Determination of Cell Fate Selection During Phage Lambda Infection

by

François St-Pierre

M.A., Natural Sciences, University of Cambridge, U.K. (2005)
B.A., Natural Sciences, University of Cambridge, U.K., (2002)

Submitted to the Department of Biology
in partial fulfillment of the requirements for the degree of

Doctor of Philosophy

at the

MASSACHUSETTS INSTITUTE OF TECHNOLOGY

February 2009

Author .....
Department of Biology
Jan 15, 2009

Certified by .....
Drew Endy
Cabot Assistant Professor of Biological Engineering
Thesis Supervisor

Certified by .....
Chris Kaiser
MacVicar Professor of Biology
Thesis Supervisor

Accepted by .....
Stephen P. Bell
Chairman, Department Committee on Graduate Students

Determination of Cell Fate Selection During Phage Lambda Infection

by

François St-Pierre

Submitted to the Department of Biology
on Jan 15, 2009, in partial fulfillment of the
requirements for the degree of
Doctor of Philosophy

Abstract

Bacteriophage lambda infection of *Escherichia coli* can result in distinct cell fate outcomes: for example, some cells lyse while others survive as lysogens. A quantitative molecular model of lambda infection supports the hypothesis that spontaneous differences in the timing of individual molecular events during lambda infection leads to variation in the selection of cell fates. Building from this analysis, the lambda lysis-lysogeny decision now serves as a paradigm for how intrinsic biomolecular noise can influence cellular behavior, drive developmental processes, and produce population heterogeneity. The aim of this thesis is to re-evaluate lambda as a paradigm for stochastic behavior by determining whether and to what extent variation in cell fate selection results from pre-existing cell-cell differences rather than chance events during infection. I find that physical differences among cells present prior to infection can control lambda developmental outcomes. Specifically, variation in cell volume at the time of infection can be used to predict cell fate: small cells tend to produce lysogens while larger cells favor lytic growth. I then present evidence that the apparent sensitivity to host volume is encoded by components of the lambda regulatory network acting upstream or at the level of CII, a critical regulator of the lambda lysis-lysogeny decision. I also detail the construction and evaluation of new strains, tools and methodology to size-fractionate populations of cells, to detect lambda infection and gene expression at the single cell level, and to enumerate individual phage particles. My results motivate further research to understand how and to what extent natural biological systems tolerate, buffer or correct for spontaneous molecular variation during development in order to produce deterministic behavior.

Thesis Supervisor: Drew Endy
Title: Cabot Assistant Professor of Biological Engineering

Thesis Supervisor: Chris Kaiser
Title: MacVicar Professor of Biology

Acknowledgments

This thesis is dedicated to Thi, my wife, who has buffered the lows and excited the highs of my graduate experience. She has been very understanding whenever I had to spend long days I spent at the lab, and has provided a warm, fun environment at home. I also want to thank my parents for being constant supporting force and for their regular visits to Boston.

Gevorg Grigoryan and Keila Ramos have been and continue to be extraordinary friends. Gevorg has also been a gym partner, a smart scientist with whom to bounce of ideas and a wise advisor on personal and career issues.

Arun Devabhaktuni and Tony Kuzhippala went above and beyond what can be expected of UROPs. Arun in particular has worked with me since summer 2007 and has grown from not knowing how to grow a bacterial culture to performing genetic engineering and time-lapse microscopy at the level expected of graduate students and postdocs. Felix Moser and Mingjie Li are two very talented research assistants in our lab who have worked closely with me on the lambda project. Arun, Tony, Felix and Mingjie have all been fun people to work with. They have been patient with technical frustrations and constructed many tools which will revolutionarize single cell analysis of lambda infection.

Other members of the Endy lab not mentioned above - Leon Chan, Sri Kosuri, Heather Keller, Ty Thomson, Jason Kelly, Barry Canton, Jeff Gritton, Ilya Sytchev, Alex Mallet, Caitlin Conboy, Jennifer Braff, Samantha Sutton and Isadora Deese - have provided a terrific working environment. Reshma Shetty and Austin Che from the Knight lab were great de facto additions to our lab, and provided valuable input to my project during our weekly lab meetings. I'd like to thank Samantha Sutton for being a good friend, a life coach and generally a thoughtful and nice person to be around. I've also been privileged to know Ty Thomson, who's always been eager to help bouncing off some ideas or find a bug in a Matlab script; the workplace has been enlivened by his great sense of humor. Isadora has kept the Endy lab from going into anarchy, and been a great help on many different issues.

The members of my thesis committee - Bob Sauer, Tania Baker and Chris Kaiser - have helped me grow scientifically and challenged me by keeping the bar high. Don Court, my outside committee member, and Lynn Thomason in his lab, have been very generous with their time, providing technical help and knowledge.

Finally, Drew has been an extraordinary advisor. In particular, I want to thank him for letting me explore my own ideas, for emphasizing the importance of communicating research and helping me improve my oral and written communication skills. I'm sad at the prospect of our scientific journey together soon reaching an end.

Contents

List of Figures

List of Tables

Chapter 1

Introduction

Multi-cellular systems have the extraordinary ability to develop and differentiate, giving rise to many specialized cell types. Cellular differentiation is typically highly controlled, and is thus an exciting process with which to study how cells can integrate information from their environment to direct their developmental response. Of particular interest are the constraints that might limit the ability of cells to make accurate developmental decisions. For example, commitment to a given cell fate must typically be made within a limited time window and involves collecting environmental and internal cues which may be complex, ambiguous or fluctuating. Given such constraints, the reliability often observed in the development of natural biological systems is remarkable [73]. For instance, the patterns of programmed death and terminal differentiation during embryonic development of Caenorhabditis elegans are nearly invariant from one individual to the next [164].

One particularly useful model system to study the properties of cell fate decision networks is bacteriophage lambda (λ), a 48,502 bp dsDNA virus that infects the bacterium *Escherichia coli* [65, 99, 100]. Lambda-infected cells typically become lytic or lysogenic. Cells that become lytic produce and release progeny phage into the environment following lysis of the host cell. Alternatively, if infected cells become lysogenic, the phage genome integrates into the bacterial chromosome and the resulting prophage is passively replicated within the surviving cell and its offspring [65, 69, 111, 140]. The lysis-lysogeny regulatory network is one of the best-

studied natural biological networks, giving the opportunity to study system-level behaviors [2, 107, 120, 156, 178, 183].

In this Chapter, I first describe the cascade of events leading to commitment to lytic growth or lysogeny. I next describe how the lambda regulatory network may sense two important aspects of its environment: the nutritional status of the host cell and the number of phage concurrently infecting a given cell. I conclude by describing a puzzling observation that motivated my thesis research: genetically-identical cells, infected by the same number of phage, do not always adopt the same cell fates, and present two models that may explain this observation.

1.1 Timing of lambda gene expression during development

The development of phage lambda is typically described as a cascade of gene expression divided into three stages. 'Immediate-early' genes are the first to be expressed after entry of phage DNA into the host cell. It is generally thought that lambda does not commit to lytic growth or lysogeny during this stage. In the 'delayed early' phase, infected cells produce regulators of the lysis-lysogeny decision, and are thought to commit to a given cell fate. Finally, in the 'late' stage of infection, lambda implements the developmental decision made in the 'delayed early' stage. Each of these stages is now described in greater detail, and depicted in Figure 1-1 (p.21) and Figure 1-2 (p.22)

1.1.1 Immediate-early stage

See Figure 1-1a; p.21

Immediately after phage DNA entry into a cell, the strong promoters of the right (pR) and left (pL) operons are active, driving expression of the regulators Cro and N, respectively [44,125,148]. Expression of 'delayed early' genes, located downstream of *N* and *cro*, is attenuated by transcriptional terminators located beyond these two genes [110, 152]. How-

ever, these terminators are not 100% efficient, and so a limited amount of downstream genes are also transcribed during the immediate-early stage. For example, *t*R1 is only ~50% efficient [28], so that *c*II, *O* and *P* are transcribed to a certain degree. Similarly, *t*L1 is ~80% efficient, although this value was determined with *t*L1 out of the phage context [32,41,133]. Nevertheless, a limited amount of products of the *p*L operon, such as CIII, may be produced during this initial phase of lambda infection.

1.1.2 Delayed-early stage

See Figure 1-1b; p.21

Efficient expression of delayed-early genes, located downstream of the *t*L1 and *t*R1 terminators, depends on a product from the immediate-early stage: the N protein [148]. Lambda N is a transcriptional antiterminator that forms a complex with host factors, thereby allowing RNA polymerase to overcome most lambda transcriptional terminators, including *t*L1 and *t*R1 [18,52,65]. N-mediated antitermination allows efficient transcription of downstream genes, both those participating in the lytic pathway (e.g., *Q*, replication and recombination genes) and those involved in the establishment of lysogeny (*c*II, *c*III) [79]. Finally, Cro accumulates to sufficient levels to start repressing the *p*L and *p*R operons by binding to its cognate operator sites [62], thus limiting further transcription of early genes.

Commitment to lytic growth or lysogeny is thought to occur at the delayed-early stage, but the exact timing and mechanism of the lysis-lysogeny decision is still not completely understood [69,131,140]. However, the activity of the delayed-early protein CII is thought to be critical in determining cell fate: infected cells with high CII activity tend to become lysogens, while those with low CII activity tend to follow the lytic pathway [7, 9, 17, 31, 65, 69, 88, 131, 140] (see also later sections and Chapter 5). Another delayed-early product, the CIII protein, is also thought to play a critical role in the lysis-lysogeny decision by stabilizing CII [43].

1.1.3 Late stage

See Figure 1-1c,d; page 21

Cell fate selection, thought to occur predominantly during the delayed-early phase, is

implemented during the late stage. In cells slated to become lysogens, CII coordinates the repression of lytic functions and the establishment of lysogeny by binding to three promoters: *p*aQ, *p*RE and *p*I [69, 131]. CII reduces transcription of the lytic gene *Q* by binding to *pa*Q, thereby promoting transcription of a small RNA antisense to *Q* message and leading to lowering of *Q* expression [71, 161]. CII also leads to repression of lytic functions indirectly, by driving expression of the lambda repressor (CI) [144]. In turn, CI turns off lytic functions (as well as *c*II expression) by binding to its cognate operator sites within *p*R and *p*L [118, 121, 122]. Moreover, by binding to the right and left operator regions, CI can activate its own expression from the *p*RM promoter [122], thus ensuring maintenance of lysogeny. Finally, CII drives expression of the lambda integrase by binding to *p*I [130], ultimately leading to site-specific integration of lambda DNA into the host chromosome [59, 100, 177].

For cells that select the lytic pathway, CII expression is presumably not high enough to repress *Q*, another phage-encoded antiterminator. Q, a phage-encoded antiterminator, allows transcription from the constitutive *p*R' promoter to extend past the *t*R' terminator, leading to expression of genes involved in capsid formation (e.g. *D*,*J*), DNA packaging (e.g. *A*) and lysis of the host cell (*R*, *S*) [52, 65, 70, 168]. A threshold requirement for Q antitermination function has been posited to explain why there is a delay between the accumulation of Q protein and the observation of Q-mediated antitermination [89].

1.2 Environmental regulation of the lysis-lysogeny decision

1.2.1 Regulation of the lysis-lysogeny decision by the nutritional conditions of the host cell

Growth condition of the host can directly impact the lambda lysis-lysogeny decision. For example, cell fate statistics vary with the growth phase of the host cells at the time of infection (Figure 1-3, page 23). Moreover, starvation of host cells prior to infection has been shown to raise the probability of lysogeny [93, 106]. How lambda infected cells sense and respond to growth conditions remains poorly understood. In this section, I describe

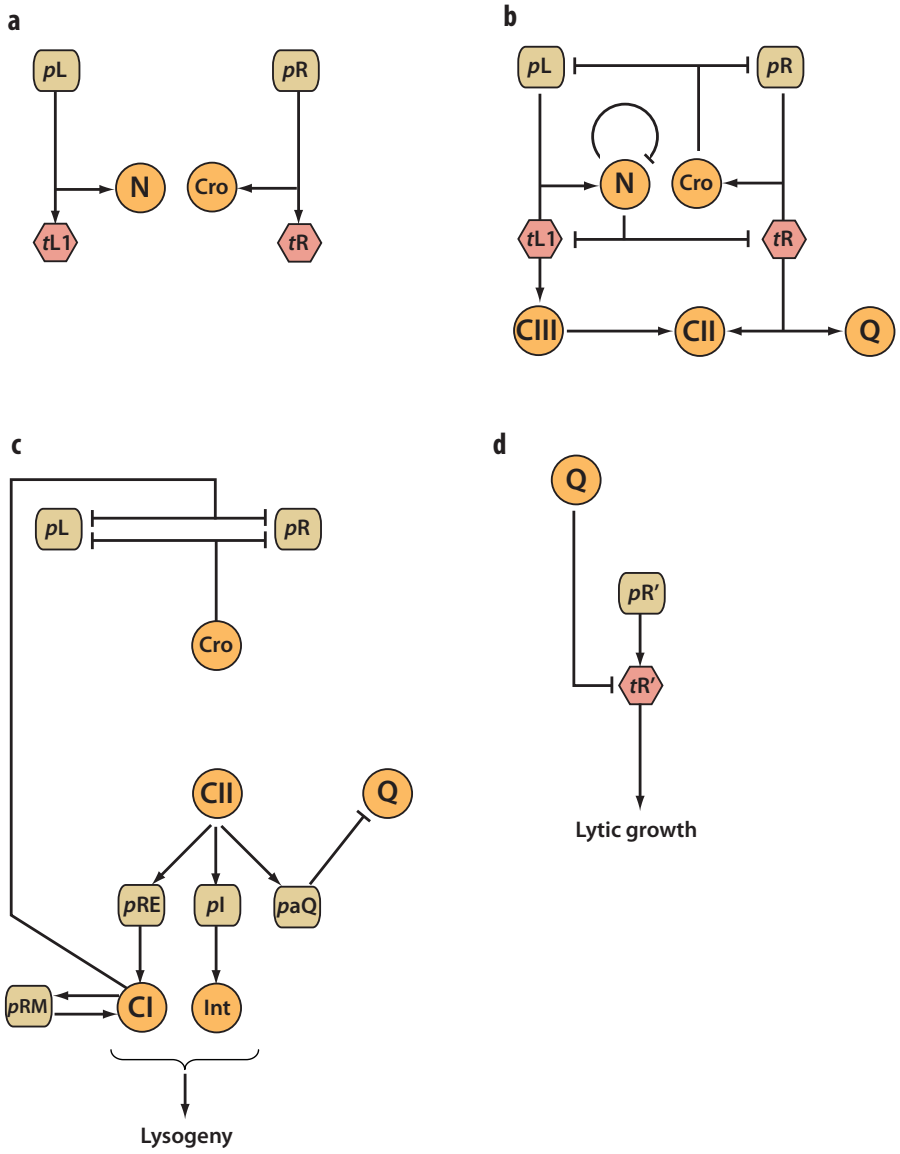

Figure 1-1: **Stages of lambda gene expression during infection. a,** immediate early gene expression. **b,** delayed early gene expression **c,** late lysogenic gene expression **d,** late lytic gene expression. Arrows indicate positive interactions, bars indicate negative interactions. Brown boxes indicate promoters, pink stop signals depict terminators and yellow circles represent genes and corresponding gene products. Not all interactions or components are depicted. A composite of subfigures a-d is shown in Figure 1-2 (page 22). This figure was inspired in part by Figure 6 of ref [131].

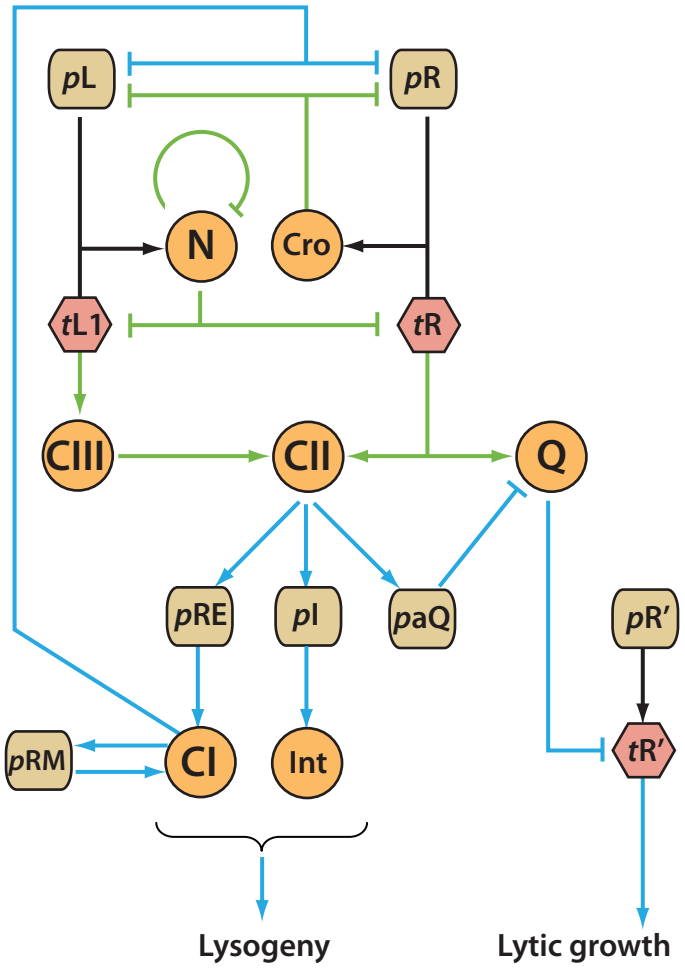

Figure 1-2: **Timing of lambda gene expression during infection.** The color of arrows and bars indicate the stage of lambda infection at which the interaction is particularly significant: black corresponds to the immediate early stage; green, delayed early stage; blue, late lytic or lysogenic stage. Other symbols are described in the legend to Figure 1-1. Not all interactions or components are depicted. This figure was inspired in part by Figure 6 of ref [131].

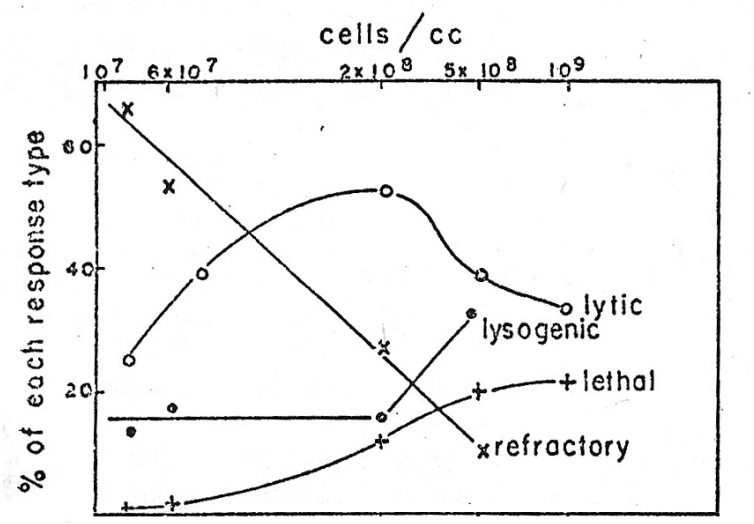

Figure 1-3: **Cell fate outcomes at different times during growth of a culture.** Aliquots from cultures of *E. coli* K12 were infected at an average of 2-4 phage per cell. The proportion of each type of response was determined. The lytic and lysogenic responses are described in the main text. In the lethal response, the cell dies but does not produce viable phage particles. Refractory cells neither die nor become lysogens, and might simply be uninfected; they produce daughter cells which, if infected, can give rise to any of the responses described here. This image was modified from reference [105]

how host-encoded factors may couple the growth rate (or nutritional status) of the host cell to the lysis-lysogeny decision statistics.

RNaseIII upregulates translation of lambda *N* and *c*III, but represses translation of *c*II

RNaseIII is a host-encoded, double-strand-specific ribonuclease. RNaseIII expression appears to be controlled by cell growth rate, with higher growth rates giving higher levels of RNaseIII [180]. RNaseIII regulates the expression of at least three lambda genes: *N*, *c*II and *c*III (Figure 1-4, p.24). RNaseIII regulates *N* translation in three ways [179,180]. First, RNaseIII can cleave and thereby remove a large stem-loop structure at +76 to +208 of the *N* open reading frame. The hairpin is thought to sterically interfere with recognition of the *N* mRNA Shine-Dalgarno sequence; higher RNaseIII levels therefore lead to higher levels of *N* expression. Second, RNaseIII also upregulates *N* expression by preventing the formation of a negative regulatory complex that represses translation of *N*. Cleavage of the *N* leader

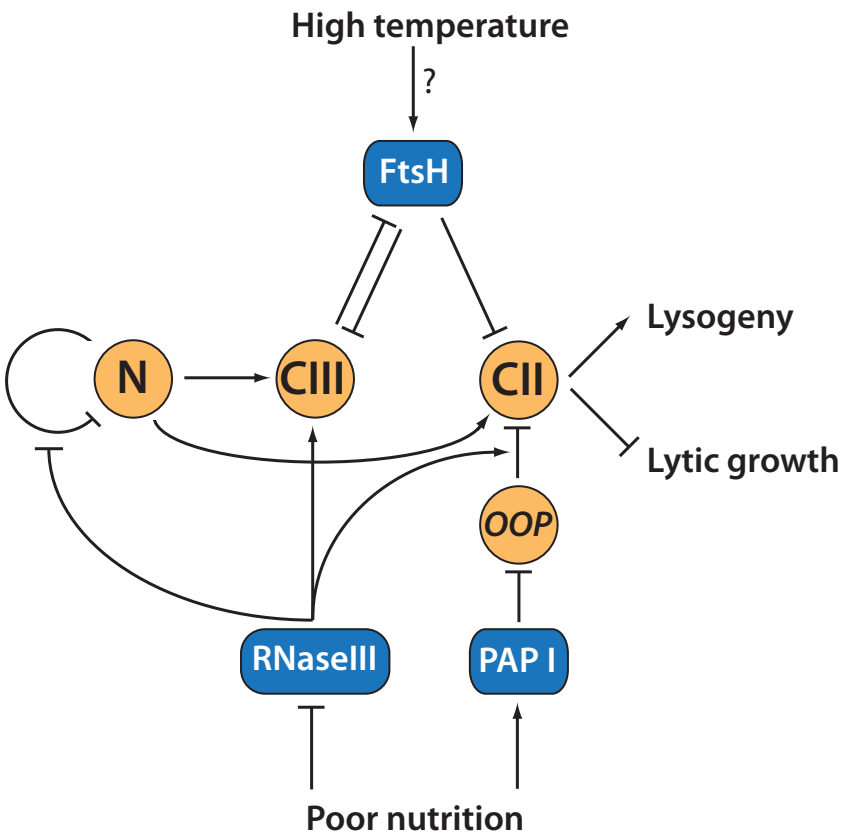

Figure 1-4: **Host influences on phage lambda regulators of the lysis-lysogeny decision.** Arrows indicate positive interactions, bars indicate negative interactions. Brown boxes indicate host factors and yellow circles represent lambda genes and corresponding gene products. Not all interactions are depicted.

sequence by RNaseIII can activate *N* expression ~200-fold under some conditions. Third, cleavage by RNaseIII upstream of *N* can reduce the half-life of the *N* message. Unlike the first two mechanisms, higher RNaseIII would, in this case, result in lower *N* expression. However, given that the levels of *N* are higher in a wild-type cell than in a mutant that cannot express RNaseIII (rnc^-), the net effect of RNaseIII is the upregulation of *N*.

The levels of N may play a role in determining the outcome of the lambda lysis-lysogeny decision. For example, infection of cells that constitutively overexpress N from a plasmid results in clear plaques, a phenotype indicative of a lower probability of lysogeny [180]. Moreover, stabilization of N by infection of a lon^- mutant also results in clear plaques [60]. However, CII is destabilized in a *lon* background [60], so it is unclear whether lytic growth is promoted due to the effect of *lon* on N, CII, or both. Nevertheless, the RNaseIII control of *N* expression therefore provides a possible mechanism by which an infected cell could

sense and respond to variation in growth rate. RNaseIII promotes *c*III translation, possibly by binding and thereby stabilizing a conformation of the *c*III mRNA that results in more efficient translation [8,9,91]. Contrary to its effect on *c*III, RNaseIII represses *c*II translation by cleaving the double-stranded RNA formed by *c*II mRNA and *oop* RNA, a short transcript antisense to the 3' end of the *c*II message [97].

In summary, RNaseIII downregulates translation of *c*II, but upregulates translation of lambda *N* and *c*III. What is the net effect of RNaseIII on the fate statistics of lambda infected cells? Growth of lambda on *rnc*$^-$ cells produces clear plaques; this phenotype can be suppressed by mutations that increase translation of *c*III [7–9]. These observations suggest that upregulation of *c*III by RNaseIII may be the dominant effect. However, the impact of a quantitative reduction of RNaseIII levels may be distinct from complete abolishment of RNaseIII activity (as in *rnc*$^-$ cells) [180].

FtsH/HflB degrades CII and CIII, but is inhibited by CIII

FtsH/HflB is an essential ATP-dependent protease thought to play a key role in the lambda lysis-lysogeny decision [17, 56, 76, 88, 131, 132]. FtsH is located in the membrane [76]; it associates with HflK and HflC, possibly assembling into a $FtsH_6HflKC_6$ holoenzyme, of which there are less than 100 per cell [76]. HflK and HflC appear to act as functional modulators of FtsH function [5, 82–84].

FtsH is thought to impact the lysis-lysogeny decision by affecting the stability of lambda CII and CIII ([83, 88], Figure 1.4). CII carries a flexible C-terminal domain of 16 amino acids that is necessary and sufficient for FtsH-mediated degradation [36,87,88]. *In vivo*, CII has a half-life of ∼1-2 minutes [83, 88]. Conditions or mutations that increase the stability of CII typically result in a consequent increase in the frequency of lysogeny. For example, mutations in *ftsH*, *hflK* and *hflC* which increase the half-life of CII also promote lysogeny [67, 83]. Given that loss-of-function mutants of *hflK* and *hflC* allow a higher frequency of lysogeny, is it surprising that overexpression of HflKC also stabilizes CII and increases the frequency of lysogeny [83]. Overexpression of FtsH and loss-of-function mutations of CII have the more expected finding of promoting lytic growth: in these conditions, lambda infection results in clear plaque formation [17, 170]. Higher temperature results in higher FtsH activity and lowered CII half-life [87]; however, higher temperature does not always increase the frequency of lysogeny [67, 87]. Finally, mutations in *hflD*, a peripheral host

membrane protein posited to recruit CII to the membrane for FtsH-mediated proteolysis, also reduce CII stability and probability of lysogeny *in vivo* [85].

CIII, a small phage-encoded 54-residues peptide, inhibits FtsH-mediated degradation of CII by acting as a competitive inhibitor [90]. CIII is itself degraded by FtsH, but with slower kinetics (half-life of ∼7 min) than CII [68]. CIII inhibits FtsH by binding to FtsH but not to CII [63]. CIII can be associated with the membrane, either by a direct interaction with the inner membrane, or by virtue of its association with FtsH [68]. CIII can dimerize [63] or oligomerize [90], and the formation of higher-order structures may be critical for its function [90]. Conditions that increase CIII expression increase the frequency of lysogeny, while those which lower CIII levels favor lytic growth [9, 17, 44, 74, 86, 92].

The evidence presented above is consistent with a model wherein stability of CII is critical in regulating the lysis-lysogeny decision. However, deletion or mutation of the signal which identified CII for FtsH-mediated degradation increases CII stability but does not consistently result in higher frequencies of lysogeny [87]. Nevertheless, FtsH-mediated degradation of CII appears to play an important role in the lysis-lysogeny decision.

How might FtsH sense nutritional conditions and respond by affecting fate outcomes of lambda infected cells? It has been suggested that at higher levels of nutrition, FtsH-related proteolytic activity is increased, leading to shorter CII and CIII half-lives [13]. However, to my knowledge, this hypothesis has never been tested. One mechanism by which the activity of FtsH may be modulated during growth phase involves the C-terminal self-processing by FtsH *in vivo*, which results in the removal of the last 7 C-terminal residues [4]. This processing is affected by the growth phase of the cells, with increased processing observed in stationary phase relative to exponential phase. However, both processed and unprocessed forms of FtsH are able to degrade CII. Nevertheless, CII stability may be quantitatively affected by the processing of FtsH. It is therefore not known whether C-terminal processing of FtsH may be responsible for the increased frequencies of lysogeny observed as host cells are growth to saturation.

Polyadenylated oop RNA downregulates cII expression

As discussed previously (see section 1.2.1 on p.23), *oop* RNA can lower translation of the *c*II message via a double-stranded association with *c*II mRNA, and subsequent cleavage of double-stranded product by RNaseIII. In bacteria, polyadenylated RNA molecules are typ-

ically degraded faster than non-modified transcripts [77]. Degradation of *oop* RNA appears to be more efficient in slower growing cells due to higher levels of the RNA polyadenylation enzyme PAP I [77]. For example, the half-life of the oop message is ∼1.5 min in cells grown in LB (doubling time = 34 min) but ∼0.1 min in cells grown in a glycerol minimal medium (doubling rate = 119 min). This finding suggests that CII expression may be greater in slower growing cells due to lower expression of the oop transcript, presumably resulting in higher frequencies of lysogeny. The regulation of *oop* degradation by growth conditions is therefore a potential mechanism by which the environment may tune the frequency of lysogeny.

Why does the frequency of lysogeny vary with growth rate?

The mechanisms by which the lambda regulatory network can sense and respond to variation in environmental conditions is still not fully understood [38]. In this section, I have described three possible mechanisms (RNaseIII activity, FtsH activity, *oop* polyadenylation), which may couple growth rate to cell fate statistics. Given the extensive interactions between the bacterial host and lambda infection, there remains the possibility that other mechanisms are at play too [33, 53, 88, 114, 134].

1.2.2 Regulation of the lysis-lysogeny decision by the multiplicity of infection

The frequency of lysogeny increases with the multiplicity of infection (MOI), the number of lambda particles concurrently infecting a given cell ([54, 86, 93, 105]; Figure 1-5, page 28). Increased frequencies of lysogeny with higher MOI have also been observed for other temperate phages, such as λ_{22} [54] or P22 [24, 101]. How lambda senses and responds to MOI is not completely understood [131]. Which phage-encoded genes are involved in the multiplicity dependent character of lysis-lysogeny decision? Increasing copy number of *c*I [144,145], *c*II [43] and *c*III [43,144,145] were all observed to promote CI synthesis, which is typically considered to be a marker of lysogeny [9, 65, 86, 145].

Kourilsky identified different determinants of the MOI response depending on the genotype of the phage used. When using Q^- phage strains, he found that the copy number of *c*II (and possibly of *c*III), but not of *c*I, impacts the probability of lysogeny [94]. In

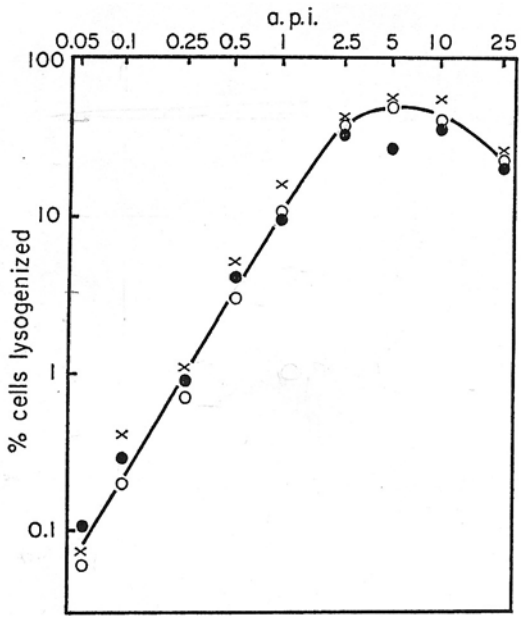

Figure 1-5: **Frequency of lysogeny as a function of the average phage input.** Exponentially growing cells were starved in 10 mM $MgSO_4$ and infected with different phage:cell ratios (here termed "average phage input" or a.p.i.). The different symbols represent different experiments where the frequency of lysogeny was calculated using different protocols. Note that the frequency of lysogeny is represented here as the percentage of all cells (infected or uninfected) which became lysogens. The frequency of lysogeny as the percentage of infected cells which become lysogens also increases as a function of a.p.i. (data not shown). This image is reproduced from reference: [92].

replication-deficient phages (P^-), however, cI, cII and cIII all promoted lysogeny. The use of P^- and Q^- phage strains complicates the interpretation of Kourilsky's results for understanding the lysis-lysogeny decision with wild-type lambda, which is replication-competent (P^+) and able to activate late lytic functions (Q^+). Nevertheless, all the studies presented in this section, considered together, identify cI, cII and cIII as candidate genes involved in the MOI response. These results are consistent with other studies suggesting that CII and CIII can be rate-limiting for lysogenization (e.g. [20, 78]).

Several mechanistic models may explain the multiplicity dependent character of lysogenization [94]. Perhaps the most parsimonious is the "gene dosage" model, whereby additional copies of certain lambda pro-lysogeny genes may increase the overall rate of expression of those genes [29,94]. However, higher MOI also increases lytic genes such as *cro* or Q. Perhaps lysogeny is comparatively favored at higher MOI because of the products of lysogenic genes may require oligomerization for their activity, and exhibit a significant concentration dependence for oligomerization [29]. Consistent with this hypothesis, tetramerization of CII [36] and oligomerization of CI [39, 137, 139] appear to have functional consequences on their activity. Nevertheless, further experimentation is needed to directly test whether lambda responds to the MOI via its effect on the dosage of specific lambda regulator genes.

1.3 Genetically identical cells, infected by a single phage, can produce different developmental outcomes

Across many conditions, genetically identical cells grown in the same environment and each infected with a single lambda particle select different cell fates: some cells lyse while other cells become lysogens [87, 105, 106]. This variability in cell fate is unlikely to be due to genetic variation within the phage population or to an artifact of the experimental methods used to grow infected cells or quantify developmental outcomes ([105], Chapter 2). Given this, how do genetically identical cells infected with the same number of phage particles give rise to distinct cell fates?

In considering this question, cell fate selection during lambda infection has emerged as a paradigm for how biochemical "noise" might account for differences in developmental

outcomes [13, 115, 166, 176]. In particular, Arkin and colleagues used a detailed stochastic chemical kinetics model of lambda infection to analyze if the lysis-lysogeny decision might be driven by spontaneous differences in the timing of individual biochemical reaction events [13]. In the "Arkin model", initially identical newly infected cells are expected to spontaneously accumulate quantitative differences in the abundances of key regulatory molecules, which then propagate through the lysis-lysogeny "decision circuitry" and result in distinct cell fates (Figure 1-6a, p.31).

The Arkin model is important for at least two reasons. First, the model revitalized study of how lambda infected cells produce distinct cell fates, recognizing that the existing detailed descriptions of the individual molecular components of phage lambda are not sufficient to explain such system-level behavior. Second, Arkin and colleagues mapped the process of cell fate selection onto an explicit model of intracellular physics, which forces a recognition of the fact that many systems in biology are comprised of components whose cellular abundances are far below levels for which continuous approximations of chemical kinetics are valid [57], and for which precision of behavior cannot be expected to emerge via the bulk averaging of many individual reaction events [154].

The Arkin model also makes a strong claim — cell fate differences in lambda-infected *E. coli* arise due to spontaneous biochemical noise during infection. However, to my knowledge, no experiments have been carried out to test this hypothesis. Thus in framing my thesis research, I considered an alternative model for lambda infection suggested by Lieb, Gros and Kourilsky decades ago [92, 95, 105]. In the alternative model, variation in the lysis-lysogeny decision may result from cell-cell variability present prior to infection (Figure 1-6b, p.31). This PhD thesis describes my efforts to test and explore these models.

1.4 Thesis overview

Chapter 2* — Host volume is a predictor of the lambda lysis-lysogeny decision, population measurements

I first explain why I selected cellular volume as a plausible predictor of cell fate. I then describe how I developed and optimized methods to size-fractionate asynchronous populations of cells via counterflow centrifugal elutriation. Results obtained with cultures of stationary phase cells show that host volume can be used to predict the

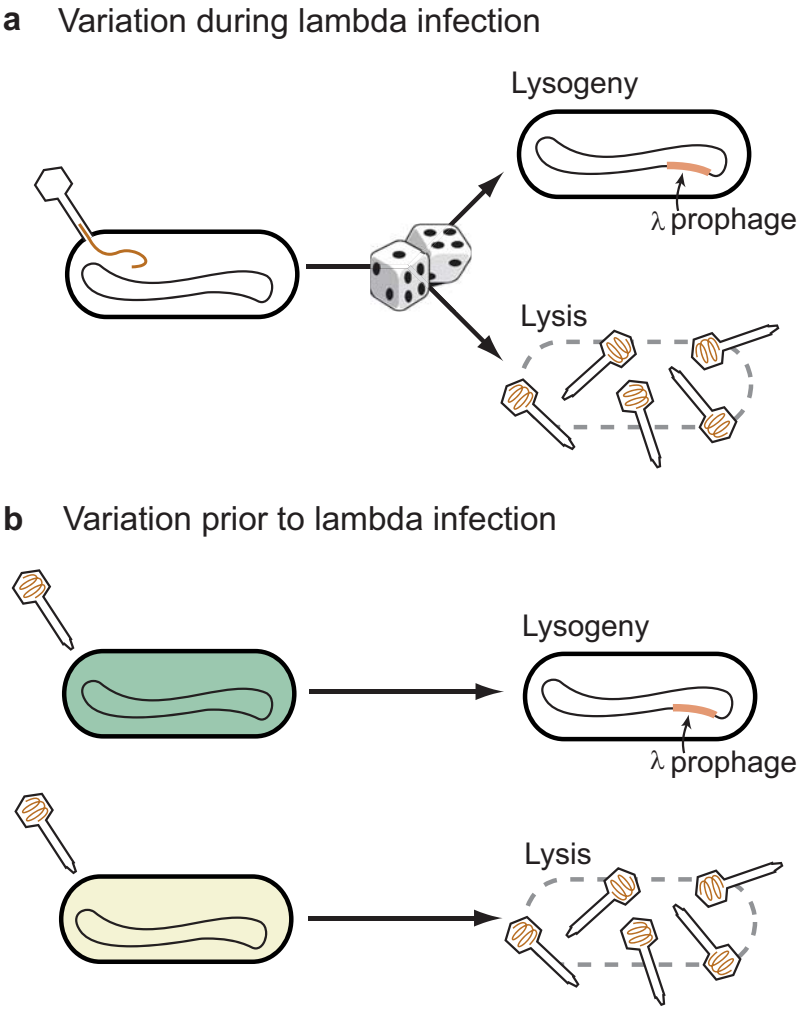

Figure 1-6: **Alternative models for cell fate selection in a population of genetically identical cells. a,** Variation during infection (for example, spontaneous chemical kinetic noise) leads to qualitative differences in cell fate. **b,** Variation in the physical state of individual cells prior to infection predetermines cell fate.

fate of lambda infected cells: smaller cells tend to become lysogens, while larger cells tend to follow lytic growth.

Chapter 3* — Host volume is a predictor of the lambda lysis-lysogeny decision, single-cell microscopy measurements

I present the development of a microscopy platform to study lambda infection in single cells. Using this platform, I present results that further support the main conclusion of Chapter 2: the lambda lysis-lysogeny decision is correlated with the volume of individual, stationary phase cells. My single cell results show that while volume is a strong predictor of cell fate, it does not fully account for the observed variability in cell fate selection.

Chapter 4* — Identification of host-encoded determinants of lambda's "volume sensor"

I describe efforts to understand whether lambda may be sensitive to a cellular parameter correlated with volume rather than volume more directly. I first show that sensitivity to host volume is not specific to infection of stationary phase cells. I then describe ongoing efforts to determine whether lambda may be sensitive to cell cycle position rather than volume.

Chapter 5 — Identification of phage-encoded determinants of lambda's "volume sensor"

I describe how characterization of the timing of the lysis-lysogeny decision can help to identify phage-encoded components underlying lambda's apparent sensitivity to host volume. In particular, I discuss the construction of a fluorescent reporter of CII activity. Preliminary results using this reporter suggest that the lysis-lysogeny decision has been made before or at the level of CII activity.

Chapter 6 — Detection and enumeration of individual phage particles

I describe ongoing attempts to create a reporter of the multiplicity of infection (MOI), and how such a reporter would enable the study of the decision in wild-type hosts grown to exponential phase.

Chapter 7 — Summary

Here, I summarize the results from previous Chapters, highlight opportunities for future research, and put my work in the larger context of research on cell fate selection.

* Parts of Chapters 2, 3 and 4 are published in: F. St-Pierre and D. Endy. Determination of cell fate selection during phage lambda infection. *Proceedings of the National Academy of Sciences of the United States of America*, 105(52):20705-10, Dec 30 2008.

Chapter 2

Host volume is a predictor of the lambda lysis-lysogeny decision, population measurements

2.1 Host volume is a plausible marker of cell fate

In Chapter 1, I briefly described an alternative model for lambda infection in which cell-cell variability that exists prior to infection determines individual cell fates (Figure 1-6b). Given the extent of interactions between host and phage (1; [53]), variability in a large number of host functions could plausibly impact the lambda lysis-lysogeny decision.

To select a candidate predictor[1] of cell fate onto which to focus my initial efforts, I considered past work showing that the frequency of lysogeny increases with the average number of infecting phage per cell ([93]; Chapter 1). To explain this observation, Kourilsky proposed that lysogeny requires the concentrations of one or more phage-encoded factors to exceed a critical threshold [94, 96]. The amount of pro-lysogeny factors produced in an infected cell may be greater when the levels of their corresponding genes are high, either because many phage are simultaneously infecting the same cell [93], or because the infected

[1]For the purpose of this thesis, I define "predictor" as a cellular characteristic, measured prior to (or immediately after the start of) infection by phage lambda, that correlates with the eventual fate of the cell (lysis or lysogeny). Examples of such cellular characteristics may be morphological parameters (volume, surface area, shape), or the abundance, activity or localization of a given molecular species (e.g. a given protein or mRNA). A predictor implies correlation, not causality.

cell is small (this work). For cells infected with the same number of phage, I might therefore predict that, at least early during infection, smaller cells will have an increased concentration of pro-lysogeny gene products and may tend to become lysogens; larger cells will have a lower concentration of pro-lysogeny gene products and might favor lytic growth. Particularly important examples of such pro-lysogeny factors are lambda CII and CIII, whose levels are known to impact the lysis-lysogeny decision (see section: 1.2, p.20). However, the levels of other phage-encoded gene products – for example, lambda N – may also play a role (also discussed in section 1.2, p.20).

According to this "gene dosage" model, host volume may be a plausible marker of lambda infected cells. Modeling of the lambda right operator region (oR), performed prior to the start of my experimental work, also suggested that sensitivity to host volume can be encoded in lambda regulatory circuit (see Chapter 5), further motivating the experimental validation of volume as a marker of cell fate.

Note that the precise nature of a putative correlation between the volume and fate of lambda infected cells is considered in Chapter 4. For example, lambda might be sensitive to position within the cell division cycle rather than host volume. Thus, with the understanding that volume may be a proxy for other cellular parameters, I next considered experiments to test whether host volume may be used to predict the outcome of the lysis-lysogeny decision.

2.2 Macroscopic plate methods can be used to quantify cell fate statistics

2.2.1 Preparation of stationary phase *Escherichia coli* MG1655

Before testing host volume as a candidate marker of the lambda lysis-lysogeny decision, I evaluated and developed methods to quantify cell fate selection statistics. For my experiments, I used the "wild-type" *Escherichia coli* K12 strain MG1655 (F^- *lambda*$^-$ *rph*-1) whose genome has been completely sequenced [22].

Because the multiplicity of infection (MOI) is known to impact cell fate selection (see above and Chapter 1), I ensured that virtually all cells were infected at the same MOI (MOI=1) by using a low phage-to-cell ratio (0.005 or otherwise noted). However, wild-

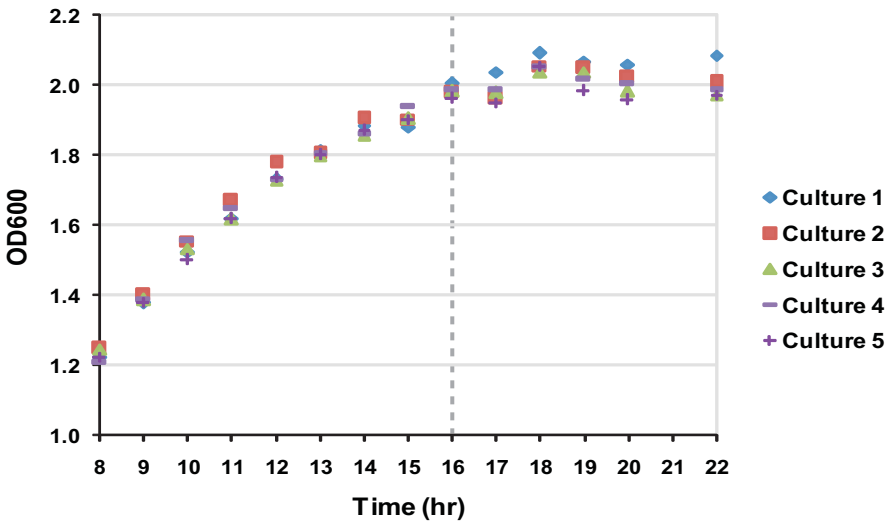

Figure 2-1: **Growth curves of *Escherichia coli* MG1655 approaching stationary phase in tryptone broth at 37°C.** I grew five cultures of *Escherichia coli* MG1655 from independent colonies as described in the main text. Aliquots from each culture were diluted 3-fold into TB for OD600 measurement via a Shimatzu UV160U spectrophotometer (Shimadzu Scientific Instruments, Columbia, MD, USA). The time represents the number of hours following the 500-fold dilution in 0.5L TB (see main text). I typically harvested cells for size-fractionation and/or infection 16 hours post-dilution. Dilution and time-independent measurement error was determined by comparing the OD600 readings of 10 separate 3-fold dilutions of stationary phase cells. The coefficient of variation of those measurements was <1%.

type cells grown to exponential phase and infected with a single phage typically follow the lytic pathway exclusively [93]. Thus, to raise the frequency of lysogeny to measurable levels, I starved the cells by growing them to stationary phase, a growth phase reported to produce high fractions of both lytic events and lysogens [93, 105]. Specifically, I first grew MG1655 cultures in tryptone broth (TB; [153]) at 37°C to an OD600 of 0.40, as measured by a UV160U spectrophotometer (Shimadzu Scientific Instruments, Columbia, MD, USA). I then diluted the culture 500-fold into 0.5L of TB in a 2.8 L baffled flask, and continued growth with shaking (220rpm) and aeration for 16 hours at 37°C (see Figure 2-1 for growth curves).

2.2.2 Quantification of cell fate outcomes

I measured developmental outcomes using λ *c*I857 *bor*::*KanR*, a lambda strain constructed by Lynn Thomason in the laboratory of Donald L. Court (NCI-Frederick, Frederick, MD,

USA). This strain has two important characteristics. First, the phage produces only lytic cells at temperatures above 40℃ due to the temperature sensitive allele (*c*I857) of the lambda repressor *c*I. Second, the phage contains a *KanR* cassette integrated into the lambda genome as a partial replacement of the *bor* locus. This cassette permits selection of lysogens as kanamycin-resistant colonies. Note that *bor* is not known to be involved in the lysis-lysogeny decision. I confirmed that inactivation of *bor* does not impact lambda decision by comparing population-average cell fate statistics in MG1655 cells infected with *c*I857 *bor*::*KanR* or with wild-type lambda (Figure 2-2, page 39).

To measure cell fate outcomes, I followed the procedure sketched in Figure 2-3 (p.40). I first resuspended cells to 1E9 cells/ml in ice cold TB supplemented with 10 mM $MgSO_4$. I added phage at an average phage-to-cell ratio of 0.005 (λ *c*I857 *bor*::*KanR*) or 0.05 (λ^+). This phage-to-cell ratio was calculated by titering phage and cells using standard methods [11]; because of unadsorbed phage, the actual (i.e. effective) phage-to-cell ratio was typically 40-60% lower (data not shown).

I incubated cell-phage mixtures at 4℃ for 30 min to allow for adsorption. I removed unadsorbed phage by centrifugation. I then diluted cells 10-fold in TB supplemented with 1mM $MgSO_4$ pre-warmed to 30℃. I incubated cells at 30℃ with shaking and aeration for 45 min, after which I placed cultures on ice; this incubation step is necessary to allow newly lysogenic cells to develop kanamycin resistance (λ *c*I857 *bor*::*KanR*) or superinfection homoimmunity (λ^+). I removed any remaining unadsorbed phage by a final centrifugation step.

I independently measured lysis, lysogeny, and total infected cells. I measured the number of lytic cells by using TB soft agar to disperse cells on TB agar plates containing ∼6E7 plating cells, incubating at 30℃, and counting plaque forming units (PFU). Plating cells are simply additional cells that are sensitive to lambda infection and allow propagation of lambda infection, so that individual infected cells can produce clear areas (plaques) on a lawn a bacterial cells. I made plating cells by growing MG1655 in TB supplemented with 0.2% maltose to exponential phase and resuspending the culture to ∼6E8 cells/ml in TB supplemented with 10 mM $MgSO_4$.

For experiments using λ *c*I857 *bor*::*KanR*, I measured the number of lysogenic cells by spreading cells on TB agar supplemented with 20 μg/ml kanamycin sulfate. When plating uninfected cells on kanamycin agar, I usually obtained no false positives; in a few cases,

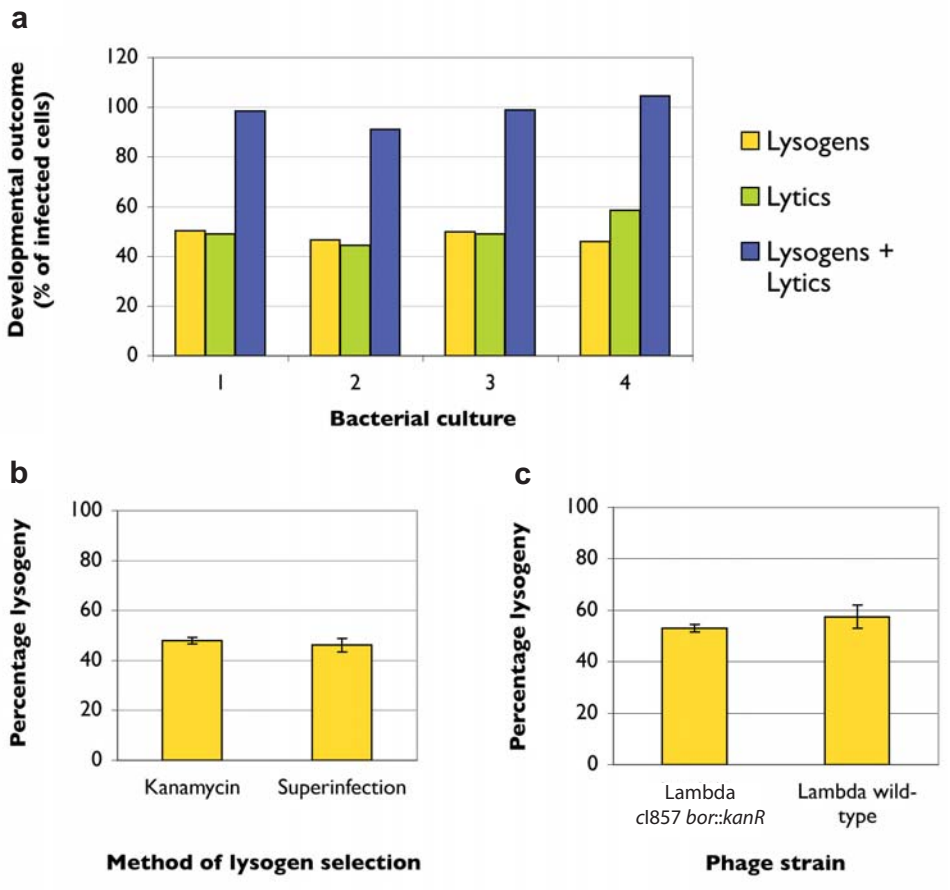

Figure 2-2: **Genetically identical cells, each infected with a single phage, can produce distinct developmental outcomes. a,** Four independent infected cultures produce similar fractions of lytic and lysogenic outcomes, the sum of which equals an independent measure of total infected cells. **b,** Population-wide cell fate statistics are insensitive to the method of lysogeny quantitation. The error bars represent the standard error of the mean of three infections made with independent stocks of λ *c*I857 *bor*::*KanR*. **c,** A culture of stationary phase cells was infected with three independent stocks of λ^+ and three independent stocks of λ *c*I857 *bor*::*KanR*. The percentage lysogeny is the number of lysogens over the total number of infected cells (here calculated as the sum of lysogens and lytic events). The error bars represent the standard error of the mean of infections made with three independent stocks of λ *c*I857 *bor*::*KanR* or λ^+.

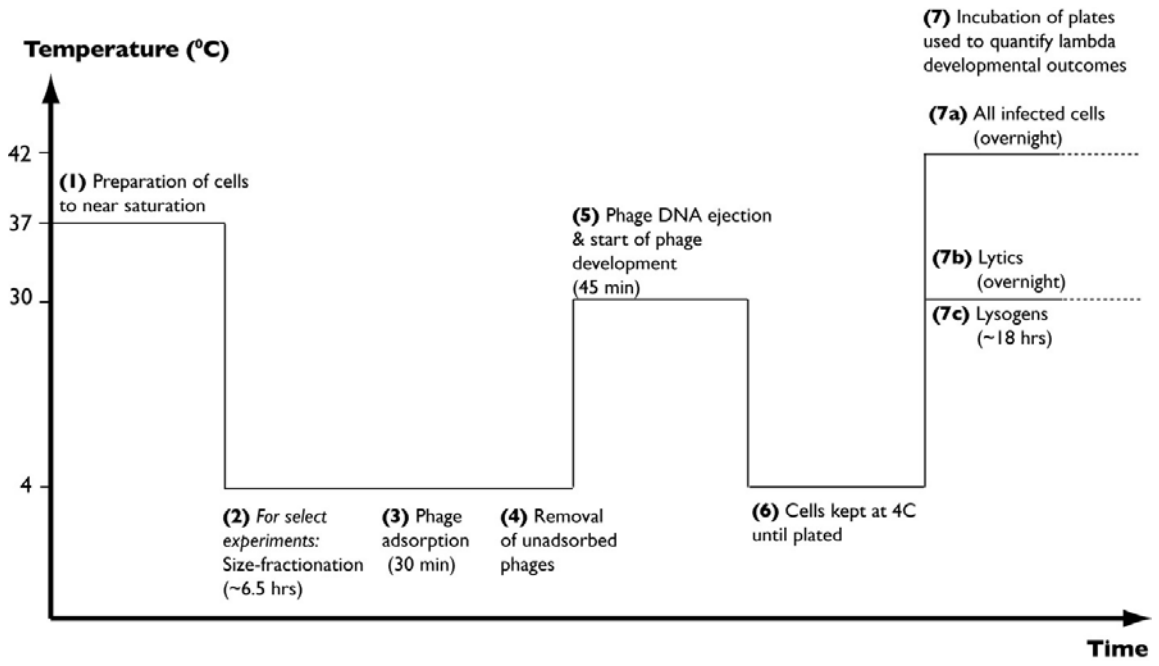

Figure 2-3: **Macroscopic plate tests to quantify developmental outcome of lambda infected cells, sketch of experimental procedure.** The major steps of the experimental protocols are shown above. The duration of the steps is indicated where appropriate.

up to 0.001% of plated cells gave false positives (data not shown). For experiments using λ^+, I selected lysogens as cells resistant to homoimmune superinfection. Specifically, I spread infected cells on TB agar seeded with ~1E9 *c*I26, a lambda mutant that kills any non-lysogenic lambda-sensitive cells. When plating uninfected cells on *c*I26-seeded agar, ~0.01% of cells produced colonies (false positives). For both λ^+ and λ *c*I857 *bor*::*KanR*, I incubated plates at 30℃ and scored lysogens by counting the number of colony forming units (CFU).

For cells infected with λ *c*I857 *bor*::*KanR*, I independently measured the total number of infected cells by preparing plates as if to count lytic events, with the exception that the plates were incubated at 42℃. At 42℃, the temperature-sensitive lambda repressor *c*I857 is inactive, so all infected cells select the lytic pathway and can be counted as PFU.

I found that stationary phase MG1655 produced 45-50% lysogeny (Figure 2-2a, p.39). Across four replicate experiments, the sum of independent measurements of lysogens and lytic centers was equivalent to my independent measurement of the total number of infected cells. I saw no difference in the frequency of lysogenization whether I used kanamycin or

resistance to homoimmune superinfection as a method to select lysogens (2-2b). Both λ *c*I857 *bor*::*KanR* and λ^+ produced identical frequencies of lysogeny (Figure 2-2c, p.39), suggesting that the *c*I857 and *bor*::*KanR* alleles do not interfere with the lambda lysis-lysogeny decision in my experimental conditions. Because selection using kanamycin is simpler and produces a lower false positive background, I used λ *c*I857 *bor*::*KanR* for all subsequent experiments in this Chapter, unless otherwise noted.

2.3 Counterflow centrifugal elutriation can produce fractions of *E. coli* cells with different mean cell volumes

2.3.1 Size fractionation of cultures of *Escherichia coli*

To test whether host size can be used to predict the fate of infected cells, I required a method to obtain fractions of different mean cell volume from stationary phase cultures of *Escherichia coli*. I present here two methods that were initially considered:

"Baby machine"

One method developed by Helmsletter and Cummings, the "baby machine", involves the collection of recently divided cells, which are typically the smallest cells of a culture [19,64]. Briefly, exponentially growing cells are attached to a nitrocellulose membrane, and growth medium is flowed onto the cells. Newborn cells simply fall in a receptacle. Larger cells (cells further into the cell division cycle) can be obtained by growing smaller cells in culture media for a given amount of time. Unfortunately, this method can probably only be used with exponentially growing cells, because growth media needed to allow cells to divide (to obtain newborns) and to grow (to obtain larger cells) prevent cells from remaining in stationary phase.

Flow cytometry

Forward angle light scatter (FALS) has been used to estimate bacterial cell size [23, 149]. I therefore performed pilot studies using a MoFlo flow cytometer and cell sorter (Dako,

Glostrup, Denmark) at the MIT Flow Cytometry Core Facility. I collected two cell fractions, one for cells with the 10% smallest FALS signal, and one with cells with the 10% largest FALS signal. However, volume measurements using a Coulter counter (see later this Chapter) showed identical mean cell volumes for the two fractions. Discrepancy between published data and the results from my pilot experiment might be due to instrumentation differences. I did not consider this method further, and concentrated on counterflow centrifugal elutriation (next).

2.3.2 Development of counterflow centrifugal elutriation methods

Counterflow centrifugal elutriation (elutriation) fractionates cell based on differences in terminal sedimentation velocity, which is correlated with cell size [51]. Elutriation has previously been used to isolate fractions of small *E. coli* cells from asynchronous populations [51]. Here, I developed protocols to obtain many fractions of *E. coli* cells across a range of mean cell volumes (MCV). I used a JE5.0 counterflow centrifugal elutriation (elutriation) system equipped with a single 40 ml chamber pre-cooled to 4℃ (Beckman Coulter, Fullerton, CA, USA). I controlled cell and medium flow rate via a peristaltic pump loaded with small pump head cartridges and fitted with L/S14 silicon tubing (Cole-Parmer, Vernon Hills, IL, USA). I increased fraction quality by using two anti-parallel pump heads and a pulse-damping chamber to improve continuity of flow in the elutriation chamber; the damping chamber also trapped small bubbles that otherwise would have disrupted flow within the chamber or caused rotor vibration. I switched the pulse-damping chamber on-line after cell loading by means of a three-way valve. Figure 2-4 (p.44) depicts the most important features of my setup.

Note that I also designed an air purge system to remove air from the JE5.0 elutriation rotor equipped with a large (40ml) elutriation chamber. The necessary flow rate to remove air from my system is 200 ml/min (Ref. The JE5.0 Elutriation System, Instruction Manual, © 2004). Unfortunately, the maximal flow rate of my system is only ∼31 ml/min: at the maximal pump drive speed of 100rpm, small cartridges equipped with L/S 14 tubing give an output of ∼15.6 ml/min per cartridge. I therefore had to use a second drive with the same maximal speed of 100rpm, but equipped with an Easyload pump head loaded with L/S 17

Part	Part Number
Elutriation pump*	
1. Masterflex L/S variable speed digital economy drive	HV-07524-50
2. Masterflex L/S 2-channel, 6-roller pump head	HV-07519-10
3. Masterflex L/S small cartridges	HV-07519-85
Air purge pump*	
1. Masterflex L/S variable speed digital economy drive	HV-07524-50
2. Masterflex L/S Easy-Load pump head	HV-07518-10
3. Masterflex L/S 17 tubing (6.4mm inside diameter), peroxide-cured	HV-96400-17
Masterflex pulse dampener*	HV-07596-20
Masterflex L/S 14 tubing (0.6mm inside diameter), peroxide-cured*	HV-96400-14
3-way valves i.e. 3-way stopcocks with Luer connections, male-lock*	HV-30600-02
JE5.0 elutriation system with large (40ml) chamber and pressure gauge**	Contact Beckman Coulter

*Cole-Parmer Instrument Company **Beckman-Coulter

Table 2.1: **Elutriation system parts list.** All equipment was from Cole-Parmer Instrument (Vernon Hills, IL, USA, www.coleparmer.com), with the exception of the JE5.0 elutriation system, which is from Beckman Coulter (Fullerton, CA, USA, www.beckmancoulter.com). See Figure 2-4 (p.44) for a sketch of my elutriation system.

tubing. This second drive was able to achieve flow rates of up to 280ml/min. A 3-way valve was used to control whether the "air purge pump drive" or my normal "elutriation pump drive" was switched on-line. Note that it may be possible to find a pump system (pump drive, pump head and tubing) that could be used both to purge air out of the elutriation system and to produce the flow rates used in my protocols.

I developed two elutriation protocols, optimized to isolate smaller and larger MG1655 cells, respectively. During an experiment, I carried out each protocol in parallel using two independent elutriation systems. For both protocols, I first filled the system with an ice-cold solution of M9 salts, purged any air from each elutriation system and brought the rotors to 4800 RPM for at least 15 minutes before cell loading. I vortexed cells vigorously for 2 minutes prior to loading to reduce cell clumping in the elutriation chambers. I then loaded each elutriation system with 120 ml of cells at a flow rate of 3 ml/min. To collect fractions of small MG1655 cells, I kept the flow rate at 3 ml/min for 20 min to allow cells to equilibrate

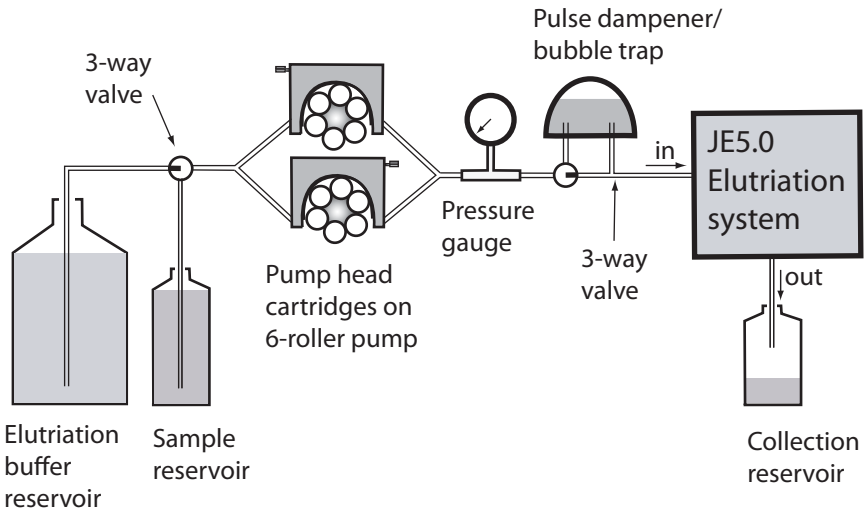

Figure 2-4: **Schematic of counterflow centrifugal elutriation system.** The specific parts used in my system are listed in Table 2.1 (p.43). This setup was inspired by [172] and the JE5.0 elutriation system instruction manual (©2004). As described in the main text, I used two identically-configured elutriation systems in parallel for most of my experiments.

in the chamber. I then increased the flow rate to 4, 5 and then 6 ml/min, collecting 0.5 L at each flow rate. I collected small cells from the 6 ml/min fraction, and discarded all other fractions. To collect fractions of larger MG1655 cells, after loading the cells into the elutriator, I slowly increased the flow rate to 7 ml/min. I then increased the flow rate from 7 to 13 ml/min in 1 ml/min steps, collecting 0.5 L at each flow rate. I collected increasing volume cells from the 9, 10, 11, 12 and 13 ml/min fractions (I only collected 0.1 L at the 13 ml/min flow rate) (Table 2.2).

2.3.3 Elutriation does not grossly affect cell fate selection statistics

I tested if elutriation may have affected cellular physiology in such a way that it grossly influenced the lysis/lysogeny decision. To do this, I performed elutriation using the described methods except that elutriated cells were continuously pumped back into the system. Cells that underwent elutriation in this way exhibited the same developmental statistics as cells from the same culture that were not loaded into my elutriation systems (Figure 2-5).

I tested if subjecting cells to elutriation, and thus to centrifugal and counterflow forces, can affect their physiology in such a way that it influenced the lysis-lysogeny decision fol-

Flow rate at which the fraction was collected (ml/min)	**Fraction volume** (L)	**Approximate yield** (% of loaded cells collected in the fraction)
6	0.5	1
9	0.5	5
10	0.5	6
11	0.5	6.5
12	0.5	6.5
13	0.1	1

Table 2.2: **Yield of fractions collected by counterflow centrifugal elutriation.** Fractions produced by elutriation were concentrated ∼100-fold in 1x M9 by centrifugation. Cells from the asynchronous population used to load the elutriation system were resuspended in the same medium (1x M9). The OD600 of the resulting cell suspensions was measured using an ND-1000 spectrophotometer (NanoDrop, Wilmington, DE, USA). Assuming 1E9 colony forming units (CFUs) per OD600 per ml for all fractions independently of mean cell volume, I calculated an estimate of the number of cells collected in each fraction. The numbers shown above represent the average of measurements made on elutriated fractions from three independent stationary phase cell cultures. Note that yields do not sum up to 100% of loaded cells, because only collected fractions were included in this analysis.

lowing infection by phage lamdba. To do this, I performed elutriation for the same duration (∼6.5 hours) as for the elutriation experiments presented in the next sections of this Chapter. Moreover, to increase the probability of observing an impact of elutriation on the lysis-lysogeny decision, fractionated cells – that is, cells which left the elutriation system – were continously reintroduced into the elutriation apparatus. Cells that underwent elutriation in this way exhibited the same developmental statistics as cells from the same culture that were not loaded into my elutriation systems (Figure 2-5, 46). This result suggests that the process of elutriation, performed as described earlier, does not cause a measurable impact on the lambda lysis-lysogeny decision.

2.3.4 Electronic and microscopy measurements of cell size

I measured the volumes of individual cells in each fraction by two methods: light microscopy and electronic volume. For microscopy measurements, I spread cells on 0.85% NaCl agarose pads and took pictures using a TE2000-E inverted microscope equipped with a 60x DM phase contrast objective, 1.5x intermediate magnification (Nikon USA, Melville, NY, USA)

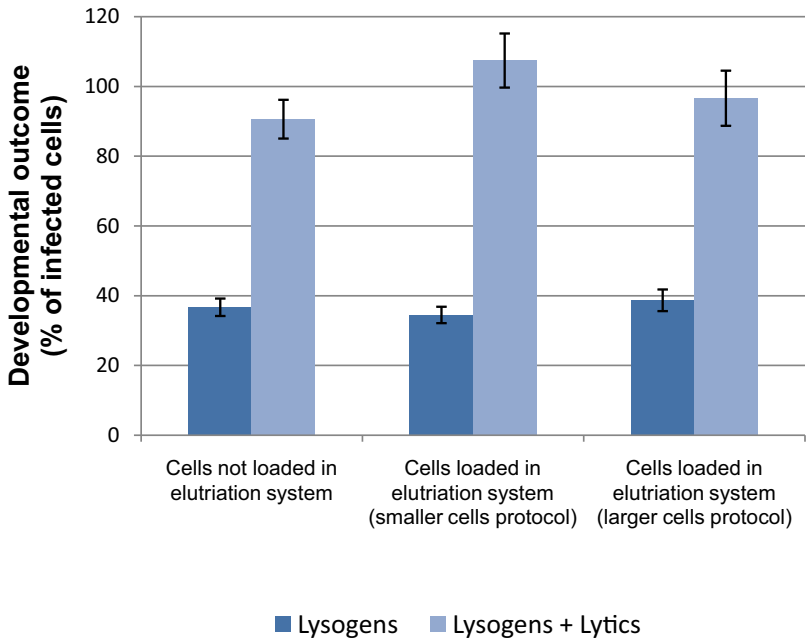

Figure 2-5: **Counterflow centrifugal elutriation does not result in qualitative changes in developmental outcome statistics of lambda-infected cells.** Elutriation was performed as described in Section 2.3.2 (p.42). However, as explained in the text, I continously reintroduced fractionated cells back into the elutriation system. To do this, I made two changes to the setup depicted in Figure 2-4 (44). First, the sample reservoir was the only reservoir used. The outflow of the system, including fractionated cells, was collected into the sample reservoir so that it could then be pumped back into the system. Second, the pulse dampener was not used to avoid cells accumulating in its chamber. This setup was used for both elutriation systems, and the two protocols described earlier (Section 2.3.2, p.42) were followed in parallel. At the end of the procedure, cells were collected into separate containers by using a high flow rate (>20 ml/min) to wash out the cells, and manual removal of the cell pellet which usually forms at the distal end of the elutriation chamber. Cells loaded in the two elutriation systems, as well as cells from the same population but which were not loaded in either of the elutriation systems, were infected with phage lambda and their developmental outcomes quantified. The error bars represent the Poisson error of plating.

and an ORCA-AG CCD camera (Hamamatsu Photonics K.K., Japan) controlled by IPLab v3.9 software (BD Biosciences, Rockville, MD, USA). I manually measured the long axis of more than 500 cells per fraction. I converted cell length measurements (pixels) to absolute length (microns) using a calibration slide (AppliedPrecision, Issaquah, WA, USA). I converted measured cell lengths to cell volumes by modeling cells as hemisphere-capped cylinders: cell volume = $4/3\pi r^3 + (L-2r)\pi r^2$, where 'L' is the cell length and 'r' is the half the cell diameter 'r' was assumed to be identical (0.44 μm) for all cells. I chose this value of 'r' by measuring the mean cell diameter of over 500 cells from an asynchronous MG1655 population grown as described above.

To obtain electronic volume measurements, I used an NPE Cell Quanta Hg/488 equipped with 25 μm flow chamber (NPE Systems, Pembroke Pines, FL, USA)(106). To better separate cell volume measurements from electronic noise, I stained cells Syto-9 (Invitrogen, Carlsbad, CA, USA) and triggered on fluorescence rather than volume. For staining, I first diluted cells to ~1E6 cells/ml in NPE isodiluent (NPE Systems, Pembroke Pines, FL, USA) and incubated with 2 μM Syto-9 for 30 min at 4℃ in the dark. I calibrated my electronic volume measurements by spiking cell suspensions with 1.51 μm yellow-green fluorescent polystyrene beads (Excitation: 425 nm, Emission: 480 nm; Catalog No. FS04F, Bangs Labs, Fishers, IN, USA). Cells and beads were excited with a 488 nm laser and their emission monitored using a 525/30 nm emission filter. Electronic volume (gain setting=10) and fluorescence were recorded for more than 10,000 cells and 5,000 beads per fraction. Electronic and microscopy measurements of fraction mean cell volumes gave similar values (Figure 2-6, p.48), and confirmed that elutriation can be used to produce fractions with different mean cell volumes (Figure 2-7,p.49).

Volume measurements of septating cells

Many cells in fractions of larger cells appear to be septating (see Figure 2-7, p.49). I assumed that both "halves" of septating cells can freely exchange molecules during phage infection, so that size measurements should include the entire cell. This assumption is further supported by time-lapse movies of individual cells infected by a phage strain constitutively expressing GFP (see Chapter 3, p.61). In these movies, GFP is seen to fill up the entire cell, rather than only half of the cell (data not shown). However, I cannot exclude the possibility that certain macromolecules, such as phage DNA, cannot cross partially formed septa.

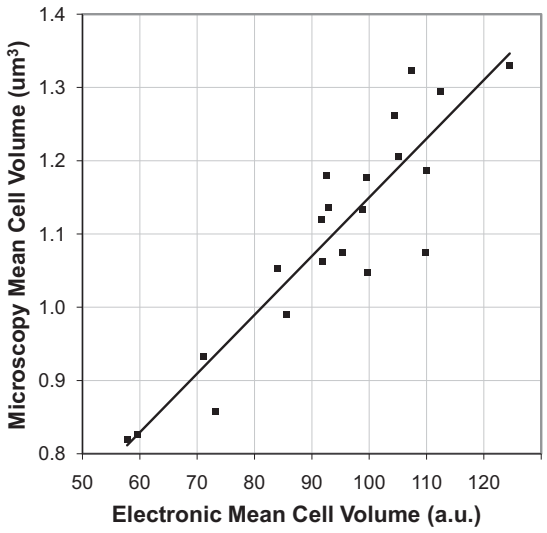

Figure 2-6: **Comparison of mean cell volume obtained by electronic and microscopic measurements.** Mean cell volume for the 21 fractions included in 2-11 (p.53) was obtained by microscopic and electronic measurements as described earlier. The equation of the linear trendline is y = 0.0069x + 0.4668, and the correlation coefficient (r^2) is 0.823.

The volume of a septating cell was calculated identically to the volume of a non-septating cell with the same length. My microscopy measurements therefore overestimate the volume of septating cells. However, this overestimation may be slight, as electronic and microscopy measurement gave similar results (Figure 2-6, p.48).

2.4 Host volume is a marker of cell fate

Having established methods to segregate cells based on size, measure cell volumes and quantify cell fate outcomes, I next set out to test the hypothesis that host volume can be used to predict the fate of lambda infected cells. I grew three independent cultures of MG1655 as described earlier and collected cell fractions with mean cell volumes (MCV) between 0.82 and 1.33 μm^3, giving a MCV ratio of ∼1.6 between the largest and smallest fractions (Figure 2-11, p.53; Figure 2-8, p.50; Figure 2-9, p.51; Figure 2-10, p.52).

I infected each cell fraction and quantified developmental outcome. Across the ∼1.6-fold range of MCV fractions, I observed a ∼3-fold difference in the percentage lysogeny (Figure

I also tested whether my results might be due to differences in the number of dead or

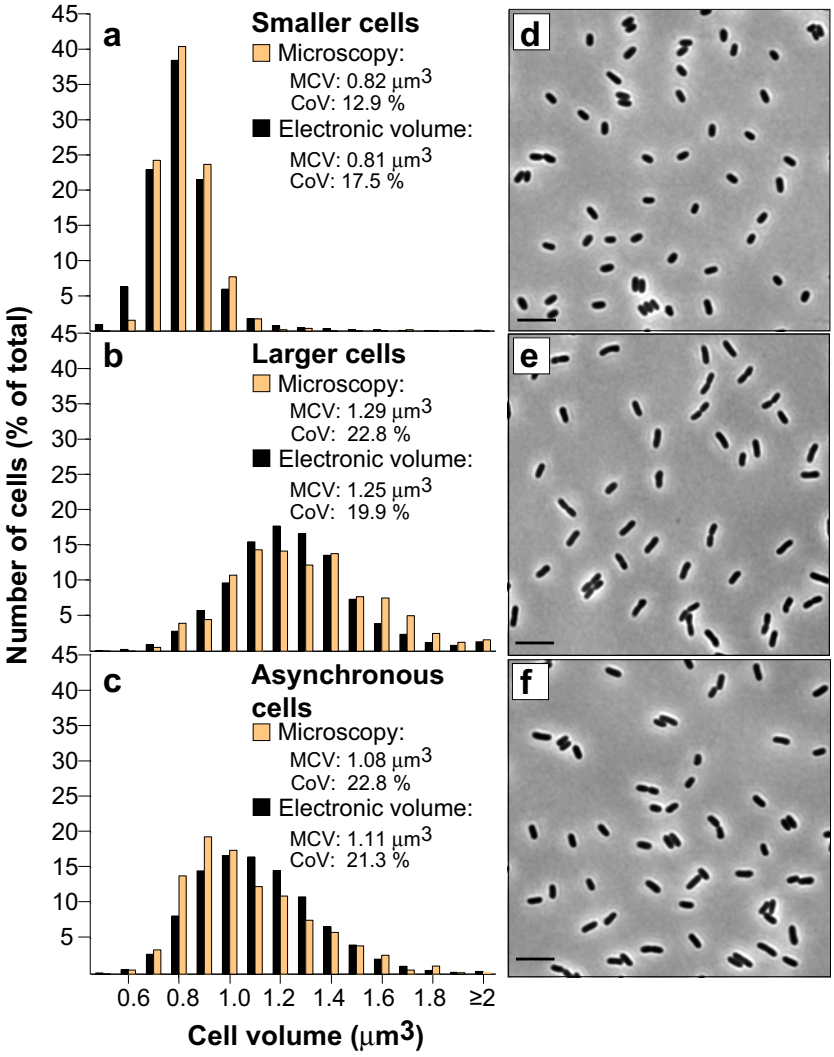

Figure 2-7: **Genetically identical cells can be separated into many fractions with different mean cell volumes.** Asynchronous cultures of stationary phase *E. coli* MG1655 were sorted using counterflow centrifugal elutriation (Methods). The distribution of cell volumes obtained by microscopy (n > 500) and electronic (n > 10,000) measurements are shown for representative small **(a)** and large **(c)** fractions, as well as for the starting asynchronous population **(e)**. Representative phase contrast pictures **(b, d, f)** are shown to the right of the corresponding volume distributions. The black bar at the bottom right corner of each image represents a length of 5 μm. MCV = mean cell volume; CoV = coefficient of variation.

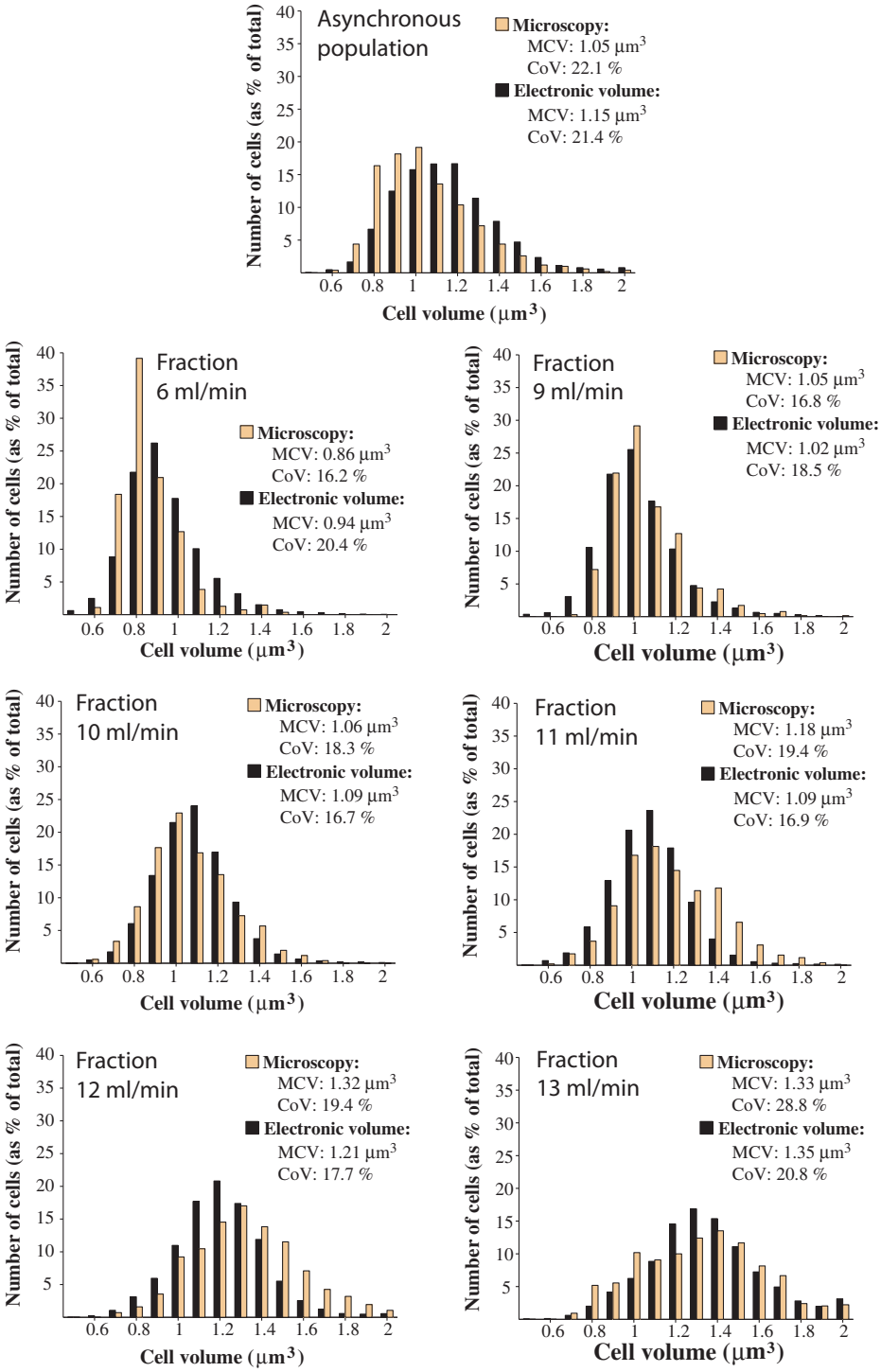

Figure 2-8: **Volume histograms of elutriated fractions of Figure 2-11 (p.53), squares series**

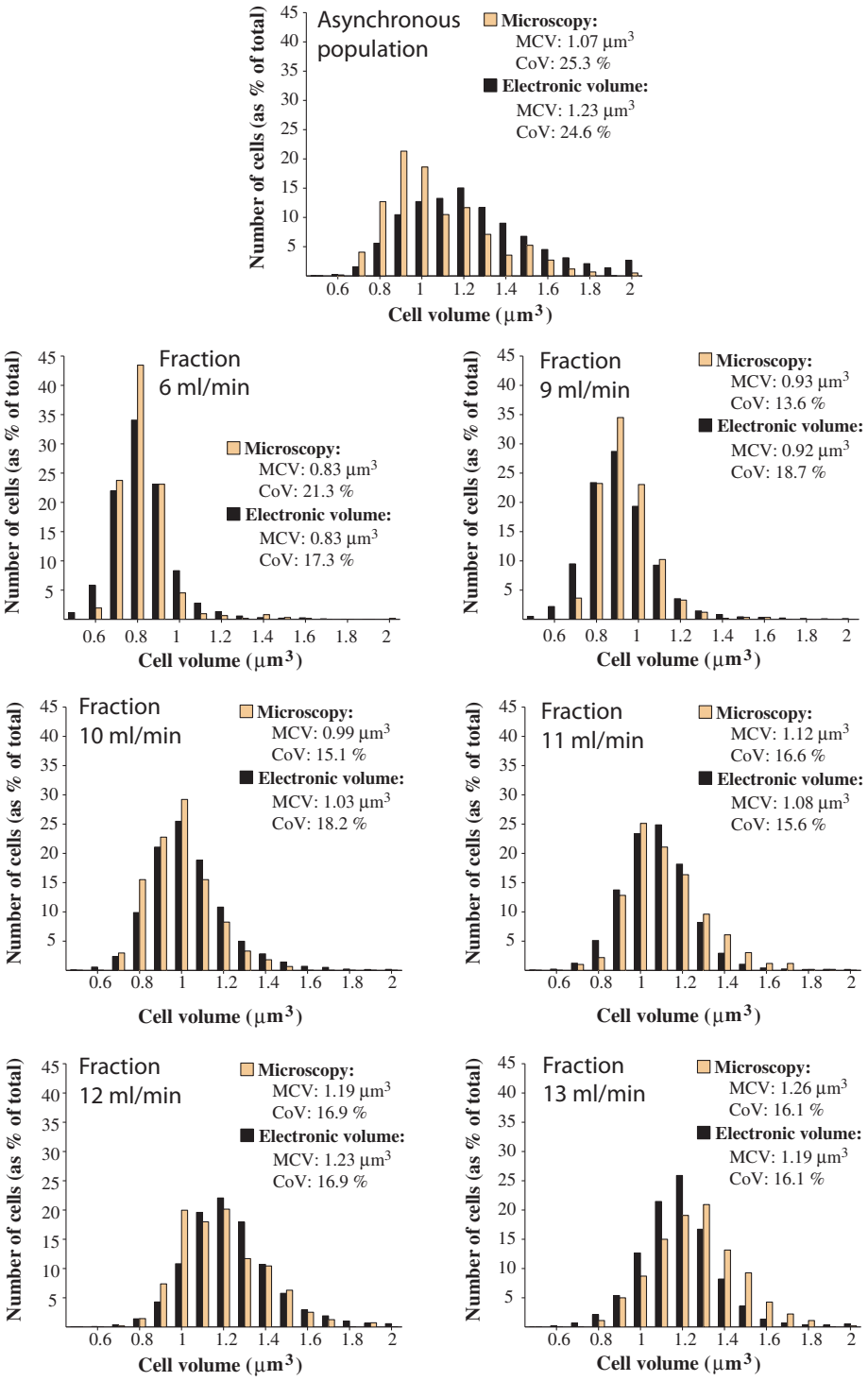

Figure 2-9: **Volume histograms of elutriated fractions of Figure 2-11 (p.53), triangle series**

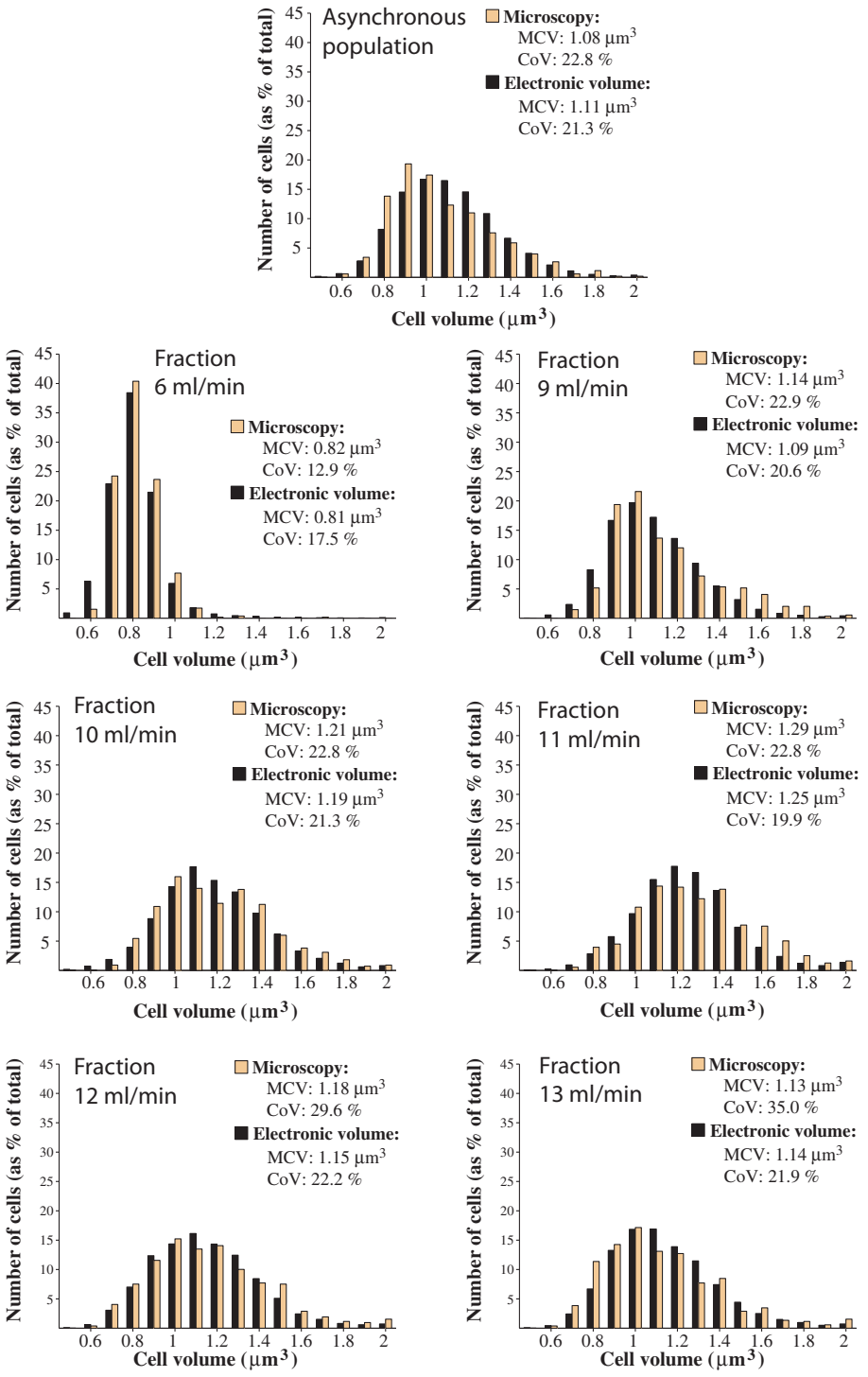

Figure 2-10: **Volume histograms of elutriated fractions of Figure 2-11 (p.53), circles series**

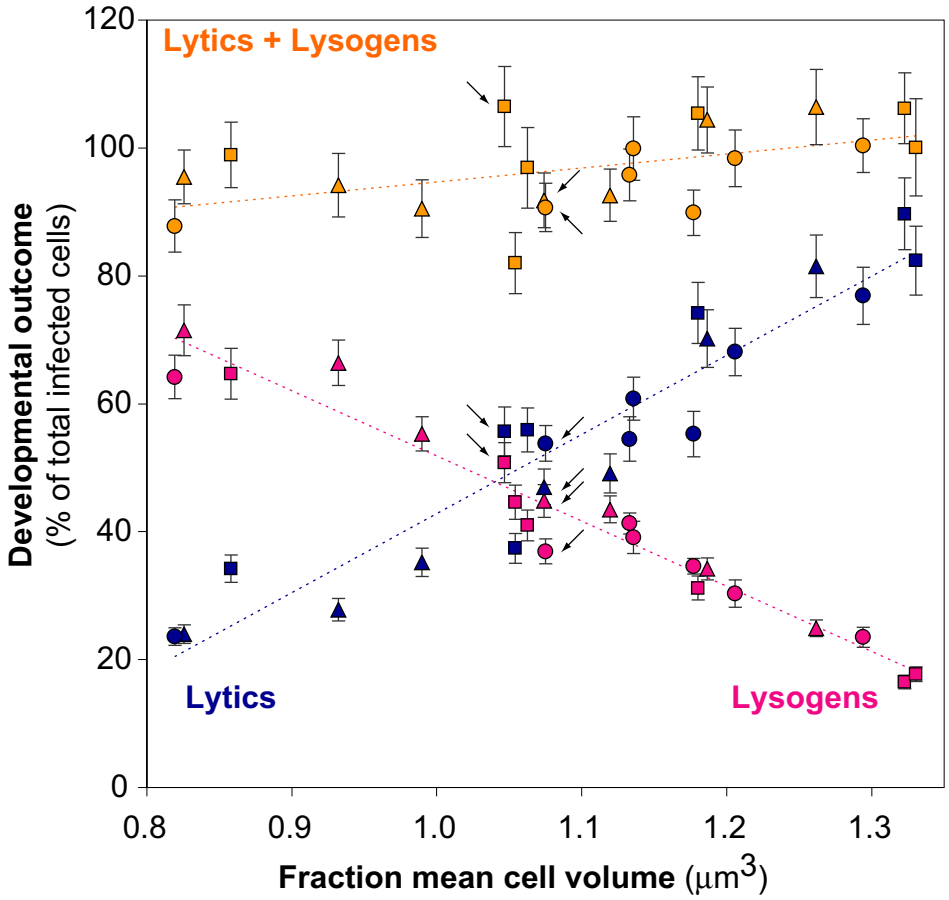

Figure 2-11: **Physical variation can be used to predict the lysis-lysogeny decision (population measurements of stationary phase MG1655 cells).** Independent measurements of the fraction of lytic events and lysogeny as a function of the mean cell volume for different cell fractions. Developmental outcome is expressed as a percentage of an independent measure of the total number of infected cells for each fraction. Circles, triangles, and squares depict fractions collected from independent experiments. The three starting asynchronous (unfractionated) cultures are also shown (arrows). Error bars depict the Poisson standard error of the mean from plating. Dashed lines depict linear regression lines for percentage lysis and lysogeny, and the sum of lytic events and lysogens.

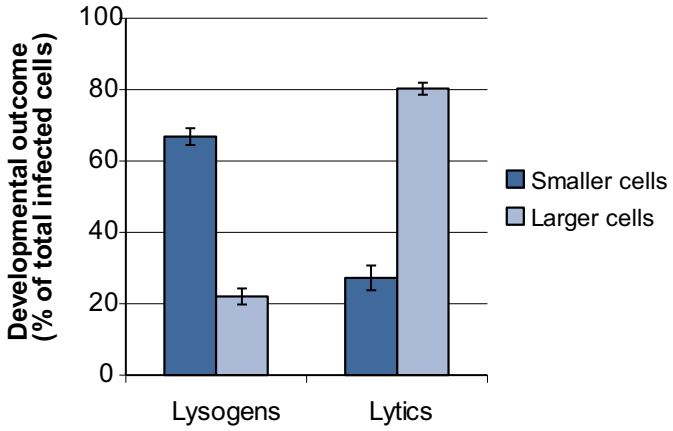

Figure 2-12: **Comparison of developmental statistics of fractions of smaller and larger infected cells.** From the fractions illustrated in Figure 2.9, I further analyzed three small MCV fractions and three large MCV fractions. Each group was composed of fractions obtained from independent cultures. The small MCV fractions gave an average of 66.8% lysogeny, over 3 times the percentage lysogeny observed in the large MCV fractions, 22.0% (p=0.002, 2-tail paired t-test). The same fractions gave a corresponding change in frequency of lytic events: I observed 27.3% lytic events in the small MCV fractions compared to 80.3% in the large MCV fractions (p=0.003, 2-tail paired t-test). The error bars represent the standard error of the mean of three independent fractions.

non-growing cells across the different fractions used. To do this, I followed via microscopy over 250 cells from both a low MCV fraction (0.83 μm^3 MCV; 71.5% lysogeny) and a high MCV fraction (1.26 μm^3 MCV; 24.9% lysogeny). In both cases more than 98% of observed cells grew and divided.

Since cells were incubated for 45 min at 30°C in liquid medium between phage adsorption and plating (above), cell division or lysis could have occurred during this period, potentially skewing the developmental outcome statistics. However, I found no increase in colony or plaque counts during this incubation period for uninfected or infected fractions at both high and low MCV, respectively (Figure 2-13, p.56; Figure 2-14, p.57). I confirmed the absence of cell division using time-lapse microscopy (data not shown). This lag in cell division may result from my use of stationary phase cells.

Finally, my experiment used unpurified stocks of phage lambda. However, I confirmed that a correlation between volume and fate of infected cells is also observed with purified phage stocks (See section 3.2, p.64).

My initial results therefore strongly suggested that host volume immediately prior to

infection can be used to predict the fate of lambda infected cells: larger cells tend to lyse, while smaller cells tend to become lytic.

2.5 Critical volume analysis

No cell fraction obtained via the elutriator and plating method produced 100% lysogens or 100% lytic events (Figure 2.9). However, each elutriated fraction was comprised of cells spanning a range of volumes (Figure 2-7,49; Figure 2.8). Thus, I was unsure if the occurrence of both lysis and lysogeny in each fraction might be due to stochastic processes intrinsic to infection within individual cells, or to remaining pre-existing extrinsic differences in cell volume (or another variable) that were beyond the segregation capabilities of my elutriation method.

Given the observed sensitivity to pre-existing differences in cell volume, I was particularly curious if volume at the time of infection might entirely account for the eventual fate of infected cells. To quickly consider this possibility I used a single parameter abstract "all-or-none" model to posit that any cells smaller than a "critical volume" might produce a lysogen, while any larger cell would undergo lysis (Figure 2.13a). I then used this critical volume model to analyze data obtained by elutriation and plating. Specifically, I compared the observed frequency of lysogeny to the frequency of lysogeny that would be predicted using the all-or-none model, fitting for the best critical volume across all cell fractions. The best-fit critical volume model (1.04 m3) is a good predictor (r^2=0.93, $p < 1E\text{-}04$) of observed cell fate (Figure 2.13b).

For comparison, I also calculated a critical volume for each fraction independently by determining the volume at which the percentage of cells of lesser volume is equal to the observed probability of lysogeny in that fraction. For example, the observed percentage lysogeny for the indicated fraction (Figure 2.13c, arrow) is 17.7%, and the critical volume for this fraction is determined as the volume for which 17.7% of the cells are of lesser volume (1.02 μm^3). From this complementary analysis I observed that the critical volumes across all MCV fractions were concentrated within a range of cell volumes that are much narrower than the volume distribution of the starting asynchronous population.

To be clear, my mathematical analysis does not conclusively establish a critical volume all-or-none model, nor reveal anything about molecular mechanisms that would underlie

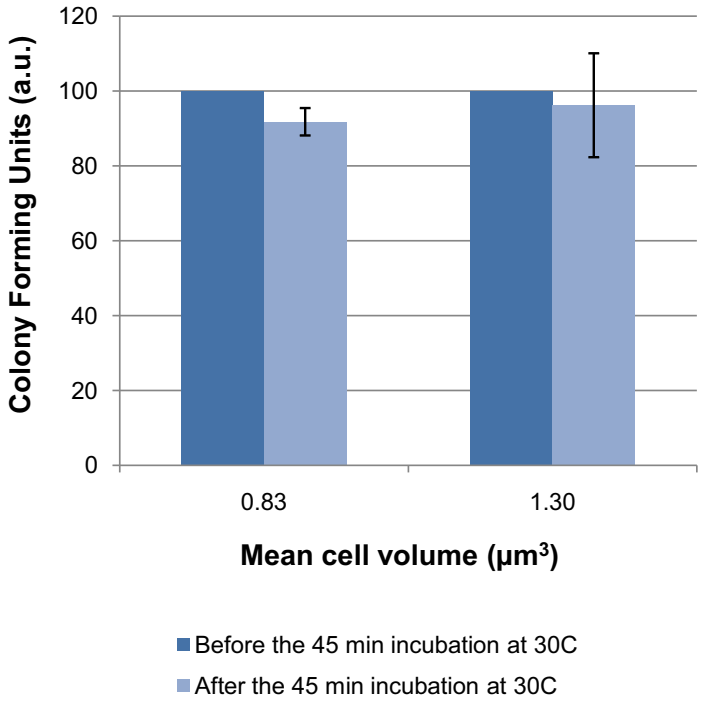

Figure 2-13: **The total number of cells does not increase during the 45-minute incubation step between adsorption and plating.** I grew and size-fractionated three independent cultures of bacterial cells. For each culture, I selected the fraction with the smallest mean cell volume (MCV) and the fraction with the largest MCV. To replicate experimental conditions of my usual infection protocol (except for the addition of phages), I resuspended cells in TB supplemented with 10 mM $MgSO_4$, incubated them at 4℃ for 30 minutes and diluted them in TB pre-warmed to 30℃. Cells were then plated on TB agar either immediately following dilution, or after a 45-minute incubation at 30℃ with aeration in a roller drum. Plates were incubated at 30℃ for ∼18 hours and scored for colony forming units (CFUs). For each experiment and each fraction, the number of CFUs obtained after the 45 min incubation period was normalized to the value obtained when cells were plated before incubation. The error bars represent the standard error of the mean of those three independent experiments. The values given for the mean cell volume represent the mean of the MCV of three fractions.

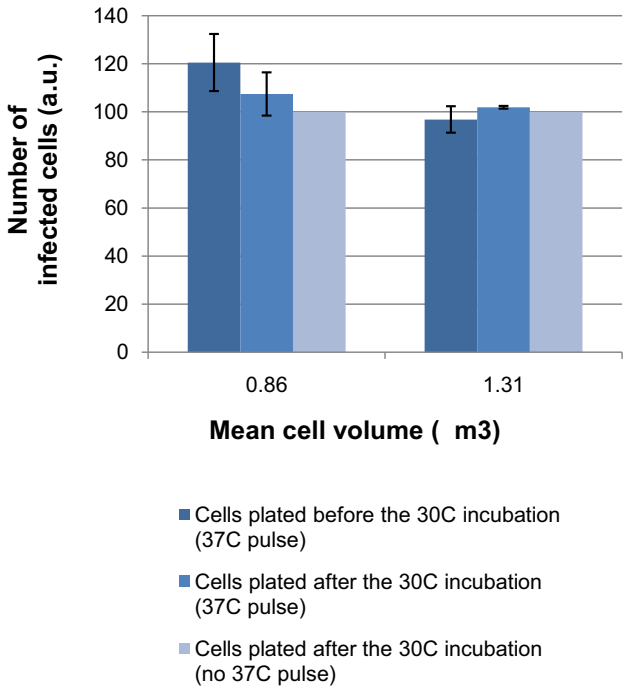

Figure 2-14: **The total number of infected cells does not change during the 45-minute incubation step between adsorption and plating.** I grew and size-fractionated a culture of bacterial cells. The fraction with the largest mean cell volume (MCV) and the fraction with the smallest MCV were infected with λ *c*I857 *bor*::*KanR*. After the usual adsorption step (30 min, 4℃), cells from each fraction were split into three treatment groups. Some cells were submitted to a 5-min pulse at 37℃ and plated either immediately (Condition A), or after the usual 45-min incubation at 30℃ (Condition B). The 37℃ pulse was performed to ensure phage DNA ejection prior to plating [?], thus avoiding potential effects of plating conditions on DNA entry probability. Cell treated exactly as described in Supplementary Methods (i.e. 45 min incubation at 30 C but no 5-min pulse at 37℃) were also plated (Condition C). Infected cells were scored as plaque forming units (PFUs) on plates incubated at 42℃. The error bars represent the standard error of the mean of three replicate experiments performed using cells from the same fraction. For each replicate experiment, the number of PFUs obtained in Conditions A and B was normalized to the number of PFUs obtained from Condition C.

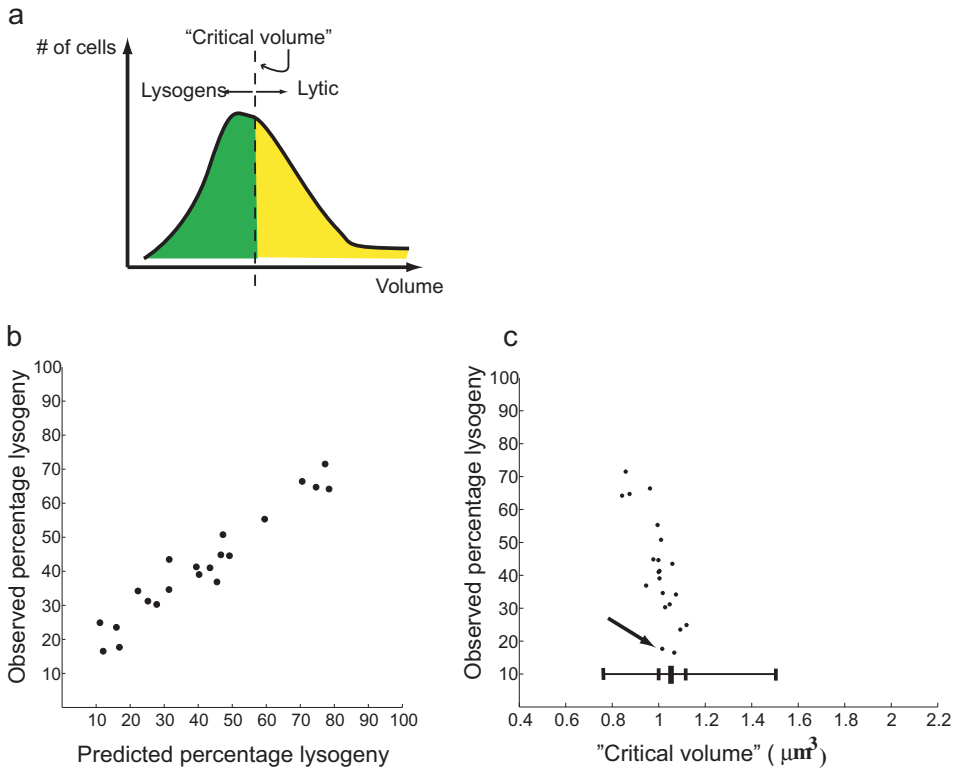

Figure 2-15: **"Critical volume" analysis. a,** Cartoon representation of my concept of "critical volume". In this simple hypothesis, all cells greater than this critical volume become lytic, while all cells smaller than the critical volume become lysogens. **b,** Correlation between the observed frequency of lysogeny obtained by experimentation, and the percentage lysogeny predicted by my critical volume model. Each data point represents one of the 21 fractions analyzed in Figure 2.9. **c,** Fraction-specific "critical volumes". The horizontal bar: the center dash represents the mean, 10% of the population fall within the inner dashes, and 90% within the outer dashes. Most critical volume points fall within the inner dashes.

such behavior. However, it suggests that my cell fraction data is not grossly or obviously inconsistent with an all-or-none deterministic model for lambda infection (Figure 1.6b) in which cells smaller than a putative critical volume ($\sim$1 μm^3) will become lysogens. My analysis also highlighted the need to develop experimental methods for directly exploring the correlation between host volume and ensuing cell fate at the single cell level, the topic of the next Chapter.

2.6 Chapter summary

Re-interpretation of experiments by Lieb, Kourilsky and others [54, 86, 93, 105] motivated the selection of cellular volume as a possible predictor of cell fate. I developed and optimized methods of counterflow centrifugal elutriation to size-fractionate asynchronous populations of *E. coli* cells. Results obtained with cultures of stationary phase cells show that physical variation present prior to infection can control the fate of lambda infected cells: smaller cells tend to become lysogens, while larger cells tend to follow lytic growth.

Chapter 3

Host volume is a predictor of the lambda lysis-lysogeny decision, single-cell microscopy measurements

In Chapter 2, I demonstrated that host volume can be used to predict the fate of lambda infected cells. In this Chapter, I present the development and utilization of a microscopy platform to study lambda infection at the single cell level. I wished to develop this platform for two primary reasons. First, I wanted to confirm the results of Chapter 2 using a different method to observe cells of different volume and determine cell fate selection statistics. Second, to quantify, at the single cell level, the extent to which host volume is correlated with the fate of lambda infected cells.

3.1 Design and construction of λ *A*am19 *b*::*GFP* *c*I857

3.1.1 Designing a phage strain for single-cell microscopy

Detecting all infected cells using a phage-encoded GFP cassette

I first set out to replicate the experimental conditions described in the previous Chapter, namely infection of MG1655 grown to stationary phase in tryptone broth (TB). As in Chapter 2, I controlled the multiplicity of infection (MOI) by using a low average number (0.03) of phage per cell. Lytic events can be simply detected using brightfield microscopy due to cell lysis. However, I needed a method to distinguish lysogens from uninfected cells. To detect all infected cells, including lysogens, I integrated into the lambda genome a cassette that results in the constitutive expression of the green fluorescent protein. The cassette was inserted in the "*b*" region of phage lambda [30], a region not thought to play a role in the lambda lysis-lysogeny decision. I considered alternative methods of detection such as those further described in Chapter 6. However, I chose the phage-encoded GFP cassette method because it is relatively simple and less likely to significantly perturb lambda regulatory network.

Using an amber mutation in gene *A* to prevent re-infection of lambda infected cells

I wished to avoid complications arising from re-infection of infected cells by the progeny of neighboring cells which underwent lysis. To this end, I introduced an amber mutation in gene *A* (*A*am19 allele) into λ *b*::*GFP*. The *A* gene encodes an essential phage DNA packaging enzyme [48] not thought to be involved in the cell fate selection process. Strains which do not suppress the amber mutations, such as those used in my experiments, can still lyse because the phage-encoded holin-endolysin system for host cell lysis (genes *R* and *S*) remains intact. Importantly, lysed cells only release empty (uninfectious) lambda particles, thus preventing re-infection.

To allow a simpler detection of *A*am19 mutants, I engineered a *c*I857 mutation onto λ *b*::*GFP* prior to engineering the *A*am19 mutation (see construction section below). The

*c*I857 allele results in fully active CI repressor at temperatures of $< \sim$32℃, but non-functional CI at temperatures $> \sim$40℃ [165].

At 40℃-42℃, λ *A*am19 *c*I857 mutants produce clear plaques when plated on an amber-suppressor strain (e.g. C600) but cannot be propagated on non-suppressor strains(e.g. MG1655). They are thus easily distinguished from the A^+ *c*I857 parental strain which forms clear plaques when plated on either strain [132]. The details of the construction of λ *A*am19 *b*::*GFP* *c*I857 are presented below:

3.1.2 Construction of λ *A*am19 *b*::*GFP* *c*I857

Recombineering of a GFP cassette onto lambda genome

I first selected a GFP cassette from pSB3K3-I20115 [1], a plasmid constructed by Heather Thompson and Matt Gethers in my laboratory. When using the primers described below for PCR amplification, the resulting GFP cassette contained the following critical elements:

1. BBa_E0040 [1], a BioBrick^{TM} version of the bright GFP variant *gfpmut3b*, with a strong ribosome binding site (RBS) from phage T7 gene 2.0. BBa_E0040 was driven by a strong, LacI-repressible promoter BBa_R0011 [1]. In the presence of IPTG or in a Δ*lacI* strain, this cassette produces GFP constitutively, as desired for my application.

2. The kanamycin resistance marker from the plasmid, to allow selection for phage carrying the GFP cassette.

3. Two terminators, BBa_B0015 and the *E. coli his* operon terminator, separating *gfp* from the kanamycin marker.

I first PCR-amplified the above mentioned GFP cassette using primers containing 20 bp of homology to the GFP cassette and 48-50 bp of homology to lambda *b* region:

- Forward primer:
  5'-aggcagcaaaatcatcagaaacgaacgcatcatcaagtgccggtcgtgca-
  aactttatccgcctccatcc-3'

- Reverse primer:
  5'-ccgtatccttcacccaggctgtgccgttccacttctgatattcccctcc-

cgtgaagaaggtgttgctga-3'

I used ethanol purification to desalt and concentrate my PCR product, and performed membrane dialysis for further desalting. I performed recombineering on an infectious lambda wild-type particle using the recombineering strain DY380 and published methods [169]. To select for recombinants, I infected MG1655 cells grown to stationary phase with the recombineering lysate and plated on LB supplemented with 20 μg/ml kanamycin. Putative λ *b*::*GFP* lysogens were confirmed by PCR and fluorescence microscopy. Stocks of λ *b*::*GFP* were derived from these lysogens using standard methods [65].

The resulting phage contained the 2,662 nt GFP cassette integrated into the *b* region [30] of the phage genome, replacing the wild-type lambda sequence between lambda coordinates 20430-22278 and producing a phage whose genome is only slightly longer (813 nt or 1.7%) than wild-type λ. The added sequence is well within the range giving efficient DNA packaging [49]. I reconfirmed the presence of the cassette on the phage by fluorescence microscopy and by DNA sequencing.

Recombineering *c*I857 and *A*am19 onto λ *b*::*GFP*

I next engineered the *A*am19 (C→T at lambda coordinate 1917) and *c*I857 (C→T at lambda coordinate 37742) mutations onto λ *b*::*GFP* using published methods of recombineering using single stranded oligonucleotides [132, 169]. I identified recombinants by plaque morphology and confirmed the presence of the mutations by DNA sequencing and fluorescence microscopy.

3.2 Host volume is a predictor of the fate of single lambda infected cells

The newly constructed phage strain, λ *A*am19 *b*::*GFP* *c*I857, produces bright fluorescence upon infection, allowing easy detection of infected cells. I performed single cell experiments using the same bacterial strain and culture conditions as previously used in the elutriation and plating experiments (wild-type *E. coli* grown to stationary phase in TB). I infected cells at low multiplicity (average phage:cell ratio of ~0.03) and recorded time-lapse movies via automated fluorescence and brightfield microscopy. For all single cell experiments men-

tioned in this thesis, the phage:cell ratio was determined directly by counting the number of infected (i.e. GFP expressing) cells and the total number of cells. The phage:cell ratio was approximately what was expected given the number of phage added, and the number of unadsorbed phage which I removed by centrifugation prior to imaging (data not shown).

I determined the cell size of infected cells by direct manual measurement of cell length of the first frame of each time-lapse movie. Cell size could also have been measured using the movie frame where GFP fluorescence is first detected. However, such a method would result in measurement bias if either:

1. fluorescence is detected at different times in cells fated to become lysogens compared to cells fated to produce lytic events, or:

2. the lysogeny and the lytic pathway differentially impact cell growth prior to appearance of GFP. If true, differences in volumes between cells fated to become lytics and cells fated to become lysogens may be caused by the chosen pathway, rather than being a true predictor of cell fate.

Measurements of cell lengths were converted into measurements of cell volume as described in Section 2.3.4 (p.45).

I established cell fates as described in Figure 3-1 (p.66). Briefly, I scored an infection as a lytic event when a GFP-expressing cell or both of its daughters lysed. I did not observe any instance of lysis in cells that did not previously express GFP. An infected cell was presumed to be a lysogen when it survived the infection, producing two daughters which also divided. Stable lysogeny requires integration of lambda DNA into the host chromosome [131]. While my system did not allow me to determine whether integration took place, the overall cell fate selection statistics from my microscopy experiments were equivalent to those obtained via my elutriation and plating method (see later).

In a minority of cases, I observed an infected cell giving rise to two daughters, one which lysed and one which survived and divided; such events were scored as 'mixed fate'. In some 'mixed fate' events, fluorescence appeared to decrease as the surviving cell grew and divided. Perhaps such loss of fluorescence is due to changes in growth conditions as the agarose pad became crowded and cells presumably left exponential phase. Increased number of cells may also reduce accessibility of IPTG, which is required to induce expression from the GFP cassette (see 3.1.2, p.63). An alternative possibility is that the surviving cell and

Cell fates			Classification	% of total (counts)
Infected cell	Daughters of infected cell			
	Daughter A	Daughter B		
Lyses	n/a	n/a	Lytic event	55.6 (175)
Divides	Lyses	Lyses	Lytic event	0.3 (1)
	Lyses	Divides	Mixed fate	5.1 (16)
	Divides	Divides	Lysogeny	39.0 (123)
				100 (315)

Figure 3-1: **Cell fate selection statistics via time-lapse microscopy, stationary phase MG1655 cells.** Cultures of MG1655 were grown to stationary phase in tryptone broth and infected at low API (phage:cell, ∼1:30) with λ *A*am19 *b*::G*FP* *c*I857. The developmental outcome of infected (GFP-expressing) cells and, if applicable, their daughter cells, was monitored by time-lapse microscopy. The "classification" column outlines my mapping of developmental outcomes (lysis or division) of infected cells to overall cell fate outcomes. In some cases, the fate of an infected cell or one or both of its daughters could not be determined either because (1) the cell moved out of the field of view or became obscured by neighboring cells, (2) the cell did not divide or lyse before the end of the time-lapse movie. Such ambiguous cases were not included in this table or in any analyses.

its progeny somehow remained uninfected. A direct reporter of lysogeny, such as a reporter of integration, would help distinguish between these hypotheses.

The percentage lysogeny from my microscopy experiments (41.1%) closely matched that obtained via my elutriation and plating method (44.2±4.0% S.E.M). The majority of infected cells which divided produced lysogens (123 of 140). Interestingly, a minority of infected, dividing cells (16 of 140) produced offspring that obtained distinct cell fates - one daughter cell lysed while the other formed an lysogen or continued to grow and divide. I also observed one case in which a cell appeared to have divided, giving rise to daughters that both gave a lytic response.

I estimated the initial size of each infected cell by measuring cell length immediately following infection. I combined the initial cell size and cell fate data in order to determine to what extent the size of individual cells predetermines cell fates. Consistent with my

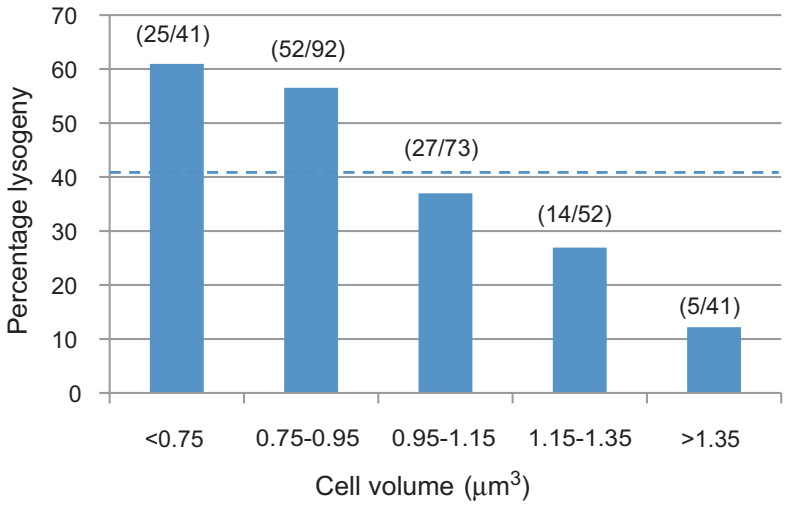

Figure 3-2: **Physical variation can be used to predict the lysis-lysogeny decision (single cell measurements of stationary phase MG1655 cells).** Probability of lysogeny as a function of the length of individual MG1655 grown to stationary phase. The numbers in parentheses represent the number of lysogens over the total number of infected cells within each volume bin. The dashed lines correspond to the average percentage lysogeny.

elutriation-based results, I observed that in individual stationary phase cells the probability of lysogeny is greatest in the smallest cells (p=0.61) and decreases with increasing cell size (p=0.12) (Figure 3-2, p.67). While volume was a predictor of cell fate, I did not find a "critical volume" below which all cells became lysogens, and above which all cells produced lytic events.

Phage stocks used in my microscopy and elutriation experiments were unpurified; my results might therefore be an artifact of some component present in my phage stocks. To test this possibility, I purified a stock of λ *A*am19 *b*::G*FP* *c*I857 by differential sedimentation and isopycnic centrifugation in CsCl gradients, using standard protocols [11]. Using this purified phage stock, I infected one culture of MG1655 grown to stationary phase in TB, and found that volume remained a predictor of cell fate. For example, the average volume of lysogens (count=22 cells) was 0.84 μm^3, while the average volume of lytics (count=89 cells) was 1.16 μm^3. For comparison, in the experiments shown in Figure 3-2 (p.67), the average volume of lysogens was 0.92 μm^3 (count=123 cells) while the average volume of lytics was 1.11 μm^3 (count=176 cells). For all data points presented above, the standard

error of the mean is $<0.03\ \mu m^3$. This control experiment suggests that the presence of a correlation between the volume and fate of infected cells is not due to a component present in my phage stocks. However, purification of phage stocks might affect the strength of the correlation; additional experiments would be needed to determine whether this may be the case.

3.3 Chapter summary

I constructed a specialized phage strain to observe lambda development at the single cell level. This strain produces GFP during infection, thereby identifying infected cells. Moreover, it is unable to produce infectious virion progeny, avoiding complications from reinfection of the initially infected cells. Results obtained with cultures of stationary phase cells confirm the main result of Chapter 2: following infection, smaller cells tend to become lysogens, while larger cells tend to follow lytic growth. Cell volume has thus been shown to be a marker of cell fate using two different methods of observing cells of different volumes and quantifying cell fate statistics (Chapter 2 and this Chapter). Volume does not appear to be a perfect predictor of cell fate. Other variation, arising before or during infection, must therefore play a role in regulating the lambda lysis-lysogeny decision.

3.4 Chapter acknowledgments

Felix Moser (Endy lab) introduced the *c*I857 marker into λ *b*::*GFP* by recombineering with single-stranded oligos (Section 3.1.2, p.64).

Chapter 4

Identification of host-encoded determinants of lambda's "volume sensor"

In Chapters 2 and 3, I presented experimental support to the hypothesis that the volume of stationary phase cells can be used to predict their fates following lambda infection: larger cells tend follow the lytic pathway, while smaller cells tend to become lysogens. How might the lambda regulatory network sense host volume (or a correlated cell parameter)? The the lambda lysis-lysogeny decision circuit includes both phage- and host-encoded components [53, 65, 131]. I now describe ongoing efforts to identify host (this Chapter) and phage (Chapter 5) determinants of lambda's apparent volume sensitivity. More specifically, in this Chapter, I first demonstrate that host volume can be a marker of cell fate for both stationary and exponentially growing cells. Lambda is thus unlikely to "sense" volume via a host factor present exclusively during stationary phase. I then consider whether lambda might be responsive to cell cycle position rather than host volume, and describe how these two host parameters may be decoupled.

4.1 Is lambda's sensitivity to host volume specific to stationary phase?

Stationary phase cultures are known to be particularly heterogeneous. For example, dilution of late stationary phase cultures into fresh medium can produce a subpopulation of cells which start dividing, and another subpopulation with cells which do not [151]. Heterogeneity in stationary phase is also observed when cells remain in the same medium. For example, Makinoshima and colleagues were able to fractionate stationary phase cultures into more than 10 subpopulations based on their buoyant densities and expression of stationary phase promoters [117].

Lambda may be responsive to heterogeneity within a population of stationary phase cells given its strong sensitivity to the physiological condition of the host cell (see Section 1.2, p.20). For example, Pearl *et al.* recently investigated whether persister bacterial cells are protected from phage infection and induction [135]. Persisters are cells that can survive a temporary antibiotic exposure; unlike antibiotic resistant cells, their progeny are sensitive to antibiotics. Type I persistent bacteria, which can arise during stationary phase [16] to form ∼1% of the population [81], were found to be protected from prophage induction. However, persisters were not protected from infection. The authors did not investigate whether the persistence state impacts the lysis-lysogeny decision, and whether there is a correlation between the size of a cell and its ability to persist. Nevertheless, the results of Pearl and colleagues suggest that lambda can be sensitive to phenotypic variability arising during stationary phase.

Given that cells become smaller as they approach and advance within stationary phase [3], smaller cells within a culture may tend to be those which have progressed further within stationary phase and may be phenotypically different from larger cells. Lambda may sense and respond to such variability by producing different outcome statistics that are correlated with such cell-cell physical variation. This "starvation stress" model leads to a strong, testable claim - lambda sensitivity to host volume is specific to stationary phase. Using two approaches, I collected evidence inconsistent with the "stationary stress model":

- I show direct evidence that host volume can be a predictor of the fate of exponentially growing cells (section 4.1.1, p.71)

- I describe the development of a single-cell reporter of stationary phase stress. I found no correlation between cell size and the signal from this reporter (section 4.1.2, p.75)

4.1.1 Variation in the volume of exponentially growing cells is correlated with lambda developmental outcome

Raising the frequency of lysogenization of exponentially growing cells

To directly test the starvation stress model, I set out to consider whether host volume is a marker of cell fate not only in conditions of starvation, but also in conditions where cells are growing exponentially. Unfortunately, and as stated previously, cells in early exponential phase and infected at MOI=1 typically only adopt the lytic pathway.

To raise the frequency of lysogeny to observable levels, I considered three approaches. First, because lambda developmental outcome statistics are sensitive to nutritional conditions [93, 96, 105], I tried to raise the frequency of lysogeny by using a poor medium: I grew MG1655 cells to low density (OD600∼0.07, Shimadzu UV160U) in M9 medium [153] supplemented with 0.5% acetate as the sole carbon source. In these conditions, MG1655 grows with the very slow doubling rate of 4.5-5 hrs at 30°C. I determined the frequency of lysogeny as described previously (see Section 2.2.2 on p.37), except that the recovery was performed in M9 acetate for 1 hour. From this single pilot experiment, I obtained a frequency of lysogeny of 3.5%. I also measured cell fate statistics by single cell microscopy at low MOI (∼0.03) with λ *A*am19 *b*::*GFP* *c*I857. I removed free phage and performed time-lapse microscopy as described in Chapter 3, except that I used 2% LMP agarose supplemented in M9 acetate (rather than TB). All ∼50 cells observed lysed, suggesting a frequency of lysogeny of $< 2\%$. Given the low number of cells observed in this experiment, this result is not grossly inconsistent with the frequency of lysogeny obtained using the plating method (3.5%).

A frequency of lysogeny of ∼3.5% (and possibly lower) was determined too low to do microscopy experiments. As explained in previous Chapters, I wanted to keep the frequency of cells infected at MOI ≥ 2 small compared compared to the frequency of lysogeny. For example, and assuming a Poisson distribution of phage onto cells [37], an infection at a phage:cell ratio of ∼1:143 would result in ∼0.35% of infected cells being infected at MOI ≥ 2, which is small (10-fold lower) than the overall frequency of lysogeny. However, this

would result in only one lysogen every 4086 cells (infected or not), making it very difficult to obtain sufficient data by microscopy to generate statistically significant results.

I also considered increasing the frequency of lysogeny by infecting cells at a higher multiplicity of infection (MOI). However, given that cell fate statistics are sensitive to MOI, this strategy requires a reporter of MOI so that only cells infected by the same number of phage can be compared. Because of the potential importance of a system to count phage particles, and because of the large number of techniques tested or considered, ongoing efforts to develop a reporter of MOI are discussed separately (Chapter 6).

Because of the difficulty in developing conditions or technology to obtain a high fraction of lysogeny in wild-type strains, I next considered *E. coli* mutants giving the high frequency of lysogeny (*hfl*) phenotype. Certain mutants, such as MA150 (*hflA*150) [74], resulted in abnormal morphology upon infection with lambda (data not shown); other mutants resulted in significant decreases in cell growth rate (e.g. *hflB* and *hflD* mutants). *hflK*::*kanR*, *hflC*::*kanR* and *hlfX*::*kanR* mutants from the Keio collection [15] grew at rates similar to the parental wild-type strains and did not produce aberrant morphology during lambda infection (e.g. Figure 4-1, p.73). HlfK and HflC are membrane proteins that regulate the activity of FtsH/HlfB, the main protease degrading lambda CII (Chapter 1). Deletion of these loci is therefore expected to stabilize CII, but not to change the dynamics of lambda gene expression during infection. Because the role of HlfX is not known, I was hesitant to select *hflX*::*kanR* as host strain. The remaining two strains from the Keio collection were equally suitable; I chose strain JW4132 (Coli Genetic Stock Center # 10975, genotype: F^- *lambda*$^-$ *rph*-1 Δ(*araD-araB*)567 *lacZ*::*rrnB-3* Δ(*rhaD-rhaB*)568 ***hflK*::*kanR***) for further experimentation.

Preexisting variation in the volume of exponentially growing cells correlates with cell fate outcomes

I diluted overnight cultures of JW4132 in M9GlyM + 10 μg/ml kanamycin and grew them at 30℃ with vigorous shaking to OD600 ∼ 0.07 (UV160U spectrophotometer, see above). M9GlyM is M9 [153] supplemented with 0.4% glycerol, 0.2% maltose, 2 mM $MgSO_4$ and 0.1 mM $CaCl_2$. I diluted the culture 1000-fold in fresh M9GlyM supplemented with 1 mM IPTG (to induce GFP expression following infection with λ *A*am19 *b*::*GFP c*I857) and grew the culture back to OD600 ∼ 0.07.

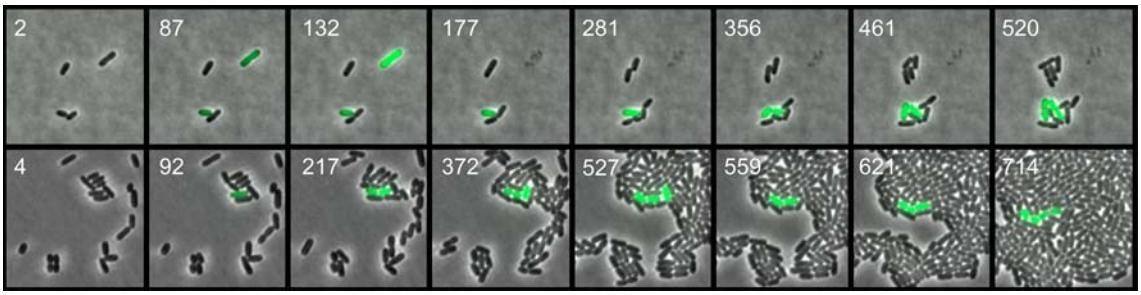

Figure 4-1: **Filmstrips of phage infection of single *hflK*$^-$ cells.** Images from time-lapse movies of exponentially growing JW4132 (*hflK*$^-$) cells infected at a phage:cell ratio of ∼1:30 with a lambda strain carrying a fluorescent reporter expression cassette. Numbers indicate the number of minutes at which the images were taken after the start of each movie. Top row: two neighboring cells are infected, each presumably at a multiplicity of one, and both cells turn green over time. The upper-right infected cell is larger and near the end of its cell division cycle, as indicated by the presence of a membrane invagination (developing septum) at mid-cell. This cell lyses between t=132 and t=177. The lower-left infected cell, which is presumably the product of a recent cell division event and is relatively small, continues to progress through a typical cell division cycle. The infected cell was presumably lysogenized by lambda as it survives the infection, producing viable progeny which also divide between t=461min and t=520min. Bottom row: an infected cell produces daughter cells with apparently distinct fates: the rightmost daughter lyses between t=527 and t=559min, while the leftmost daughter divides around t=372, producing progeny which themselves divide around t=714 min.

I concentrated cells 10-fold in TM (10 mM Tris-Cl, pH 7.5, 10 mM $MgSO_4$) and infected cells with λ *A*am19 *b*::*GFP* *c*I857 at a phage:cell ratio of ∼1:30. After 30 min at 4℃ for adsorption of phage onto cells, I removed unadsorbed phage by centrifugation and spread cells on M9GlyM + 1 mM IPTG + 2% LMP agarose pads. I incubated the cells in a microscope heating chamber set to 30℃, taking phase contrast and GFP fluorescence images (75 ms) every ∼ 15 minutes for at least 11 hours at 60-100x magnification.

Most infected cells lysed (382 of 449), with the majority of the remaining cells producing lysogens (54 of 67). Figure 4-1 (p.73; top filmstrip) presents an example filmstrip showing two infected cells: one cell produces a lytic response while the other cell survives the infection as a presumed lysogen. As with the stationary phase conditions (Chapter 3), I again observed a small number of infected, dividing cells whose offspring obtained distinct cell fates (7 of 82; and see Figure 4-1, p.73, bottom filmstrip). Complete cell fate selection statistics are provided (Figure 4-2, p.74).

As in Chapter 3, I estimated the initial size of each infected cell by measuring cell

Cell fates			Classification	% of total (counts)
Infected cell	Daughters of infected cell			
	Daughter A	Daughter B		
Lyses	n/a	n/a	Lytic event	85.1 (382)
Divides	Lyses	Lyses	Lytic event	1.3 (6)
	Lyses	Divides	Mixed fate	1.6 (7)
	Divides	Divides	Lysogeny	12.0 (54)
				100 (449)

Figure 4-2: **Cell fate selection statistics via time-lapse microscopy (single cell measurements of exponentially growing *hflK*$^-$ cells).** Cultures of JW4132 were grown to stationary phase in tryptone broth and infected at low API (phage:cell, ∼1:30) with λ *A*am19 *b*::*GFP* *c*I857. The developmental outcome of infected (GFP-expressing) cells and, if applicable, their daughter cells, was monitored by time-lapse microscopy. The "classification" column outlines my mapping of developmental outcomes (lysis or division) of infected cells to overall cell fate outcomes. In some cases, the fate of an infected cell or one or both of its daughters could not be determined either because (1) the cell moved out of the field of view or became obscured by neighboring cells, (2) the cell did not divide or lyse before the end of the time-lapse movie. Such ambiguous cases were not included in this table or in any analyses.

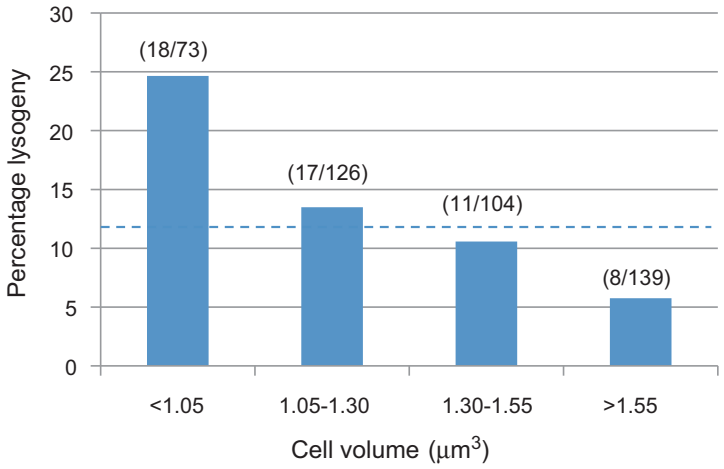

Figure 4-3: **Physical variation can be used to predict the lysis-lysogeny decision (single cell measurements of exponentially growing *hflK*$^-$ cells).** Probability of lysogeny as a function of the length of individual JW4132 (*hflK*$^-$) grown to exponential phase. The numbers in parentheses represent the number of lysogens over the total number of infected cells within each volume bin (excluding "mixed fate" cells).. The dashed line corresponds to the average percentage lysogeny.

length immediately following infection. I combined the initial cell size and cell fate data in order to determine to what extent the size of individual cells predetermines cell fates. The probability of lysogeny is greatest in the smallest cells (p=0.25) and decreases with increasing size (p=0.06) (Figure 4-3, p.75). While volume was strongly correlated with cell fate, once again I did not find a "critical volume" below which all cells became lysogens, and above which all cells produced lytic events.

4.1.2 No correlation is observed between cell size and fluorescence from a reporter of stationary phase stress

The experiments described in the first section of this Chapter were started at approximately the same time as those discussed in Chapter 3. At that time, I did not know whether I would be able to develop a platform to directly test whether host variation in the volume of exponentially growing cells impacts the lambda lysis-lysogeny decision (Section 4.1.1, p.71). I therefore decided to find a second method to investigate whether the apparent sensitivity

to host volume was specific to stationary phase. In particular, I tried to find a correlation between cell size and a marker of stationary phase, as described next.

Selection and construction of a reporter of stationary phase

Stationary phase is often accompanied and defined by large-scale changes in gene expression [128]. In narrowing the field for potential physiological variables that may impact lambda development, I considered that the stationary stress response is highly dependent on the alternative RNA polymerase sigma factor σ_s [55, 66, 128, 158]. Moreover, σ_s amount and activity is promoted by the "alarmone" ppGpp [128]. ppGpp is reported to impact the lambda pR promoter, thereby modulating the frequency of lysogeny [138, 160]. σ_s activity may therefore be a plausible marker of lambda developmental outcome.

I decided to test whether σ_s activity, as a prototypical marker of stationary phase stress, might be correlated with cell volume. I used the BioBrick^{TM} device BBa_ J45995 encoding GFP under the control of the σ_s-controlled promoter pOsmY [116, 117]. To minimize the impact of the reporter on host physiology, BBa_ J45995 was ported from a high-copy copy plasmid (pSB1AT3, pMT1 origin of replication) to a low-copy plasmid (pSB4K5 [157]). As a control, I used BBa_ I7100, where GFP is driven by the constitutive promoter BBa_R0040. BBa_I7100 was also ported to pSB4K5. I transformed both plasmids — pSB4K5-J45995[1] and pSB4K5-I7100 — into MG1655, the same strain used in the experiments described in Chapters 2 and 3. BBa_J45995, BBa_I7100, pSB1AT3 and pSB4K5 where all obtained from the Registry of Standard Biological Parts [1].

pSB4K5-J45995 is a reporter of stationary phase

I grew three independent cultures of MG1655 carrying pSB4K5-J45995 in TB to stationary phase as described in Chapter 2. At different points during growth, I spread cells on M9 agarose (2%) pads and imaged at least 300 cells per culture using phase contrast and fluorescence (50 ms exposure) microscopy. Cell size (as area on the still pictures) and fluorescence were extracted by custom Matlab (Mathworks, Natick, USA) scripts. Fluorescence per μm^2 increases with OD600, as expected for a reporter of stationary phase (Figure 4-4). On

[1]Following the example of Shetty *et al.* [157], I represented BioBricks parts cloned within a BioBrick plasmids by writing the BioBricks vector name, followed by a dash, and the BioBricks part number, without the use of italics.

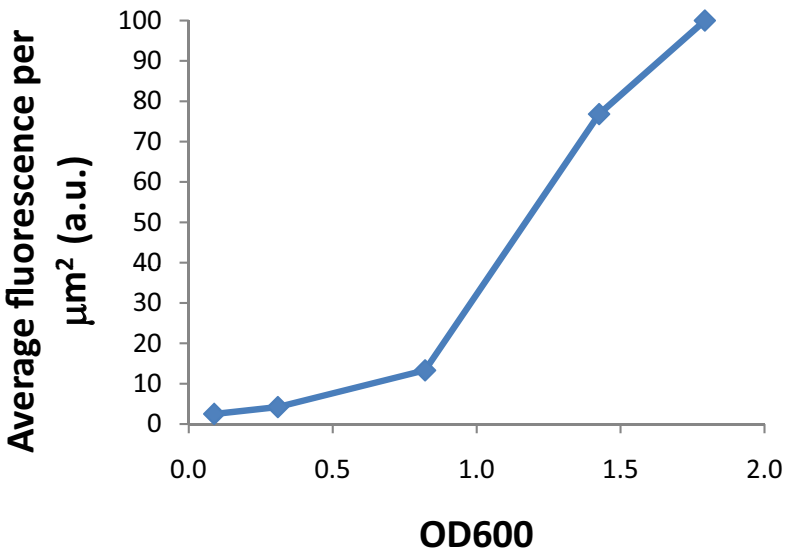

Figure 4-4: **Plasmid pSB4K5-J45995 is a reporter of stationary phase.** MG1655/pSB4K5-J45995 was grown in tryptone broth (TB) and aliquots removed at various time during growth to stationary phase. GFP signal of at least 300 cells per time point was measured by fluorescence microscopy. Fluorescence is low during exponential phase (first 2-3 points), but increase rapidly as cells approach stationary phase.

the other hand, pSB4K5-I7100 was brightly fluorescent in both exponential and stationary phase (data not shown).

The reporter of stationary phase stress does not significantly impact growth kinetics or cell fate decision statistics

I grew three independent cultures of (1) MG1655 carrying pSB4K5-J45995 and (2) MG1655 carrying pSB4K5-I7100 in TB to stationary phase, as described in Chapter 2. Aliquots from each culture were diluted 3-fold into TB for OD600 measurement via a Shimatzu UV160U spectrophotometer (Shimadzu Scientific Instruments, Columbia, MD, USA). The sampling time represents the number of hours following the 500-fold dilution in 0.5L TB (see Chapter 2). All cultures reached a plateau in OD600 at ~16 hours after the start of the culture (Figure 4-5, p.78, as was obtained with plasmid-free MG1655 (Chapter 2). pSB4K5-J45995 also did not affect cell fate decision statistics: infection of stationary phase MG1655 cells carrying pSB4K5-J45995 gave 50.8±1.0% (n=3, S.E.M.) lysogeny, compared with 48.9±2.6% (n=3, S.E.M.) for plasmid-free MG1655.

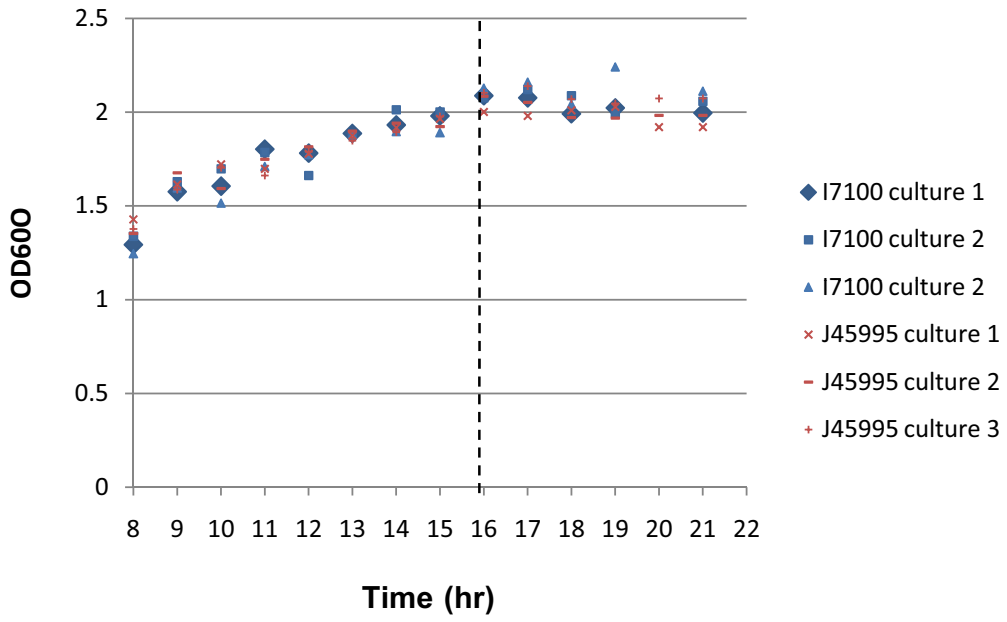

Figure 4-5: **Growth curves of 3 independent cultures of MG1655/pSB4K5-J45995 and MG1655/pSB4K5-I7100.** Both strains reach a plateau in OD600 at t ∼16 hours (dotted line), as observed with MG1655 without plasmid (Chapter 2, Figure 2-1, p.37)

No correlation is observed between cell size and fluorescence from my reporter of stationary phase stress

Three independent cultures of MG1655/pSB4K5-J45995 and MG1655/pSB4K5-I7100 were grown to stationary phase, imaged and analyzed as described above. I plotted the fluorescent per area (μm^2) as a function of cell size for MG1655/pSB4K5-J45995 (Figure 4-6a, p.79) and MG1655/pSB4K5-I7100 (Figure 4-6b, p.79).

For each strain, I divided cells into 6 bins of cell size. I then normalized the values obtained with the stationary phase reporter (J45995) with those obtained using the constitutive reporter (I7100). This normalization was necessary to remove variations in fluorescence between cells of different size that were not specific to variation in the expression of the *p*OsmY promoter.

My results are depicted in Figure 4-7 (p.80), and show no correlation between cell size and fluorescence from my stationary phase reporter. It is possible that such a correlation exists, but is either too small to detect or is masked by other sources of variation, such as cell-cell differences in plasmid copy number or gene expression capacity. Moreover, my

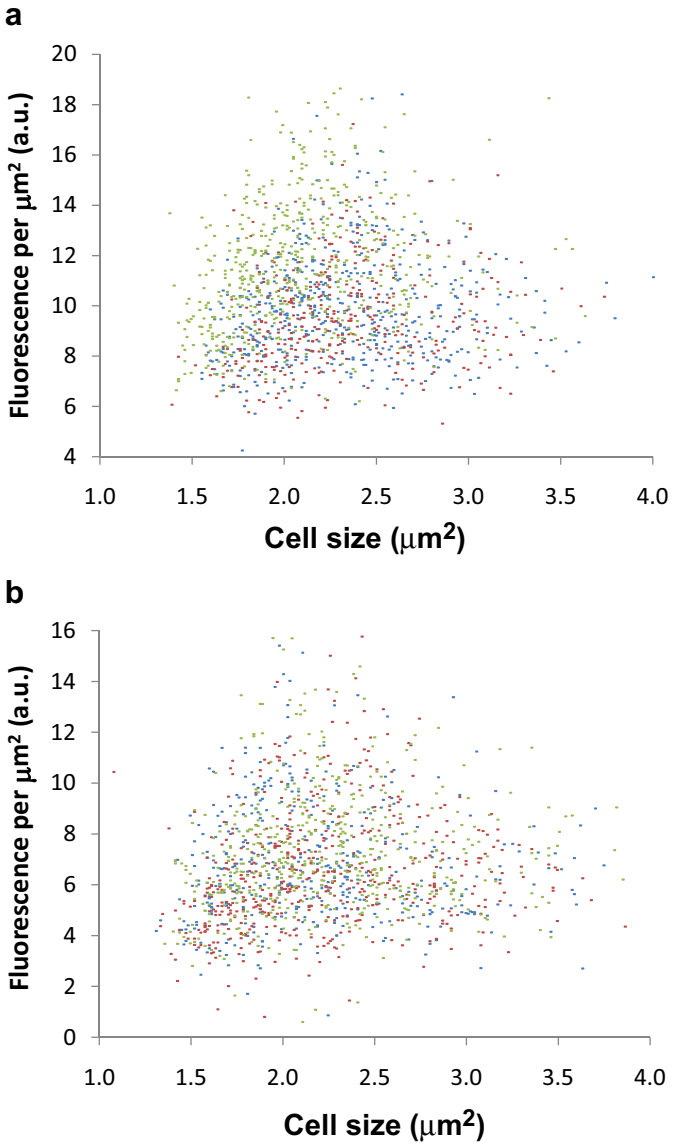

Figure 4-6: **Fluorescence per area as a function of cell size for stationary phase cultures of (a) MG1655/pSB4K5-J45995 and (b) MG1655/pSB4K5-I7100.** Cell size is given as the area (in μm^2) covered by each cell on my 2D images. Each dot represent a single cell (n>1000 for each plot), with each color represent cells from independent cultures (n>300 per culture). Exposure time was 50 ms (MG1655/pSB4K5-J45995), or 10 ms (MG1655/pSB4K5-I7100).

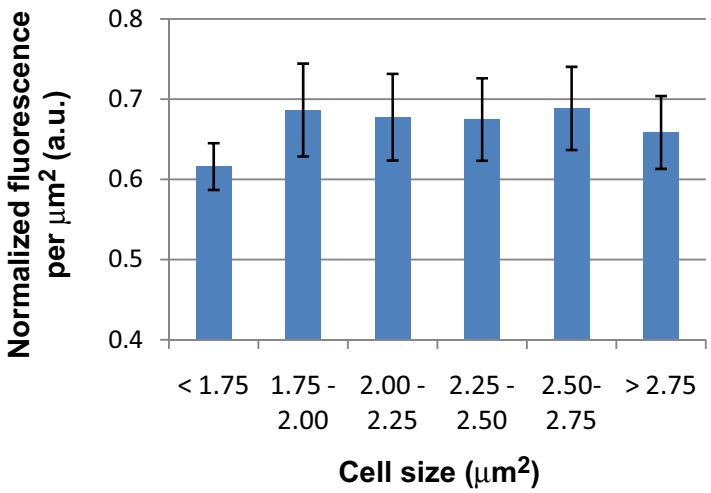

Figure 4-7: **Cell size is not correlated with signal from the stationary phase reporter (pSB4K5-J45995).** MG1655/pSB4K5-J45995 cells divided into bins, and their fluorescence per area normalized as described in the main text. Error bars represent the standard error of the mean.

reporter used GFP with a wild-type terminus, resulting in a very stable protein. The use of GFP variants with shorter half-lives may have more easily captured more transient changes in gene expression [102, 171]. Finally, I might not have used the best promoter to report on cell-cell differences during stationary phase that impact lambda developmental outcome. However, given success in developing tools and conditions to study lambda infection in exponential phase directly (see section 4.1.1, page 71), this line of investigation was not pursued further.

4.2 Is lambda sensitive to pre-existing variation in cell cycle position?

4.2.1 Consideration of cell cycle position as a determinant of the lambda lysis-lysogeny decision

The results described above show that sensitivity to host volume (or a correlated variable) can also be observed when cells are grown to exponential phase. With the caveat that these experiments were done using an *hfl* mutant rather the wild type, sensitivity to host volume

(or a correlated variable) are likely to be a more general feature of the lambda regulatory circuit rather than a property specific to stationary phase.

What aspects of host physiology, correlated with volume, might impact lambda development? In Chapter 2, I briefly described a "gene dosage" model wherein variation in host volume results in variation in the concentration of phage-encoded genes during infections at constant MOI. In an alternative model, considered here, the lambda lysis-lysogeny decision may be sensitive to the cell cycle position of its host cells, a parameter that is well correlated with cell volume [19]. In particular, cell cycle position may specify the amount, localization or activity of host-encoded regulators of the lambda regulatory circuit. For example, the localization of FtsH in *Bacillus subtilis* appears to vary throughout the cell cycle, accumulating at the septum during cell division [175].

Another possible coupling between the *E. coli* cell cycle and lambda development was posited by Kourilsky and Gros more than 30 years ago [95]. In their model, cells in which replication is not proceeding actively are more readily lysogenized. Because the ability of cells to replicate lambda DNA may be related to their ability to replicate their own genome, the position of the host cell with respect to its replication cycle may affect the lambda lysis-lysogeny decision. For example, cells which tend to be lysogenized may be those which have finished a DNA replication cycle and have not yet started a new round of replication. A possible molecular mechanism which could underlie this model might include the two main regulators of chromosome replication initiation in *E. coli*, DnaA and SeqA, which are also regulators of lambda's pR promoter [58, 77]. Activity of pR plays an important role in the regulation of lambda DNA replication [58, 77] and the lysis-lysogeny decision [131].

4.2.2 Selection of a bacterial strain to decouple cell cycle position from cell volume

I next set out to test whether lambda may be sensitive to cell cycle position, regardless of the specific mechanism that may underlie such a behavior. An obstacle to testing the "cell cycle" model of lambda infection is the high degree of correlation between cell volume and cell cycle position in wild-type *Escherichia coli* cells [19]. To decouple cell volume and cell position, I considered bacterial mutants for which cell division is controlled by temperature or by the addition of an exogenous inducer such as IPTG or arabinose. While inhibition of

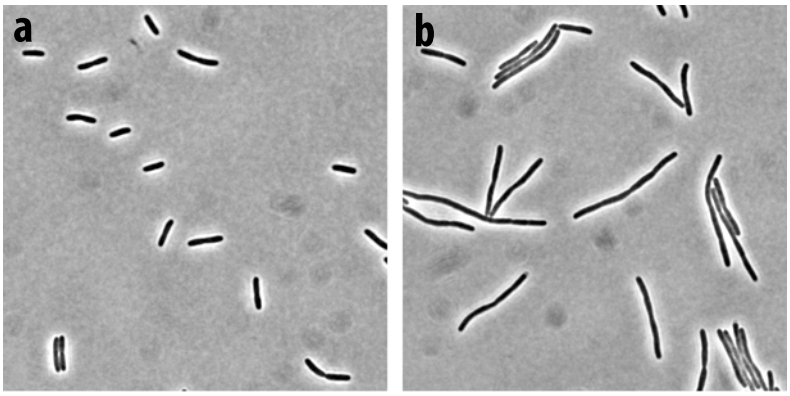

Figure 4-8: **Temperature control of septation using JW4132 *ftsA*12.** FSP-B207 (JW4132 *ftsA*12) was grown in LB to late log, diluted 10-fold in fresh LB and incubated at 30℃ **(a)** or 40℃ **(b)** for one hour. Cells were then placed on 2% LMP agarose pads supplemented with TB and imaged with a 60X phase contrast objective.

DNA replication results in inhibition of septation [75], inhibition of cell division typically does not affect progression through the cell cycle. Continued ability of filamenting cells to progress through the cell cycle is evidenced by their ability to replicate DNA and segregate bacterial chromosomes (e.g. [6, 21, 147]).

I transduced *ftsA*12 *leu*::*Tn*10 [34], a temperature-sensitive allele of the cell division gene *ftsA* [34, 40, 108] linked to a *leu*::*Tn*10 marker, from W3110 *ftsA*12 *leu*::*Tn*10 into the *hflK*::*kanR* strain JW4132 described in the previous section. The resulting strain, FSP-B207, was shown to elongate at high temperatures (e.g. > 40℃) but to be of near wild-type lengths at 30℃ (Figure 4-8, p.82).

Using FSP-B207, I can use temperature to decouple cell size from cell cycle position. The cell cycle model predicts that the frequency of lysogeny should be largely independent of cell size. On the other hand, the gene dosage model predicts that the frequency of lysogeny will decrease as cells elongate. Experiments are underway to test those predictions.

4.3 Chapter summary

I obtained evidence that lambda's apparent sensitivity to host volume is not specific to stationary phase. First, using an *E. coli* mutant strain producing a high frequency of lysogeny (*hflK*$^-$), I found that host volume can be a predictor of the fate of cells grown to exponential phase. Second, I found no correlation between the size of a cell and the signal

from a plasmid-based reporter of stationary phase. Apparent sensitivity to host volume may thus be a general property of the lambda decision circuit. As with stationary phase cells, the volume of exponentially growing cells is not a perfect predictor of cell fate. Experiments are underway to determine whether lambda may be directly sensitive to cell cycle position rather than volume.

4.4 Chapter acknowledgments

- Mingjie Li (Endy lab) collected much of the data for the experiments with the reporter of stationary phase (Section 4.1.2, p.75) and constructed JW4132 *ftsA*12 (Section 4.2.2, p.81).
- Felix Moser (Endy lab) ported (1) the GFP reporter of stationary phase (BBa_J45995) and (2) the cassette expressing GFP constitutively (BBa_I7100) into the low-copy plasmid pSB4K5 (Section 4.1.2, p.76).

Chapter 5

Identification of phage-encoded determinants of lambda's "volume sensor"

The lambda regulatory network consists of both host-encoded regulators (e.g. FtsH, RNaseIII) and phage-encoded factors (e.g. CII, CIII). In the previous Chapter, I presented efforts to uncover what aspect of host physiology, volume or a correlated parameter, impact the lambda lysis-lysogeny decision. In particular, I found that this "volume sensor" is unlikely to rely on stationary phase factors, given that host volume is a predictor of cell fate for both stationary and exponential phase cells. In this Chapter, I describe efforts to identify phage-encoded determinants of the volume sensor.

5.1 Timing of the lambda lysis-lysogeny decision

To narrow the list of candidate lambda factors critical for lambda sensitivity to host volume, I first considered the use of known lambda mutant strains. Using either the elutriation or microscopy platforms, I could directly test whether certain genes are critical for the volume effect. Unfortunately, most of lambda regulators are thought to be critical for lambda's ability to lysogenize (e.g., CI, CII), to lyse (e.g., Q, Cro) or both (e.g., N). The use of most loss-of-function alleles would therefore be expected to reduce the frequency of lysis or lysogeny to undetectable levels, to significantly affect the dynamics of the lambda decision

circuit, or both.

I detail here a different strategy to identify plausible phage factors which participate in sensing volume (or a correlated variable). In this method, I aim to find when the lambda lysogeny decision is set. Variation in host volume must impact phage-encoded factors acting upstream of the decision point. As an initial test, I decided to consider whether the decision is set at the level of CII activity. While the precise timing of the lambda lysis-lysogeny decision is not known [131,140], CII is often thought as the master regulator of the decision (see Chapter 1). According to this model, events downstream of CII are involved in the implementation of the lysis/lysogeny decision, rather than the making of the decision itself. For example, the lambda repressor (CI) or the lytic antitermination factor Q, would simply execute the decision made at the level of CII activity.

However, it is not known whether events downstream of CII may play a part in determining cell fate. Indeed, some researchers have questioned the role of CII as the sole master regulator of the lysis-lysogeny decision [38]. In another example, my advisor Drew Endy made a computational model of lambda right operator region (oR) which suggests that asymmetry of cooperativity of CI and Cro at the oR may sense variations in host volume, resulting in different transcription rates of promoters pR and pRM (D.Endy, unpublished). In his model, events largely downstream of CII, such as activation of pRM and repression of pR by CI, play a role in the decision. Knowing whether and to what extent the lysis-lysogeny decision is set at the level of CII would allow us to refine my list of plausible phage-encoded factors responsible for the decision and, plausibly, lambda's apparent sensitivity to host volume.

5.2 Construction of a CII activity reporter

To construct a reporter of CII activity, I cloned the lambda pRE promoter upstream of BBa_ Z0301 [1], an *E. coli* codon-optimized version of Venus YFP. pRE is a CII-activated promoter which exhibits little transcription in the absence of CII [50]. I chose Venus YFP due to its brightness and fast (∼15 min) maturation rate, and because of the low amount of autofluorescence in the yellow part of the spectrum [124]. Moreover, YFP, unlike GFP, allows the use of CFP (cyan fluorescent protein) in the same system with minimal spectral overlap [155]. *Venus* was cloned with a strong RBS from phage T7 gene 5

(5'-aatcaataggagaaatcaat-3') upstream of the ATG site, with no BioBrick scar, into the BioBrick vector pSB1AK3. *p*RE (lambda coordinates 5'-38635 and 38336-3', [89] and *venus* then were cloned into BioBrick vectors using standard BioBrick cloning techniques [1, 157].

In choosing suitable BioBrick vectors to clone my *p*RE-*venus* construct, I considered the following criteria. To start, I wanted to minimize copy number to avoid perturbing the lambda regulatory network via titration of too many CII molecules. Yet, I wanted the signal to be strong enough for detection. I initially tried pSB4C5, a low-copy (∼5-12 copies/cell, [14, 109, 153]), chloramphenicol-resistant BioBrick vector with pSC101 origin of replication [157]. However, very little fluorescence was detected when JW4132/pSB4C5-*p*RE-Z0301 was grown to exponential phase in M9GlyM (Chapter 4) and infected at low multiplicity. I obtained similar results when using pSB4A5 [157], which is identical to pSB4C5 except for the resistance marker (*ampR* rather than *camR*), or pSB3C5 [157] which has the higher-copy p15A origin of replication (∼15-30 copies/cell, [14,109,153]). I obtained significantly stronger signal using pSB4A3, another low-copy vector with ampicillin resistance and pSC101 origin of replication. Additionally, BBa_I739204 a kanamycin-resistant, pACYC177-derived BioBrick vector with p15A origin gave us particularly strong signal. I do not know why pSB4A3 and BBa_ I739204 gave us stronger signal than pSB4A5, pSB4C5 and pSB3C5.

I next transformed BBa_I739204-*p*RE-Venus and pSB4A3-*p*RE-Venus into JW4132, the *hflK*::*kanR* strain described in the previous Chapter. However, because BBa_I739204 is resistant to kanamycin, I first removed the FRT-flanked *kanR* marker from JW4132 using the flippase from plasmid pCP20 [35], resulting in a partial deletion of the *hflK* locus. The resulting strain, FSP-B208, was transformed with each of the two plasmids using published methods [153].

5.3 Construction of λ *A*am19 *b*::*RFP c*I857

My reporter of CII activity and λ *A*am19 *b*::*GFP c*I857 employ fluorescent proteins whose spectra overlap (YFP and GFP, respectively), motivating the construction of a different lambda strain for detection of infected cells. I decided to use a cassette expressing a red fluorescent protein (RFP) because RFP spectra shows minimal overlap with the YFP spectra, and many RFP variants have maturation times significantly faster than the latent period

of phage lambda in M9GlyM [155].

I first tested a version of the *GFP* cassette identical to that described in Chapter 3, with the exception that the RFP variant *mCherry* replaces *GFP*. I performed recombineering on phage lambda as described before, using the same primers as those described in Chapter 3, resulting in λ *b*::*mCherry*. Unfortunately, the RFP signal from λ *b*::*mCherry* was weak when monitoring infection by time-lapse microscopy, even when using exposure times of 0.5-1 second and 2x2 binning (data not shown). To obtain stronger signal, I used a different RFP cassette, BBa_E13521. When using the primers described below for PCR amplification, the resulting RFP cassette contained the following critical elements:

- BBa_E1010 encoding the red fluorescent protein mRFP1, with the strong ribosome binding site BBa_B0034. BBa_E1010 is driven by a strong, TetR-repressible promoter BBa_R0040. In the absence of TetR, BBa_R0040 is constitutive, as desired for my application. Two terminators, BBa_B0010 and BBa_B0012 are downstream of *mRFP1*, to stop transcription from BBa_R0040 past the boundaries of the cassette.

- The ampicillin resistance marker from the plasmid harboring the cassette (pSB1A2), to allow selection for phage carrying the RFP cassette.

I first PCR-amplified the above-mentioned RFP cassette using primers containing 20-22 bp of homology to the GFP cassette and 49-50 bp of homology to lambda *b* region. The sequences homologous to the lambda genome are the same as those described in Chapter 3.

- Forward primer (72 bp):
  5'-Aggcagcaaaatcatcagaaacgaacgcatcatcaagtgccggtcgtgca
  ggatcttcacctagatcctttt

- Reverse primer (69 bp):
  5'-Ccgtatccttcacccaggctgtgccgttccacttctgatattcccctcc
  gagtcagtgagcgaggaagc

I used ethanol purification to desalt and concentrate my PCR product, and performed membrane dialysis for further desalting. I performed recombineering on an infectious lambda *c*I857 particle using the recombineering strain DY380 and published methods [169].

To select for recombinants, I infected MG1655 cells grown to stationary phase with the recombineering lysate and plated on LB supplemented with 20 μg/ml carbenicillin. Putative λ *b*::*RFP* *c*I857 lysogens were confirmed by PCR and fluorescence microscopy. Stocks of λ *b*::*RFP* *c*I857 were derived from these lysogens using standard methods [65].

The resulting phage contained my 2,247 nt *GFP* cassette into the *b* region [30] of the phage genome, replacing sequence between lambda coordinates 20430-22278 and producing a phage only slightly longer (398 nt or ∼0.8%) longer than wild-type λ. The added sequence is well within the range giving efficient DNA packaging [49]. I reconfirmed the presence of the cassette on the phage by fluorescence microscopy and by sequencing. The *mRFP1* cassette showed significantly stronger fluorescence than the *mCherry* cassette, albeit less than the GFP cassette. Maturation of mRFP1 (and mCherry) also appeared ∼3 times slower than the maturation of GFPmut3, the GFP variant used in my GFP cassette. I crossed λ *A*am19 mutation with λ *b*::*RFP* *c*I857 using standard procedures [65], resulting in λ *A*am19 *b*::*RFP* *c*I857, and confirmed the presence of the amber mutation by plating on suppressor and non-suppressor strains, and by fluorescence microscopy.

5.4 CII is an almost perfect predictor of cell fate

I grew FSP-B208 harboring the low-copy CII reporter pSB4A3-*p*RE-*venus* in M9GlyM as described in the previous Chapter. For pilot experiments, I infected cells at an API (phage:cell ratio) of ∼1.5, removed free phage by centrifugation, spread cells on M9GlyM agarose pads and recorded phase contrast and fluorescence (YFP, RFP) images every ∼15minutes (see Figure 5-1, p.90, for example filmstrips).

I followed 63 infected (RFP-expressing) cells, 24 that adopted lytic growth and 39 that became lysogens. YFP signal was first detected ∼30 min, and peaked ∼75 min after the start of infection. All 39 cells which became lysogens expressed significant YFP signal. 23 of the 24 cells which became lytic expressed no or little YFP signal. One cell that became lytic expressed more YFP fluorescence than some cells that became lytic. CII activity was thus a marker of cell fate for 62 of the 63 cells analyzed in this pilot experiment, suggesting CII is an almost (98%) perfect predictor of cell fate. Preliminary results with the medium-copy BBa_I739204-*p*RE-*venus* vector were qualitatively similar (data not shown). These results are qualitatively consistent with past work suggesting that CII is a critical regulator of the

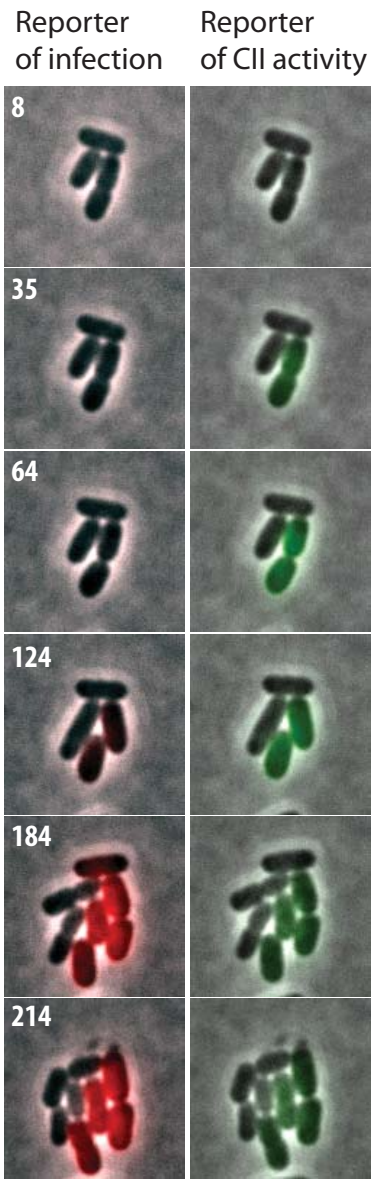

Figure 5-1: **Filmstrips of infection of single *hflK*$^-$ cells harboring a reporter of CII activity.** Images from time-lapse movies of exponentially growing FSP-B208 (Δ*hflK*) harboring the plasmid-based, CII activity reporter pSB4A3-*p*RE-*venus*. Cells were grown to exponential phase in M9GlyM and resuspended in TM as previously described. I infected cells at an API (phage:cell ratio) of ~1.5, removed free phage by centrifugation, spread cells on M9GlyM agarose pads and recorded phase contrast and fluorescence (YFP, RFP) images every ~15 minutes. Numbers indicate the number of minutes at which the images were taken after the start of each movie. The left column pictures are overlays of phase contrast and red fluorescence images. The top cell and the bottom right cell show red fluorescence, indicative of infection with λ *A*am19 *b*::*RFP* *c*I857. The bottom left cell is not infected. The right column pictures are overlays of phase contrast and yellow fluorescence (depicted green for visualization purposes). The top cell does not produce visible fluorescence and lyses between t=184 and t=214 min. The bottom right cell produces significant fluorescent signal and survives the infection, presumably as a lysogen.

lysis-lysogeny decision (Chapter 1).

The experiments presented above merit repetition, ideally at low MOI for comparison with results presented in Chapter 4. Nevertheless, my preliminary findings suggest that events largely downstream of CII — such as activation of *p*RM and repression of *p*R by CI — play a minor role in deciding between lysis and lysogeny. However, such events are likely to be important in *implementing* the lysis-lysogeny decision. If my preliminary results hold up to further experimentation, next steps should involve exploring events upstream of CII activity.

5.5 Chapter summary

I obtained preliminary results suggesting that CII activity is a near-perfect predictor of the lambda lysis-lysogeny decision. Lambda's "volume sensor" is therefore more likely to involve factors acting upstream of (or at the level of) CII, rather than factors acting downstream of CII.

5.6 Chapter acknowledgments

- Arun Devabhaktuni (Endy lab) tested the fluorescent reporters of CII activity (Section 5.4, p.89) and constructed strain λ *b*::*RFP c*I857 (Section 5.3, p.87).
- Mingjie Li (Endy lab) introduced the *A*am19 mutation into λ *b*::*RFP c*I857 (Section 5.3, p.87).
- Felix Moser (Endy lab) constructed the fluorescent reporters of CII activity (Section 5.4, p.89).

Chapter 6

Detection and enumeration of individual phage particles

In Chapter 4 (section 4.1.1, p.71), I described how I used an *hflK*$^-$ mutant to raise the frequency of lysogeny to levels observable by single-cell analysis of lambda infection. Because I am interested in studying the lambda regulatory network in wild-type conditions, I also set out to raise the frequency of lysogeny by infecting wild-type cells at a higher multiplicity of infection (see Chapter 1). Such conditions require the design of a reporter of multiplicity of infection (MOI), so that only cells infected with the same number of phage are compared. To develop a reporter of MOI, I followed two approaches in parallel. In the first (section 6.1, this page), I explored methods to determine the MOI by counting the number of phage capsids adsorbed onto a given cell. In the second method (section 6.2, page 97), I tested technology to enumerate single phage DNA particles inside host cells.

6.1 Quantification of the MOI by labeling phage capsid

I set out to develop a system to quantify the MOI by labeling phage capsids adsorbed onto cells. The MOI could then be determined by counting the number of fluorescent foci detected on a given cell surface. Labeling capsids should have the advantage of minimal (if any) perturbation of the lambda lysis-lysogeny decision. However, such a system also has

possible drawbacks. First, phage capsids may be empty (Ian Molineux, pers.comm.); empty capsids would therefore need to be removed by phage purification prior to labeling [65]. Second, not all phage bound to cells eject their DNA [113]. For maximum accuracy in determining MOI, a system based on enumerating capsid would need to be used alongside a system to detect phage DNA ejection. Third, it is unclear whether two phage particles bound near one another could be reliably resolved, especially if the individual particles do not change relative position on the cell surface over time.

6.1.1 Labeling phage capsids with Quantum Dots

I initially considered labeling phage capsids using quantum dots (Qdots), which are fluorescent semiconductor nanocrystals [123]. Methods to bind Qdots to bind to phage have been published [45, 46]. However, the authors were only able to label ∼80% of phage [46], making this method unsuitable for accurate determination of MOI.

6.1.2 Labeling phage capsids with fluorescent proteins

I tested the lambda strain λ *D-eyfp* *c*I857 *S*am7 constructed in the laboratory of Phillippe Thomen [10]. In this strain, the enhanced yellow fluorescent protein (EYFP) is attached to the C terminus of the minor lambda capsid protein D via a $GL(GSGG)_3TA$ linker. There are typically 405-420 D proteins per capsid [65]. The $GL(GSGG)_3TA$ linker has been used by other researchers for fusing D to different proteins, and was found not to interfere with binding of D to the lambda capsid [181].

I grew host cells to exponential phase in M9GlyMMC (M9 [153] supplemented with 0.4% glycerol, 0.4% maltose, 10mM $MgSO_4$ and 0.1% casamino acids). Cells were resuspended in TM [65] and infected with λ *D-eyfp* *c*I857. Infected cells were placed on 2% agarose pads supplemented with M9GlyMMC. I made time-lapse movies of infection, taking phase contrast and YFP fluorescence pictures every ∼15min.

Infected cells which became lytic were easily detected by fluorescence microscopy due to the production of D-EYFP during the late lytic stage of infection. However, I did not detect yellow fluorescent foci on the surface of the majority of infected cells (see Figure 6-1, bottom filmstrip for an example). The absence of fluorescent foci at the beginning of infection was not due to a mutation in *eyfp*, because infected cells produced fluorescence (presumably

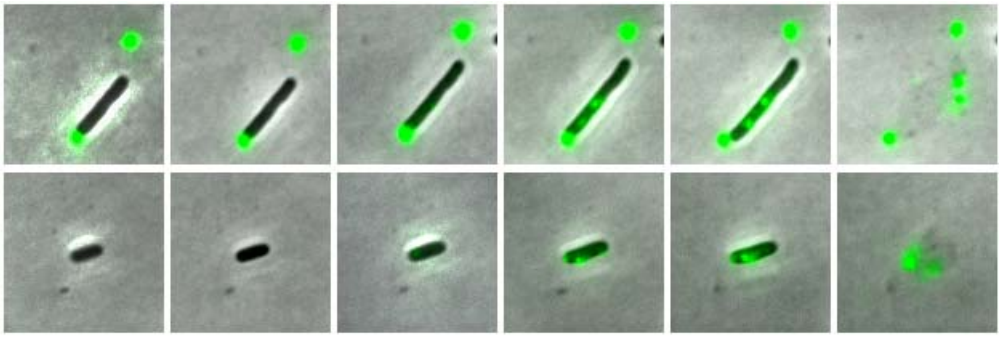

Figure 6-1: **Infection of MG1655 with λ *D-eyfp c*I857 *S*am7.** MG1655 was grown in M9GlyM and infected at an average API of ∼0.5 with λ*D-eyfp c*I857 *S*am7. Time-lapse movies were made as described earlier. The top filmstrip shows a bacterial cell apparently infected (fluorescent focus at one pole). A second fluorescent focus is also seen in the top right corner of each image, but does not seem to be attached to the cell. Fluorescence is observed inside the cell from t=33 min, presumably from production of D-EYFP protein. The cell lyses between t=57 and t=59 min. The bottom filmstrip shows a cell which initially does not appear infected (no fluorescent focus seen near the cell). However, from t=35 min, fluorescence is produced from t=35 min and the cell ultimately lysis between t=73 and t=75 min.

from D-EYFP) prior to lysis. To test if the absence of foci may be due to poor maturation of the EYFP in my conditions, I incubated my phage stock at room temperature with aeration for several hours prior to infection. However, this procedure did not qualitatively increase the number of infected cells detected using the D-EYFP fusion.

My results suggest the presence in my phage stocks of a large number of non-fluorescent phage capsids, perhaps because they contained fewer D proteins than wild-type phage, or because the linker between D and EYFP was cleaved during capsid formation. Cleavage of different linkers between D capsid and fusion proteins has been reported for fusions between D and other proteins [182], and is thus a plausible explanation. This issue cannot be remedied by creating fusions to D without the use of linkers, because both termini of protein D are located in the interface between D and the rest of the capsid [181]; linkers are therefore necessary to allow the fused portion to reach the outside of the capsid. Linkers known to better resist proteolytic cleavage — for example, PT linkers [80] — are less flexible and therefore likely to perturb the interface between D and the rest of the capsid, thereby interfering with capsid formation. Fusions to other phage capsid proteins might work but were not attempted.

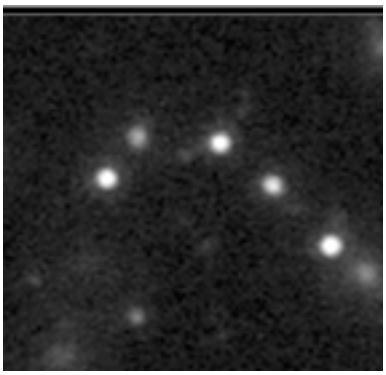

Figure 6-2: **Cy3-labed phage lambda particles.** Purified phage lambda particles were purified and labeled using the cyanide-based dye Cy3 as described [61], with the exception that I used Cy3 instead of Cy5. Labeled phage were placed on 2% agarose pads in TM [65], and imaged using a GFP filter set and a ∼200ms exposure time. Individual foci may be single phage particles.

6.1.3 Labeling phage capsid with chemical dyes

An alternative to using genetic fusions of fluorescent proteins to capsid proteins is to stain capsid proteins using chemicals. For example, CyDyes NHS Esters (GE Healthcare) have been previously used by the Phillips lab at Caltech to stain lambda capsid proteins [61]. These fluorescent dyes of the cyanine family react with exposed amine, forming covalent adducts.

I purified, stained and visualized stocks of wild-type lambda particles as described previously [61]. While staining resulted in reasonably fluorescent particles (Figure 6-2, p.96), I was unable to find fluorescent foci adsorbed onto cells, and time-lapse movies of infection showed no infection. Possibly CyDye formed adducts with the J protein of the lambda tail, thereby interfering with binding of lambda onto its cognate receptor, LamB [141, 167]. To test this hypothesis, I divided a common phage stock into two fractions which were treated identically, with the exception that one fraction was labeled in Cy3 and another was not labeled. I found that Cy3 labeling resulted in a $>$ 500-fold reduction of in titer, presumably by interfering with adsorption, so I abandoned this line of work.

6.2 Quantification of the MOI by labeling phage DNA

A different set of methods to determine the multiplicity of infection (MOI) could rely on the detection and enumeration of phage genomes following their entry into host cells. Unlike the methods presented in the previous section, direct detection of phage DNA is not complicated by the possible presence of empty phage capsids and of phage which did not eject their DNA. However, the systems describe below have a greater probability of interfering with phage development (e.g. replication, transcription). I considered the following two methods:

1. Labeling phage DNA using fluorescent repressor-operator systems (FROS) (see section 6.2.1 below)

2. Labeling phage DNA using ParB-*parS* systems (see section 6.2.2, p.99)

6.2.1 Labeling phage DNA using the FROS system

I tested the use of fluorescent repressor operator systems (FROS). In these systems, a DNA segment — typically containing 64-240 *lac* or *tet* operators (*lacO*, *tetO*) — is introduced in the desired DNA locus. When in the presence of fusions of the operators' cognate binding proteins fused to GFP (i.e. LacI-GFP or TetR-GFP), a fluorescent focus can be seen using a fluorescent microscope [98, 146]. I introduced a cassette of (a) 120 *lac* operators and a kanamycin marker or (b) 120 *tet* operators and a gentamycin marker into the *b* region of a wild-type phage lambda using recombineering [169]. A $[lacO]_{120}$-*kanR* array (5313bp) was PCR-amplified from pLau43 [98] using the following primers:

- Forward primer:
  5'-acggcatccacgaaggcgacagaggctgcgggaagtgcggtatcagcatc
  CTATGACCATGATTACGAATTC-3'

- Reverse primer:
  5'-gtggcgtacagtcatagatggtcggtgggaggtggtacaaattctctcat
  CTATGACCATGATTACGAATTC-3'

Sequences in capital letters are those homologous to the plasmid containing the array, while those in small letters are homologous to lambda's *b* region, replacing sequences

between lambda coordinates 20620 and 24268. The $[tetO]_{120}$-*gentR* array (4931bp) was PCR-amplified from pLau44 [98] using the following primers:

- Forward primer:

  5'-acggcatccacgaaggcgacagaggctgcgggaagtgcggtatcagcatc
  CTAGATTAGGTGGCGGTACTTGGG-3'

- Reverse primer:

  5'-gtggcgtacagtcatagatggtcggtgggaggtggtacaaattctctcat
  CTATGACCATGATTACGAATTC-3'

Recombinants λ *b*::$[lacO]_{120}$-*kanR* or λ *b*::$[tetO]_{120}$-*gentR* were selected as described in Chapter 2 (for the TetO arrays, I used 15μg/ml gentamycin), and confirmed by PCR. λ *b*::$[lacO]_{120}$-*kanR* and λ *b*::$[tetO]_{120}$-*gentR* strains have genomes 3% and 2.2% greater than wild-type, respectively. Genome length no greater than $\sim$5% of wild-type length can be efficiently packaged [49].

I transformed MG1655 with plasmids expressing LacI and/or TetR fused to fluorescent proteins, under the control of a weak constitutive promoter [173, 174]:

- pWX6 expresses LacI-CFP and TetR-YFP;

- pWX18 expresses LacI-CFP

I resuspended the resulting cells to OD600$\sim$2.0 in TM [65], added phage at average MOI of $\sim$2 and incubated at 4℃ for 30 min for adsorption to occur. Free phage were removed by centrifugation and infected cells were placed on a 2% LMP agarose supplemented with TM. Infected cells were then imaged by fluorescent microscopy.

Only a few weak fluorescent foci were visible following infection with λ *b*::$[lacO]_{120}$-*kanR* (Figure 6-3b,c; p.99), while foci from λ *b*::$[tetO]_{120}$-*gentR* were easily visible (Figure 6-3a). Using PCR, I found this was because the *lacO* array of most phage of my various stocks of λ *b*::$[lacO]_{120}$-*kanR* had shrunk drastically, thereby reducing the number of binding sites for LacI-GFP (data not shown). This result was unexpected, because the LacI binding sites in these arrays were separated by random sequences to minimize recombination and thereby shrinking/expansion of the arrays [98]. Array size modifications were found to occur while amplifying phage to make phage stocks. Using a *recA*$^-$ strain as host for making phage stocks did not eliminate the problem (data not shown).

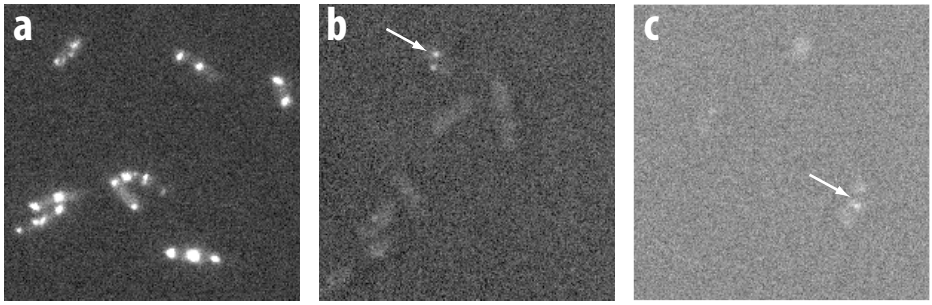

Figure 6-3: **Infection of MG1655 with λ *b*::[*lacO*]$_{120}$-*kanR* and λ *b*::[*tetO*]$_{120}$-*gentR*. a,** MG1655/pWX6 infected with λ *b*::[*tetO*]$_{120}$-*gentR*. **b,** MG1655/pWX6 infected with λ *b*::[*lacO*]$_{120}$-*kanR* **c,** MG1655/pWX18 infected with λ *b*::[*lacO*]$_{120}$-*kanR*

Shrinking of *tetO* arrays was also observed, but to a lesser extent (data not shown). However, I found that the *tetO* array appeared to block normal replication of the phage (6-4, first two columns). Wang and colleagues had observed some block of replication when *lacO* or *tetO* arrays were used on the chromosome, and found that addition of low concentrations of the cognate inducer (IPTG for *lacO* arrays; anhydrotetracycline (aTc) for *tetO* arrays) eliminated replication blocks [174]. Unfortunately, addition of aTc at the suggested concentration (40 ng/ml) also elimininated foci formation (Figure 6-5,p.101). In light of these problems, I shifted my research focus to ParB/*parS* systems (next).

6.2.2 Labeling phage DNA using ParB/*parS* systems

Another system to label DNA loci is based on the partition protein ParB, which can spread along the DNA from a nucleation site, the ∼25bp parS DNA sequence [150]. When fusions of ParB and GFP are expressed in a cell containing a *parS* sequence, GFP fluorescent foci can be observed in the location of the *parS* sequence [103, 104]. Because of a deletion of 30 amino acids, the ParB proteins using in these systems cannot function as partition proteins, but they are still able to bind to their cognate *parS* (and subsequently spread to neighboring sequences) [103]. There exist ParB/*parS* of different specificities, one from phage P1 and one from plasmid pMT1. ParB proteins of the opposite specificities do not cross react with *parS* sequences of the opposite specificity [127].

I set out to test whether the ParB/*parS* system can be used to count individual phage genomes in infected cells. I introduced the P1*parS-kanR* cassette into the *b* region of a wild-

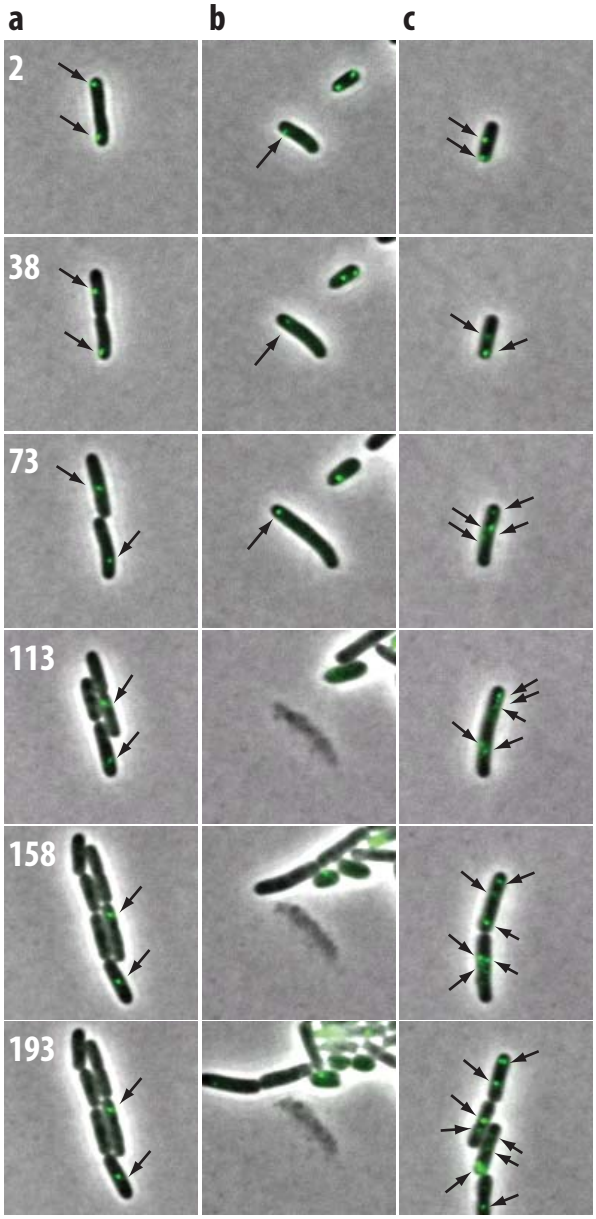

Figure 6-4: ***tetO* arrays may interfere with phage DNA replication.** MG1655/pWX6 was infected with λ b::$[tetO]_{120}$-*gentR* at a population-average MOI of $\sim$2. Infected cells were placed on 2% LMP agarose pads supplemented with M9GlyMMC. Growth at 30℃ was monitored, taking both phase contrast and fluorescent pictures. **a,** An infected cells displays two fluorescent foci, perhaps corresponding to two individual phage particles. Lambda may have chosen the lysogeny pathway in this cell, given that the cell survives and divides. However, even after a few rounds of division, no increases in the number of fluorescent foci are seen (compare with c). **b,** One fluorescent focus is seen in the infected cell in the middle of the field. The putative phage particle does not appear to replicate (no additional foci are observed) prior to lysis on the fourth frame. **c,** A cell displays two foci which replicate, giving rise to at least 8 foci on the last frame. I do not know why replication was observed in some cells (filmstrip c) but not others (filmstrips a,b)

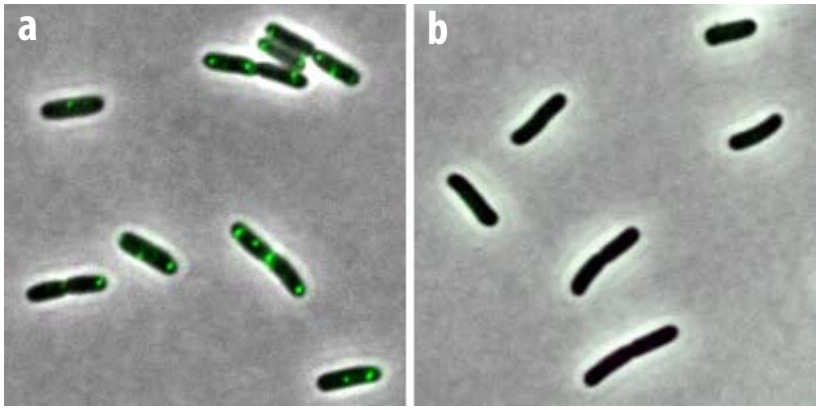

Figure 6-5: **Effect of anhydrotetracycline (aTc) on fluorescent foci formation following infection of MG1655 with λ b::[*tetO*]$_{120}$-*gentR*.** MG1655/pWX6 was infected with and was grown on M9GlyMMC alone **(a)** or supplemented with 40ng/ml aTc **(b)**.

type phage lambda. I first amplified the cassette from pALA1073 [103] using the following primers:

- Forward primer:

  5'- aggcagcaaaatcatcagaaacgaacgcatcatcaagtgccggtcgtgca

  CACAGCTTTAGAGCGTTTTGCGAT -3'

- Reverse primer:

  5'- ccgtatccttcacccaggctgtgccgttccacttctgatattcccctcc

  CGATAAAAAGCCGAAGCCTTAAAC -3'

Sequences in capital letters are those homologous to the plasmid containing the cassette, while those in small letters are homologous to lambda's *b* region. The resulting phage, λ *b*::P1*parS-kanR*, has the 1,563 nt P1*parS-kanR* cassette replacing lambda coordinates 20430 and 22278. The newly constructed phage has 286 nt ($\sim$0.6%) fewer nucleotides than wild-type lambda, and should therefore show no decrease in packaging efficiency [49]. *A*am19 and *c*I857 alleles were introduced by recombineering as described in Chapter 3.

I used the resulting phage, λ *A*am19 *b*::P1*parS-kanR c*I857, to infect MG1655 expressing ParB-GFP from pALA2705 [103]. Fluorescent foci could be detected (Figure 6-6, 102). Experiments are underway to determine to what extent the ParB/*parS* system can be used as reporter of MOI.

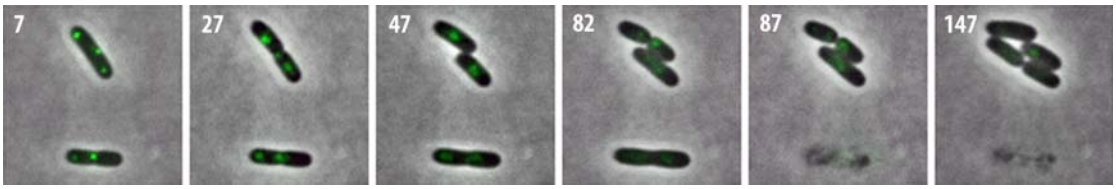

Figure 6-6: **Infection of MG1655 with λ *b*::P1*parS-kanR***. MG1655 harboring a P1ParB-GFP expression plasmid (pALA2075, [103]) was grown in M9GlyMMC + 50ug/ml carbenicillin. The culture was grown at 30℃ with vigorous agitation to OD600∼0.05. IPTG (100μM) was added to the medium and cells grown for an additional hour. Cells were infected with λ *b*::P1*parS-kanR* at a population-average MOI of ∼2. Cells were placed on 2% LMP agarose supplemented with M9GlyMMC. Phase contrast and fluorescent images were taken periodically at 30℃. For both cells, fluorescence appears to spread over a larger area over time, possibly corresponding to replication of the phage DNA.

6.3 Chapter summary

I tested several systems as potential reporters of the multiplicity of infection (MOI). Labeling phage capsid using fluorescent proteins resulted in a large fraction of phage not exhibiting detectable fluorescence, possibly because of cleavage of the linker separating the capsid protein (D) from the fluorescent protein (EYFP). Labeling phage capsid with chemical dyes resulted in inactivation of lambda particles, possibly because the dyes interfered with the binding of lambda onto its receptor (LamB). Labeling of phage DNA using the FROS system appeared to interfere with phage replication. Also, the *tetO* and *lacO* arrays were found to shrink during formation of my phage stocks, resulting in lambda particles exhibiting little or no fluorescence. Labeling of the phage DNA using the ParB/*parS* system is currently under evaluation.

6.4 Chapter acknowledgments

- Arun Devabhaktuni (Endy lab) tested λ *D-eyfp c*I857 *S*am7 (Section 6.1.2, p.94) as a reporter of MOI and constructed λ *A*am19 *b*::P1*parS-kanR c*I857 (see Section 6.2.2, 99).

- Tony Kuzhippala (Endy lab) performed the experiments with chemical labeling of the phage capsid (Section 6.1.3, p.96), and initial attempts at recombineering the *tetO* and *lacO* arrays onto phage lambda (Section 6.2.1, p.97).

Chapter 7

Conclusion

It has been known for over 55 years that apparently homogeneous cultures of *Escherichia coli* cells can bifurcate into two populations following infection by phage lambda: some cells become lytic, while others survive as lysogens [105]. Lieb, Gros and Kourilsky suggested that variation in the lysis-lysogeny decision may result from cell-cell variability present prior to infection [95, 105]. More recently, Arkin, Ross, and McAdams proposed an alternative explanation whereby spontaneous chemical "noise" in lambda gene expression creates variability in the fate of infected cells [13]. In this thesis, my primary aim has been to determine whether and to what extent variation in cell fate selection results from pre-existing phenotypic cell-cell differences (1-6b, p.31), rather than chance events during infection (1-6a, p.31).

In considering possible deterministic influences on the lambda lysis-lysogeny decision, I selected host volume as a possible marker of cell fate (Section 2.1, p.35). My results show that the fate of individual lambda-infected cells is strongly correlated with pre-existing variation in host volume. For example, a ∼2-fold increase in the size of stationary phase cells led to a ∼5-fold decrease (61% to 12.2%) in frequency of lysogeny (Figure 3-2,p.67). I initially observed that lambda was sensitive to host volume using elutriation as a method for segregating larger and smaller cells, and macroscopic plate tests (plaques, colonies) for determining cell fate (Figure 2-11, p.53). My initial finding was confirmed at the single-cell level using time-lapse fluorescent microscopy. I observed that the frequency of lysogeny decreased with increased cell size in two conditions, which differed from one another with respect to strain genotypes, culture medium and growth phase (Figure 3-2, p.67 and Figure

4-3, p.75). I also found no correlation between cell volume and the activity of a representative endogenous stationary phase promoter, as expected if the sensitivity to cell volume is not specific to stationary phase (Section 4.1.2, p.75). Sensitivity to pre-existing variation in host volume may thus be a general feature of the lysis-lysogeny regulatory network of phage lambda.

My findings challenge the view that differences in lambda cell fate outcomes are solely driven by intrinsic noise during infection. The lambda regulatory network is not only composed of phage-encoded components; rather, it operates within a bacterial environment that can also exhibit variation. Future biophysical models of lambda cell fate selection might do well to represent such variation.

The correlation between the size and fate of lambda-infected cells is particularly strong considering the limitations of the methods I used to observe and analyze the lysis-lysogeny decision. For instance, the size measurements of individual cells of Figure 3-2 (p.67) and Figure 4-3 (p.75) were made manually, considered variation in cell length only, and represented the size of cells at the start of imaging rather than at some critical time window during infection when the lysis-lysogeny decision is being set.

7.1 How does host volume impact lambda development?

Preliminary evidence presented in Section 5.4 (p.89) suggests that host volume (or a correlated variable) is likely to impact the lambda regulatory circuit upstream of (or at the level of) CII activity. However, there are still many known molecular mechanisms that could point towards a model for explaining how preexisting variation in cell volume set the level and activity of CII.

One such model is the "gene dosage" model introduced in Section 2.1 (p.35). In the conditions used for my experiments, ∼2-fold differences in volume produced 4-5 fold change in the frequency of lysogeny. One prediction of the gene dosage model is therefore that lambda decision circuit should be sensitive to relatively small (∼2 fold) variation in the concentration of one or more phage-encoded genes. I could test this prediction by determining whether and to what extent phage with different mutations can stimulate lysogenization by

a wild-type lambda particle. For example, I would infect cells with two phage strains at relatively low phage:cell ratio:

- λ *A*am19 *b*::*GFP* *c*I857
- λ *A*am19 *b*::*RFP* *c*I857 with either no additional mutations ("wild-type"), or with mutations in key regulators of the lysis-lysogeny decision (e.g. *c*II$^-$, *c*III$^-$).

Let's assume the expression level of a given gene — *c*III for the purpose of this example — is limiting for lysogeny. If true, I would expect that coinfection with λ *A*am19 *b*::*GFP* *c*I857 and λ *A*am19 *b*::*RFP* *c*I857 should result in higher frequencies of lysogeny than coinfection with λ *A*am19 *b*::*GFP* *c*I857 and λ *A*am19 *b*::*RFP* *c*I857 *c*III$^-$. These proposed experiments are the single-cell equivalent of experiments performed by Kourilsky, Kaiser and Reichardt [94, 144, 145].

There are other models than "gene dosage" that might account for the observed correlation between host volume and cell fate. For example, this correlation could also be due to physiological differences between smaller and larger cells, possibly because of their presumably distinct positions within the cell cycle. As a result, variation in volume may correlate with differences in the amount, localization or activity of host-encoded regulators of lambda development such as HflB/FtsH or RNaseIII [69, 88, 90, 140, 175, 180]. Efforts are underway to use septation mutants to decouple cell cycle position from cell volume (Section 4.2, p.80)

7.2 Is the lambda lysis-lysogeny decision completely deterministic?

While host size prior to infection is a strong predictor of cell fate, it appears that the lambda cell fate selection process may still be sensitive, in part, to other types of variation, including variation during infection. For example, Figure 3-2 (p.67) and Figure 4-3 (p.75) show that there is no "critical" volume above or below which all infected cells produce an identical developmental response.

In addition, a small number of infected cells (1.6-5.1%) divide and give rise to two daughters who obtain disparate cell fates, one that undergoes lysis and another that con-

tinues to grow and divide (Figure 3-1, p.66; Figure 4-2, p.74). If host size immediately prior to infection completely determined cell fate, I would expect the developmental response of daughter cells to be identical. Thus, mixed fate outcomes might represent an ideal case of intrinsic noise in gene expression or in partitioning of molecules (protein, DNA, mRNA) between daughter cells during cell division. Alternatively, mixed fate outcomes may still represent a deterministic process: for instance, the "age" of the poles (and other differences) of the two daughter cells might differ and affect cell fate selection following division of the originally infected cell [129]. It will be exciting to explore further if the lysis-lysogeny decision is absolutely determined by cell-cell variation present prior to infection (1-6b, p.31), or if lambda might "play dice" to some degree or on rare occasions (1-6a, p.31). It would also be interesting to find out whether the lysis-lysogeny decision of other temperate phage is similarly affected by pre-existing cellular phenotypic variation.

7.3 Why might lambda developmental outcome be correlated with host volume?

More generally, the sensitivity of lambda infection to preexisting physical variation highlights an opportunity to study how evolution shapes or delimits the molecular mechanisms underlying the behavior of biological systems. One possibility is that cell-cell variation in volume reflects physiological differences that lambda must sample to make optimal developmental decisions at the single cell level. For example, the lytic response may be preferred in infected cells capable of producing a large burst of progeny phage. Because larger cells presumably contain more material (amino acids, nucleotides, etc.) than smaller cells, they may produce greater bursts of phage particles. Alternatively, the response to pre-existing variation in host size may be an artifact of circuitry selected to be responsive to other, more dominant factors. For example, lambda's regulatory network may be tuned to respond to the MOI by measuring the concentration (rather than the absolute number per se) of phage infecting a given cell. If true, lambda would not be able to distinguish between variations in phage concentration due to differences in MOI or in host volume.

7.4 Cell fate selections in other biological model systems

Regardless of the molecular mechanism through which the lambda cell fate selection process responds to extrinsic variation, it is interesting to consider the extent to which other cell fate decisions may be predetermined. In particular, the lysis-lysogeny regulatory network of other temperate bacteriophage — such as P22, P2, HK022 and TP901-1 — are known to exhibit similarities to lambda's decision circuitry [25, 42, 65, 136]. The *Salmonella typhimurium* P22 is also known to respond to some of the same environmental parameters as lambda: for example, higher numbers of phage per cell enhances lysogenization [24, 101]. It would be valuable to determine whether a correlation between host volume and cell fate is also present in P22 and other temperate phage. The observation of such a correlation would suggest that cell size (or a correlated variable) is not simply an idiosyncrasy preserved during evolution by the particular ecology of lambda's natural habitat. If not all temperate phage exhibit an apparent sensitivity to host volume, an important challenge would be to understand why such a sensitivity has been selected during the evolution of only certain phage. In either case, comparing the regulatory networks of lambda and other temperate phage may help unraveling the molecular mechanism by which lambda appears to sense and respond to cell-cell variation in volume.

Another cell fate decision which has attracted renewed attention in recent years is the reversible entry into a state of competence for DNA uptake by a fraction of *Bacillus subtilis* cells following entry into stationary phase. Evidence is accumulating that noise intrinsic to the expression of ComK, a transcription factor necessary and sufficient for for differentiation into competence, may explain why not all cells become competent [112, 162, 163]. Indeed, reduction of comK gene expression noise by two different methods resulted in a lowered frequency of entry into competence [112, 163]. Variability in cell size does not appear to impact entry into competence (G. Suel, pers. comm.). Nevertheless, entry into competence might still determined, in part, by pre-existing cell-cell differences which have not been investigated so far. Deterministic parameters might impact the fate of *B. subtilis* by tuning the amount of noise in individual cells. However, such putative cell-cell differences would not be heritable, as sister cells are no were more or less likely to become competent if their sister became competent [162]. It will be exciting to find out whether the impact of pre-

existing variation on cell fate selection might depend on whether the resulting differentiation is transient (e.g. entry of *B. subtilis* cells into a state of competence) or largely permanent (e.g. the lambda lysis-lysogeny decision).

Consideration of deterministic and stochastic influences on differentiation is also important in understanding eukaryotic cell fate decisions, such as differentiation of stem cells. In particular, differentiation of haematopoietic stem cells is a well-studied paradigm for lineage commitment [47]. In a deterministic or "instructive" model, external factors controll cell fate choices, while in stochastic or "selective" models, external factors simply allow growth and survival of cells which, by chance, were already committed to a specific lineage. Uncovering deterministic cues are clearly important for medical applications, for example by allowing control over lineage commitment. Some evidence suggests that apparently stochastic variation in expression of lineage-specific transcription factors can prime haematopoietic stem cells for different fates [26, 47, 119]. However, it is unclear whether such spontaneous variation plays a major role in lineage commitment of stem cells in their natural context i.e. within individual animals.

Since the publication of the Arkin model [13], several hundred reports have discussed the importance of stochastic variation in gene expression and other cellular processes (e.g., [27, 143,159]). It will be interesting to find out whether stochastic variation during development actually impacts the outcome of many cell fate decisions. For comparison, development can often be predictable: for example, the patterns of programmed death and terminal differentiation during embryonic development of *Caenorhabditis elegans* are nearly invariant from one individual to the next [164]. Understanding how and the extent to which natural biological systems tolerate, buffer or correct for spontaneous molecular variation during development in order to produce deterministic behavior deserves more attention [12, 72, 73, 115, 126, 142].

Bibliography

[1] REGISTRY OF STANDARD BIOLOGICAL PARTS, *http:partsregistry.org*.

[2] G. K. Ackers, A. D. Johnson, and M. A. Shea. Quantitative model for gene regulation by lambda phage repressor. *Proceedings of the National Academy of Sciences of the United States of America*, 79(4):1129–1133, Feb 1982.

[3] T. Akerlund, K. Nordstrom, and R. Bernander. Analysis of cell size and DNA content in exponentially growing and stationary-phase batch cultures of *Escherichia coli*. *Journal of Bacteriology*, 177(23):6791–6797, Dec 1995.

[4] Y. Akiyama. Self-processing of FtsH its implication for the cleavage specificity of this protease. *Biochemistry*, 38(36):11693–11699, Sep 7 1999.

[5] Y. Akiyama, A. Kihara, H. Mori, T. Ogura, and K. Ito. Roles of the periplasmic domain of *Escherichia coli* FtsH (HflB) in protein interactions and activity modulation. *The Journal of Biological Chemistry*, 273(35):22326–22333, Aug 28 1998.

[6] J. S. Allen, C. C. Filip, R. A. Gustafson, R. G. Allen, and J. R. Walker. Regulation of bacterial cell division: genetic and phenotypic analysis of temperature-sensitive, multinucleate, filament-forming mutants of *Escherichia coli*. *Journal of Bacteriology*, 117(3):978–986, Mar 1974.

[7] S. Altuvia, D. Kornitzer, D. Teff, and A. B. Oppenheim. Alternative mRNA structures of the *c*III gene of bacteriophage lambda determine the rate of its translation initiation. *Journal of Molecular Biology*, 210(2):265–280, Nov 20 1989.

[8] S. Altuvia, H. Locker-Giladi, S. Koby, O. Ben-Nun, and A. B. Oppenheim. RNase III stimulates the translation of the *c*III gene of bacteriophage lambda. *Proceedings of the National Academy of Sciences of the United States of America*, 84(18):6511–6515, Sep 1987.

[9] S. Altuvia and A. B. Oppenheim. Translational regulatory signals within the coding region of the bacteriophage lambda *c*III gene. *Journal of Bacteriology*, 167(1):415–419, Jul 1986.

[10] L. J. Alvarez, P. Thomen, T. Makushok, and D. Chatenay. Propagation of fluorescent viruses in growing plaques. *Biotechnology and Bioengineering*, 96(3):615–621, Feb 15 2007.

[11] W. Arber, L. Enquist, B. Hohn, N. Murray, and K. Murray. *Experimental methods for use with lambda*, pages 433–466. Lambda II. Cold Spring Harbor Laboratory, Cold Spring Harbor, N.Y., 1st edition, 1983.

[12] A. M. Arias and P. Hayward. Filtering transcriptional noise during development: concepts and mechanisms. *Nature Reviews Genetics*, 7(1):34–44, Jan 2006.

[13] A. Arkin, J. Ross, and H. H. McAdams. Stochastic kinetic analysis of developmental pathway bifurcation in phage lambda-infected *Escherichia coli* cells. *Genetics*, 149(4):1633–1648, Aug 1998.

[14] Frederick M. Ausubel. *Short protocols in molecular biology : a compendium of methods from Current protocols in molecular biology*. Wiley, New York, 1995.

[15] T. Baba, T. Ara, M. Hasegawa, Y. Takai, Y. Okumura, M. Baba, K. A. Datsenko, M. Tomita, B. L. Wanner, and H. Mori. Construction of *Escherichia coli* K-12 in-frame, single-gene knockout mutants: the Keio collection. *Molecular Systems Biology*, 2:2006.0008, 2006.

[16] N. Q. Balaban, J. Merrin, R. Chait, L. Kowalik, and S. Leibler. Bacterial persistence as a phenotypic switch. *Science*, 305(5690):1622–1625, Sep 10 2004.

[17] F. Banuett, M. A. Hoyt, L. McFarlane, H. Echols, and I. Herskowitz. *hflB*, a new *Escherichia coli* locus regulating lysogeny and the level of bacteriophage lambda *c*II protein. *Journal of Molecular Biology*, 187(2):213–224, Jan 20 1986.

[18] S. Barik, B. Ghosh, W. Whalen, D. Lazinski, and A. Das. An antitermination protein engages the elongating transcription apparatus at a promoter-proximal recognition site. *Cell*, 50(6):885–899, Sep 11 1987.

[19] D. Bates, J. Epstein, E. Boye, K. Fahrner, H. Berg, and N. Kleckner. The *Escherichia coli* baby cell column: a novel cell synchronization method provides new insight into the bacterial cell cycle. *Molecular Microbiology*, 57(2):380–391, Jul 2005.

[20] M. Belfort and D. Wulff. The roles of the lambda *c*3 gene and the *Escherichia coli* catabolite gene activation system in the establishment of lysogeny by bacteriophage lambda. *Proceedings of the National Academy of Sciences of the United States of America*, 71(3):779–782, March 1974.

[21] E. Bi and J. Lutkenhaus. Isolation and characterization of *ftsZ* alleles that affect septal morphology. *Journal of Bacteriology*, 174(16):5414–5423, Aug 1992.

[22] F. R. Blattner, G. Plunkett 3rd, C. A. Bloch, N. T. Perna, V. Burland, M. Riley, J. Collado-Vides, J. D. Glasner, C. K. Rode, G. F. Mayhew, J. Gregor, N. W. Davis, H. A. Kirkpatrick, M. A. Goeden, D. J. Rose, B. Mau, and Y. Shao. The complete genome sequence of *Escherichia coli* K-12. *Science*, 277(5331):1453–1474, Sep 5 1997.

[23] T. Bouvier, M. Troussellier, A. Anzil, C. Courties, and P. Servais. Using light scatter signal to estimate bacterial biovolume by flow cytometry. *Cytometry*, 44(3):188–194, Jul 1 2001.

[24] J. S. Boyd. Observations on the relationship of symbiotic and lytic bacteriophage. *The Journal of Pathology and Bacteriology*, 63(3):445–457, Jul 1951.

[25] A. Campbell. Comparative molecular biology of lambdoid phages. *Annual Reviews of Microbiology*, 48:193–222, 1994.

[26] H.H. Chang, M. Hemberg, M. Barahona, D.E. Ingber, and S. Huang. Transcriptome-wide noise controls lineage choice in mammalian progenitor cells. *Nature*, 453:544–548, 2008.

[27] A. Colman-Lerner, A. Gordon, E. Serra, T. Chin, O. Resnekov, D. Endy, C. G. Pesce, and R. Brent. Regulated cell-to-cell variation in a cell-fate decision system. *Nature*, 437(7059):699–706, Sep 29 2005.

[28] D. Court, C. Brady, M. Rosenberg, D. L. Wulff, M. Behr, M. Mahoney, and S. U. Izumi. Control of transcription termination: a Rho-dependent termination site in bacteriophage lambda. *Journal of Molecular Biology*, 138(2):231–254, Apr 1980.

[29] D. Court, L. Green, and H. Echols. Positive and negative regulation by the *c*II and *c*III gene products of bacteriophage lambda. *Virology*, 63(2):484–491, Feb 1975.

[30] D. Court and A. B. Oppenheim. *Phage lambda's accessory genes*, pages 251–277. Lambda II. Cold Spring Harbor Laboratory, Cold Spring Harbor, N.Y., 1st edition, 1983.

[31] D. L. Court, A. B. Oppenheim, and S. L. Adhya. A new look at bacteriophage lambda genetic networks. *Journal of Bacteriology*, 189(2):298–304, Jan 2007.

[32] D. L. Court, T. A. Patterson, T. Baker, N. Costantino, X. Mao, and D. I. Friedman. Structural and functional analyses of the transcription-translation proteins NusB and NusE. *Journal of Bacteriology*, 177(9):2589–2591, May 1995.

[33] A. Czyz, R. Zielke, and G. Wegrzyn. Rapid degradation of bacteriophage lambda O protein by ClpP/ClpX protease influences the lysis-versus-lysogenization decision of the phage under certain growth conditions of the host cells. Aug 2001.

[34] K. Dai, Y. Xu, and J. Lutkenhaus. Cloning and characterization of *ftsN*, an essential cell division gene in *Escherichia coli* isolated as a multicopy suppressor of *ftsA*12(ts). *Journal of Bacteriology*, 175(12):3790–3797, Jun 1993.

[35] K. A. Datsenko and B. L. Wanner. One-step inactivation of chromosomal genes in *Escherichia coli* K-12 using PCR products. Jun 6 2000.

[36] A. B. Datta, S. Roy, and P. Parrack. Role of C-terminal residues in oligomerization and stability of lambda CII: implications for lysis-lysogeny decision of the phage. *Journal of Molecular Biology*, 345(2):315–324, Jan 14 2005.

[37] M. Delbruck. The burst size distribution in the growth of bacterial viruses (bacteriophages). *Journal of Bacteriology*, 50(2):131–135, Aug 1945.

[38] I. B. Dodd, K. E. Shearwin, and J. B. Egan. Revisited gene regulation in bacteriophage lambda. *Current Opinion in Genetics Development*, 15(2):145–152, Apr 2005.

[39] I. B. Dodd, K. E. Shearwin, A. J. Perkins, T. Burr, A. Hochschild, and J. B. Egan. Cooperativity in long-range gene regulation by the lambda CI repressor. *Genes Development*, 18(3):344–354, Feb 1 2004.

[40] W. D. Donachie, K. J. Begg, J. F. Lutkenhaus, G. P. Salmond, E. Martinez-Salas, and M. Vincente. Role of the *ftsA* gene product in control of *Escherichia coli* cell division. *Journal of Bacteriology*, 140(2):388–394, Nov 1979.

[41] D. Drahos and W. Szybalski. Antitermination and termination functions of the cloned *nutL*, *N*, and *t*L1 modules of coliphage lambda. *Gene*, 16(1-3):261–274, Dec 1981.

[42] H. Echols. Developmental pathways for the temperate phage: lysis vs lysogeny,. *Annual Review of Genetics*, 6(0):157–190, 1972.

[43] H. Echols and L. Green. Establishment and maintenance of repression by bacteriophage lambda: the role of the cI, cII, and c3 proteins. *Proceedings of the National Academy of Sciences of the United States of America*, 68(9):2190–2194, Sep 1971.

[44] H. Echols, L. Green, A. B. Oppenheim, A. Oppenheim, and A. Honigman. Role of the *cro* gene in bacteriophage lambda development. *Journal of Molecular Biology*, 80(2):203–216, Oct 25 1973.

[45] R. Edgar, M. McKinstry, J. Hwang, A. B. Oppenheim, R. A. Fekete, G. Giulian, C. Merril, K. Nagashima, and S. Adhya. High-sensitivity bacterial detection using biotin-tagged phage and quantum-dot nanocomplexes. *Proceedings of the National Academy of Sciences of the United States of America*, 103(13):4841–4845, Mar 28 2006.

[46] R. Edgar, A. Rokney, M. Feeney, S. Semsey, M. Kessel, M. B. Goldberg, S. Adhya, and A. B. Oppenheim. Bacteriophage infection is targeted to cellular poles. *Molecular Microbiology*, 68(5):1107–1116, Jun 2008.

[47] T. Enver, C. M. Heyworth, and T. M. Dexter. Do stem cells play dice? *Blood*, 92(2):348–51; discussion 352, Jul 15 1998.

[48] M. Feiss and A. Becker. *DNA packaging and cutting*, pages 305–330. Cold Spring Harbor Laboratory, Cold Spring Harbor, N.Y., 1st edition, 1983.

[49] M. Feiss, R. A. Fisher, M. A. Crayton, and C. Egner. Packaging of the bacteriophage lambda chromosome: effect of chromosome length. *Virology*, 77(1):281–293, Mar 1977.

[50] K. Fien, A. Turck, I. Kang, S. Kielty, D. L. Wulff, K. McKenney, and M. Rosenberg. CII-dependent activation of the *p*RE promoter of coliphage lambda fused to the *Escherichia coli galK* gene. *Gene*, 32(1-2):141–150, Dec 1984.

[51] C. G. Figdor, A. J. M. Olijhoek, S. Klencke, N. Nanninga, and W. S. Bont. Isolation of small cells from an exponential growing culture of *Escherichia coli* by centrifugal elutriation. *FEMS Microbiology Letters*, 10:349–352, 1981.

[52] D. I. Friedman and D. L. Court. Transcription antitermination: the lambda paradigm updated. *Molecular Microbiology*, 18(2):191–200, Oct 1995.

[53] D. I. Friedman, E. R. Olson, C. Georgopoulos, K. Tilly, I. Herskowitz, and F. Banuett. Interactions of bacteriophage and host macromolecules in the growth of bacteriophage lambda. *Microbiological Reviews*, 48(4):299–325, Dec 1984.

[54] B. A. Fry. Conditions for the infection of *Escherichia coli* with lambda phage and for the establishment of lysogeny. *Journal of General Microbiology*, 21:676–684, Dec 1959.

[55] H. Funabashi, T. Haruyama, M. Mie, Y. Yanagida, E. Kobatake, and M. Aizawa. Non-destructive monitoring of *rpoS* promoter activity as stress marker for evaluating cellular physiological status. *Journal of Biotechnology*, 95(1):85–93, Apr 25 2002.

[56] J. W. Gautsch and D. L. Wulff. Fine structure mapping, complementation, and physiology of *Escherichia coli hfl* mutants. *Genetics*, 77(3):435–448, Jul 1974.

[57] D. T. Gillespie. A general method for numerically simulating the stochastic time evolution of coupled chemical reactions. *The Journal of Physical Chemistry*, 22:403–434, 1976.

[58] M. Glinkowska, J. Majka, W. Messer, and G. Wegrzyn. The mechanism of regulation of bacteriophage lambda *p*R promoter activity by *Escherichia coli* DnaA protein. *The Journal of Biological Chemistry*, 278(25):22250–22256, Jun 20 2003.

[59] M. Gottesman and R. A. Weisberg. *Prophage insertion and excision*, pages 113–138. The bacteriophage lambda. Cold Spring Harbor Laboratory, Cold Spring Harbor, N.Y., 1971.

[60] S. Gottesman, M. Gottesman, J. E. Shaw, and M. L. Pearson. Protein degradation in *E. coli*: the *lon* mutation and bacteriophage lambda N and cII protein stability. *Cell*, 24(1):225–233, Apr 1981.

[61] P. Grayson. The DNA ejection process in bacteriophage lambda, 2007.

[62] G. N. Gussin, A. D. Johnson, C. O. Pabo, and R. T. Sauer. *Repressor and Cro protein: structure, function, and role in lysogenization*, pages 93–121. Lambda II. Cold Spring Harbor Laboratory, 1983.

[63] S. Halder, A. B. Datta, and P. Parrack. Probing the antiprotease activity of lambda CIII, an inhibitor of the *Escherichia coli* metalloprotease HflB (FtsH). *Journal of Bacteriology*, 189(22):8130–8138, Nov 2007.

[64] C. E. Helmstetter and D. J. Cummings. Bacterial synchronization by selection of cells at division. *Proceedings of the National Academy of Sciences of the United States of America*, 50:767–774, Oct 1963.

[65] R. W. Hendrix. *Lambda II*, volume 13. Cold Spring Harbor Laboratory, Cold Spring Harbor, N.Y, 1983.

[66] R. Hengge-Aronis. Interplay of global regulators and cell physiology in the general stress response of *Escherichia coli*. *Current Opinion in Microbiology*, 2(2):148–152, Apr 1999.

[67] C. Herman, T. Ogura, T. Tomoyasu, S. Hiraga, Y. Akiyama, K. Ito, R. Thomas, R. D'Ari, and P. Bouloc. Cell growth and lambda phage development controlled by the same essential *Escherichia coli* gene, *ftsH/hflB*. *Proceedings of the National Academy of Sciences of the United States of America*, 90(22):10861–10865, Nov 15 1993.

[68] C. Herman, D. Thevenet, R. D'Ari, and P. Bouloc. The HflB protease of *Escherichia coli* degrades its inhibitor lambda cIII. *Journal of Bacteriology*, 179(2):358–363, Jan 1997.

[69] I. Herskowitz and D. Hagen. The lysis-lysogeny decision of phage lambda: explicit programming and responsiveness. *Annual Review of Genetics*, 14:399–445, 1980.

[70] I. Herskowitz and E. R. Signer. A site essential for expression of all late genes in bacteriophage lambda. *Journal of Molecular Biology*, 47(3):545–556, Feb 14 1970.

[71] B. C. Hoopes and W. R. McClure. A cII-dependent promoter is located within the *Q* gene of bacteriophage lambda. *Proceedings of the National Academy of Sciences of the United States of America*, 82(10):3134–3138, May 1985.

[72] J. J. Hopfield. Kinetic proofreading: a new mechanism for reducing errors in biosynthetic processes requiring high specificity. *Proceedings of the National Academy of Sciences of the United States of America*, 71(10):4135–4139, Oct 1974.

[73] B. Houchmandzadeh, E. Wieschaus, and S. Leibler. Establishment of developmental precision and proportions in the early *Drosophila* embryo. *Nature*, 415(6873):798–802, Feb 14 2002.

[74] M. A. Hoyt, D. M. Knight, A. Das, H. I. Miller, and H. Echols. Control of phage lambda development by stability and synthesis of cII protein: role of the viral *c*III and host *hflA*, *himA* and *himD* genes. *Cell*, 31(3 Pt 2):565–573, Dec 1982.

[75] M. Inouye. Unlinking of cell division from deoxyribonucleic acid replication in a temperature-sensitive deoxyribonucleic acid synthesis mutant of *Escherichia coli*. *Journal of Bacteriology*, 99(3):842–850, Sep 1969.

[76] K. Ito and Y. Akiyama. Cellular functions, mechanism of action, and regulation of FtsH protease. *Annual Review of Microbiology*, 59:211–231, 2005.

[77] J. Jasiecki and G. Wegrzyn. Growth-rate dependent RNA polyadenylation in *Escherichia coli*. *EMBO reports*, 4(2):172–177, Feb 2003.

[78] M. O. Jones and I. Herskowitz. Mutants of bacteriophage lambda which do not require the *c*III gene for efficient lysogenization. *Virology*, 88(2):199–212, Jul 15 1978.

[79] A. D. Kaiser. Mutations in a temperate bacteriophage affecting its ability to lysogenize *Escherichia coli*. *Virology*, 3(1):42–61, Feb 1957.

[80] M. Kavoosi, A. L. Creagh, D. G. Kilburn, and C. A. Haynes. Strategy for selecting and characterizing linker peptides for CBM9-tagged fusion proteins expressed in *Escherichia coli*. *Biotechnology and Bioengineering*, 98(3):599–610, Oct 15 2007.

[81] I. Keren, N. Kaldalu, A. Spoering, Y. Wang, and K. Lewis. Persister cells and tolerance to antimicrobials. *FEMS Microbiology Letters*, 230:13–18, 2004.

[82] A. Kihara, Y. Akiyama, and K. Ito. A protease complex in the *Escherichia coli* plasma membrane: HflKC (HflA) forms a complex with FtsH (HflB), regulating its proteolytic activity against SecY. *The EMBO Journal*, 15(22):6122–6131, Nov 15 1996.

[83] A. Kihara, Y. Akiyama, and K. Ito. Host regulation of lysogenic decision in bacteriophage lambda: transmembrane modulation of FtsH (HflB), the cII degrading protease, by HflKC (HflA). *Proceedings of the National Academy of Sciences of the United States of America*, 94(11):5544–5549, May 27 1997.

[84] A. Kihara, Y. Akiyama, and K. Ito. Different pathways for protein degradation by the FtsH/HflKC membrane-embedded protease complex: an implication from the interference by a mutant form of a new substrate protein, YccA. *Journal of Molecular Biology*, 279(1):175–188, May 29 1998.

[85] A. Kihara, Y. Akiyama, and K. Ito. Revisiting the lysogenization control of bacteriophage lambda. Identification and characterization of a new host component, HflD. *The Journal of Biological Chemistry*, 276(17):13695–13700, Apr 27 2001.

[86] B. J. Knoll. Isolation and characterization of mutations in the *c*III gene of bacteriophage lambda which increase the efficiency of lysogenization of *Escherichia coli* K-12. *Virology*, 92(2):518–531, Jan 30 1979.

[87] O. Kobiler, S. Koby, D. Teff, D. Court, and A. B. Oppenheim. The phage lambda CII transcriptional activator carries a C-terminal domain signaling for rapid proteolysis. *Proceedings of the National Academy of Sciences of the United States of America*, 99(23):14964–14969, Nov 12 2002.

[88] O. Kobiler, A. B. Oppenheim, and C. Herman. Recruitment of host ATP-dependent proteases by bacteriophage lambda. *Journal of Structural Biology*, 146(1-2):72–78, Apr-May 2004.

[89] O. Kobiler, A. Rokney, N. Friedman, D. L. Court, J. Stavans, and A. B. Oppenheim. Quantitative kinetic analysis of the bacteriophage lambda genetic network. *Proceedings of the National Academy of Sciences of the United States of America*, 102(12):4470–4475, Mar 22 2005.

[90] O. Kobiler, A. Rokney, and A. B. Oppenheim. Phage lambda CIII: a protease inhibitor regulating the lysis-lysogeny decision. *PLoS ONE*, 2:e363, Apr 11 2007.

[91] D. Kornitzer, D. Teff, S. Altuvia, and A. B. Oppenheim. Genetic analysis of bacteriophage lambda *c*III gene: mRNA structural requirements for translation initiation. *Journal of Bacteriology*, 171(5):2563–2572, May 1989.

[92] P. Kourilsky. Lysogenization by bacteriophage lambda and the regulation of lambda repressor synthesis. *Virology*, 45(3):853–857, Sep 1971.

[93] P. Kourilsky. Lysogenization by bacteriophage lambda. I. Multiple infection and the lysogenic response. *Molecular General Genetics*, 122(2):183–195, Apr 12 1973.

[94] P. Kourilsky. Lysogenization by bacteriophage lambda. II. Identification of genes involved in the multiplicity dependent processes. *Biochimie*, 56(11-12):1511–1516, 1974.

[95] P. Kourilsky and D. Gros. Lysogenization by bacteriophage lambda. IV. inhibition of phage DNA synthesis by the products of genes *c*II and *c*III. *Biochimie*, 58(11-12):1321–1327, 1976.

[96] P. Kourilsky and A. Knapp. Lysogenization by bacteriophage lambda. III. Multiplicity dependent phenomena occuring upon infection by lambda. *Biochimie*, 56(11-12):1517–1523, 1974.

[97] L. Krinke, M. Mahoney, and D. L. Wulff. The role of the *OOP* antisense RNA in coliphage lambda development. *Molecular Microbiology*, 5(5):1265–1272, May 1991.

[98] I. F. Lau, S. R. Filipe, B. Soballe, O. A. Okstad, F. X. Barre, and D. J. Sherratt. Spatial and temporal organization of replicating *Escherichia coli* chromosomes. *Molecular Microbiology*, 49(3):731–743, Aug 2003.

[99] E. M. Lederberg. Lysogenecity in *E. coli* K-12. *Genetics*, 36:560, 1951.

[100] E. M. Lederberg and J. Lederberg. Genetic Studies of Lysogenicity in *Escherichia coli*. *Genetics*, 38(1):51–64, Jan 1953.

[101] M. Levine. Mutations in the temperate phage P22 and lysogeny in *Salmonella*. *Virology*, 3(1):22–41, Feb 1957.

[102] X. Li, X. Zhao, Y. Fang, X. Jiang, T. Duong, C. Fan, C. C. Huang, and S. R. Kain. Generation of destabilized green fluorescent protein as a transcription reporter. *The Journal of Biological Chemistry*, 273(52):34970–34975, Dec 25 1998.

[103] Y. Li and S. Austin. The P1 plasmid is segregated to daughter cells by a 'capture and ejection' mechanism coordinated with *Escherichia coli* cell division. *Molecular Microbiology*, 46(1):63–74, Oct 2002.

[104] Y. Li, K. Sergueev, and S. Austin. The segregation of the *Escherichia coli* origin and terminus of replication. *Molecular Microbiology*, 46(4):985–996, Nov 2002.

[105] M. Lieb. Studies on lysogenization in *Escherichia coli*. *Cold Spring Harbor Symposia on Quantitative Biology*, 18:71–73, 1953.

[106] M. Lieb. The establishment of lysogenicity in *Escherichia coli*. *Journal of Bacteriology*, 65(6):642–651, Jun 1953.

[107] J. W. Little, D. P. Shepley, and D. W. Wert. Robustness of a gene regulatory circuit. *The EMBO Journal*, 18(15):4299–4307, Aug 2 1999.

[108] J. F. Lutkenhaus, H. Wolf-Watz, and W. D. Donachie. Organization of genes in the *ftsA-envA* region of the *Escherichia coli* genetic map and identification of a new *fts* locus (*ftsZ*). *Journal of Bacteriology*, 142(2):615–620, May 1980.

[109] R. Lutz and H. Bujard. Independent and tight regulation of transcriptional units in *Escherichia coli* via the LacR/O, the TetR/O and AraC/I1-I2 regulatory elements. *Nucleic Acids Research*, 25(6):1203–1210, Mar 15 1997.

[110] D. Luzzati. Regulation of lambda exonuclease synthesis: role of the *N* gene product and lambda repressor. *Journal of Molecular Biology*, 49(2):515–519, Apr 28 1970.

[111] A. Lwoff. Lysogeny. *Bacteriological Reviews*, 17(4):269–337, Dec 1953.

[112] H. Maamar, A. Raj, and D. Dubnau. Noise in gene expression determines cell fate in *Bacillus subtilis*. *Science*, 317(5837):526–529, Jul 27 2007.

[113] D. J. Mackay and V. C. Bode. Events in lambda injection between phage adsorption and DNA entry. *Virology*, 72(1):154–166, Jul 1 1976.

[114] J. Mahajna, A. B. Oppenheim, A. Rattray, and M. Gottesman. Translation initiation of bacteriophage lambda gene *c*II requires integration host factor. *Journal of Bacteriology*, 165(1):167–174, Jan 1986.

[115] N. Maheshri and E. K. O'Shea. Living with noisy genes: how cells function reliably with inherent variability in gene expression. *Annual Review of Biophysics and Biomolecular Structure*, 36:413–434, 2007.

[116] H. Makinoshima, S. Aizawa, H. Hayashi, T. Miki, A. Nishimura, and A. Ishihama. Growth phase-coupled alterations in cell structure and function of *Escherichia coli*. *Journal of Bacteriology*, 185(4):1338–1345, Feb 2003.

[117] H. Makinoshima, A. Nishimura, and A. Ishihama. Fractionation of *Escherichia coli* cell populations at different stages during growth transition to stationary phase. *Molecular Microbiology*, 43(2):269–279, Jan 2002.

[118] R. Maurer, B. Meyer, and M. Ptashne. Gene regulation at the right operator (*o*R) bacteriophage lambda. I. *o*R3 and autogenous negative control by repressor. *Journal of Molecular Biology*, 139(2):147–161, May 15 1980.

[119] H. Mayani, W. Dragowska, and P. M. Lansdorp. Lineage commitment in human hemopoiesis involves asymmetric cell division of multipotent progenitors and does not appear to be influenced by cytokines. *Journal of Cellular Physiology*, 157(3):579–586, Dec 1993.

[120] H. H. McAdams and L. Shapiro. Circuit simulation of genetic networks. *Science*, 269(5224):650–656, Aug 4 1995.

[121] B. J. Meyer, R. Maurer, and M. Ptashne. Gene regulation at the right operator (*o*R) of bacteriophage lambda. II. *o*R1, *o*R2, and *o*R3: their roles in mediating the effects of repressor and *cro*. *Journal of Molecular Biology*, 139(2):163–194, May 15 1980.

[122] B. J. Meyer and M. Ptashne. Gene regulation at the right operator (*o*R) of bacteriophage lambda. III. lambda repressor directly activates gene transcription. *Journal of Molecular Biology*, 139(2):195–205, May 15 1980.

[123] X. Michalet, F. F. Pinaud, L. A. Bentolila, J. M. Tsay, S. Doose, J. J. Li, G. Sundaresan, A. M. Wu, S. S. Gambhir, and S. Weiss. Quantum dots for live cells, in vivo imaging, and diagnostics. *Science*, 307(5709):538–544, Jan 28 2005.

[124] T. Nagai, K. Ibata, E. S. Park, M. Kubota, K. Mikoshiba, and A. Miyawaki. A variant of yellow fluorescent protein with fast and efficient maturation for cell-biological applications. *Nature Biotechnology*, 20(1):87–90, Jan 2002.

[125] Z. Neubauer and E. Calef. Immunity phase-shift in defective lysogens: non-mutational hereditary change of early regulation of lambda prophage. *Journal of Molecular Biology*, 51(1):1–13, Jul 14 1970.

[126] J. Von Neumann. *Probabilistic logic and the synthesis of reliable organisms from unreliable components*, volume 34 of *Automata studies*, pages 43–98. Princeton University Press, Princeton, 1956.

[127] H. J. Nielsen, J. R. Ottesen, B. Youngren, S. J. Austin, and F. G. Hansen. The *Escherichia coli* chromosome is organized with the left and right chromosome arms in separate cell halves. *Molecular Microbiology*, 62(2):331–338, Oct 2006.

[128] T. Nystrom. Stationary-phase physiology. *Annual Review of Microbiology*, 58:161–181, 2004.

[129] T. Nystrom. A bacterial kind of aging. *PLoS Genetics*, 3(12):e224, Dec 2007.

[130] A. Oppenheim and A. B. Oppenheim. Regulation of the *int* gene of bacteriophage lambda: activation by the *c*II and *c*III gene products and the role of the pI and pL promoters. *Molecular General Genetics*, 165(1):39–46, Sep 20 1978.

[131] A. B. Oppenheim, O. Kobiler, J. Stavans, D. L. Court, and S. Adhya. Switches in bacteriophage lambda development. *Annual Review of Genetics*, 39:409–429, 2005.

[132] A. B. Oppenheim, A. J. Rattray, M. Bubunenko, L. C. Thomason, and D. L. Court. *In vivo* recombineering of bacteriophage lambda by PCR fragments and single-strand oligonucleotides. *Virology*, 319(2):185–189, Feb 20 2004.

[133] T. A. Patterson, Z. Zhang, T. Baker, L. L. Johnson, D. I. Friedman, and D. L. Court. Bacteriophage lambda N-dependent transcription antitermination. Competition for an RNA site may regulate antitermination. *Journal of Molecular Biology*, 236(1):217–228, Feb 11 1994.

[134] S. Peacock, H. Weissbach, and H. A. Nash. In vitro regulation of phage lambda *c*II gene expression by *Escherichia coli* integration host factor. *Proceedings of the National Academy of Sciences of the United States of America*, 81(19):6009–6013, Oct 1984.

[135] S. Pearl, C. Gabay, R. Kishony, A. Oppenheim, and N.Q. Balaban. Nongenetic individuality in the host-phage interaction. *PLoS Biology*, 6:0957–0964, 2008.

[136] M. Pedersen and K. Hammer. The role of MOR and the CI operator sites on the genetic switch of the temperate bacteriophage TP901-1. *Journal of Molecular Biology*, 384:577–589, 2008.

[137] V. Pirrotta, P. Chadwick, and M. Ptashne. Active form of two coliphage repressors. *Nature*, 227(5253):41–44, Jul 4 1970.

[138] K. Potrykus, G. Wegrzyn, and V. J. Hernandez. Multiple mechanisms of transcription inhibition by ppGpp at the lambda *p*R promoter. *The Journal of Biological Chemistry*, 277(46):43785–43791, Nov 15 2002.

[139] M. Ptashne, A. Jeffrey, A. D. Johnson, R. Maurer, B. J. Meyer, C. O. Pabo, T. M. Roberts, and R. T. Sauer. How the lambda Repressor and Cro work. *Cell*, 19(1):1–11, Jan 1980.

[140] Mark Ptashne. *A genetic switch : phage lambda revisited, publisher=Cold Spring Harbor Laboratory Press, address=New York, NY, pages=154, keywords=Bacteriophage lambda; Genetic regulation; Viral genetics, isbn=0879697164 (pbk.)*. 2004.

[141] L. Randall-Hazelbauer and M. Schwartz. Isolation of the bacteriophage lambda receptor from *Escherichia coli*. *Journal of Bacteriology*, 116(3):1436–1446, Dec 1973.

[142] C. V. Rao, D. M. Wolf, and A. P. Arkin. Control, exploitation and tolerance of intracellular noise. *Nature*, 420(6912):231–237, Nov 14 2002.

[143] J. M. Raser and E. K. O'Shea. Noise in gene expression: origins, consequences, and control. *Science*, 309(5743):2010–2013, Sep 23 2005.

[144] L. Reichardt and A. D. Kaiser. Control of lambda Repressor synthesis. *Proceedings of the National Academy of Sciences of the United States of America*, 68(9):2185–2189, Sep 1971.

[145] L. F. Reichardt. Control of bacteriophage lambda repressor synthesis after phage infection: the role of the *N*, *c*II, *c*III and *cro* products. *Journal of Molecular Biology*, 93(2):267–288, Apr 5 1975.

[146] R. Reyes-Lamothe, X. Wang, and D. Sherratt. *Escherichia coli* and its chromosome. *Trends in Microbiology*, 16(5):238–245, May 2008.

[147] M. Ricard and Y. Hirota. Process of cellular division in *Escherichia coli*: physiological study on thermosensitive mutants defective in cell division. *Journal of Bacteriology*, 116(1):314–322, Oct 1973.

[148] J. W. Roberts. Termination factor for RNA synthesis. *Nature*, 224(5225):1168–1174, Dec 20 1969.

[149] B. R. Robertson, D. K. Button, and A. L. Koch. Determination of the biomasses of small bacteria at low concentrations in a mixture of species with forward light scatter measurements by flow cytometry. *Applied and Environmental Microbiology*, 64(10):3900–3909, Oct 1998.

[150] O. Rodionov, M. Lobocka, and M. Yarmolinsky. Silencing of genes flanking the P1 plasmid centromere. *Science*, 283(5401):546–549, Jan 22 1999.

[151] J. Roostalu, A. Joers, H. Luidalepp, N. Kaldalu, and T. Tenson. Cell division in *Escherichia coli* cultures monitored at single cell resolution. *BMC Microbiology*, 8:68, Apr 23 2008.

[152] M. Rosenberg, D. Court, H. Shimatake, C. Brady, and D. L. Wulff. The relationship between function and DNA sequence in an intercistronic regulatory region in phage lambda. *Nature*, 272(5652):414–423, Mar 30 1978.

[153] Joseph Sambrook and David W. Russell. *Molecular cloning : a laboratory manual, publisher=Cold Spring Harbor Laboratory Press, address=Cold Spring Harbor, N.Y., keywords=Molecular cloning; Laboratory manuals, isbn=0879695773; 0879695765.* 2001.

[154] Erwin Schrödinger. *What is life? : the physical aspect of the living cell, publisher=University Press; Macmillan, address=Cambridge Eng.; New York, pages=91,.* 1945.

[155] N. C. Shaner, P. A. Steinbach, and R. Y. Tsien. A guide to choosing fluorescent proteins. *Nature Methods*, 2(12):905–909, Dec 2005.

[156] M. A. Shea and G. K. Ackers. The *o*R control system of bacteriophage lambda. A physical-chemical model for gene regulation. *Journal of Molecular Biology*, 181(2):211–230, Jan 20 1985.

[157] R. P. Shetty, D. Endy, and T. F. Knight Jr. Engineering BioBrick vectors from BioBrick parts. *Journal of Biological Engineering*, 2(1):5, Apr 14 2008.

[158] T. Shimada, H. Makinoshima, Y. Ogawa, T. Miki, M. Maeda, and A. Ishihama. Classification and strength measurement of stationary-phase promoters by use of a newly developed promoter cloning vector. *Journal of Bacteriology*, 186(21):7112–7122, Nov 2004.

[159] A. Sigal, R. Milo, A. Cohen, N. Geva-Zatorsky, Y. Klein, Y. Liron, N. Rosenfeld, T. Danon, N. Perzov, and U. Alon. Variability and memory of protein levels in human cells. *Nature*, 444(7119):643–646, Nov 30 2006.

[160] M. Slominska, P. Neubauer, and G. Wegrzyn. Regulation of bacteriophage lambda development by guanosine 5'-diphosphate-3'-diphosphate. *Virology*, 262(2):431–441, Sep 30 1999.

[161] F. H. Stephenson. A CII-responsive promoter within the Q gene of bacteriophage lambda. *Gene*, 35(3):313–320, 1985.

[162] G. M. Suel, J. Garcia-Ojalvo, L. M. Liberman, and M. B. Elowitz. An excitable gene regulatory circuit induces transient cellular differentiation. *Nature*, 440(7083):545–550, Mar 23 2006.

[163] G. M. Suel, R. P. Kulkarni, J. Dworkin, J. Garcia-Ojalvo, and M. B. Elowitz. Tunability and noise dependence in differentiation dynamics. *Science*, 315(5819):1716–1719, Mar 23 2007.

[164] J. E. Sulston, E. Schierenberg, J. G. White, and J. N. Thomson. The embryonic cell lineage of the nematode *Caenorhabditis elegans*. *Developmental Biology*, 100(1):64–119, Nov 1983.

[165] R. Sussman and F. Jacob. On a thermosensitive repression system in the *Escherichia coli* lambda bacteriophage. *Comptes Rendus Hebdomadaires des Séances de l'Academie des Sciences*, 254:1517–1519, Feb 19 1962.

[166] M. Thattai and A. van Oudenaarden. Intrinsic noise in gene regulatory networks. *Proceedings of the National Academy of Sciences of the United States of America*, 98(15):8614–8619, Jul 17 2001.

[167] J. P. Thirion and M. Hofnung. On some genetic aspects of phage lambda resistance in *E. coli* K12. *Genetics*, 71(2):207–216, Jun 1972.

[168] R. Thomas. Control of development in temperate bacteriphages. I. Induction of prophage genes following heteroimmune super-infection. *Journal of Molecular Biology*, 22:79, 1966.

[169] L. Thomason, D. L. Court, M. Bubunenko, N. Costantino, H. Wilson, S. Datta, and A. Oppenheim. Recombineering: genetic engineering in bacteria using homologous recombination. *Current protocols in molecular biology*, Chapter 1:Unit 1.16, Apr 2007.

[170] T. Tomoyasu, T. Yuki, S. Morimura, H. Mori, K. Yamanaka, H. Niki, S. Hiraga, and T. Ogura. The *Escherichia coli* FtsH protein is a prokaryotic member of a protein family of putative ATPases involved in membrane functions, cell cycle control, and gene expression. *Journal of Bacteriology*, 175(5):1344–1351, Mar 1993.

[171] J. A. Triccas, R. Pinto, and W. J. Britton. Destabilized green fluorescent protein for monitoring transient changes in mycobacterial gene expression. *Research in Microbiology*, 153(6):379–383, Jul-Aug 2002.

[172] A. F. Wahl and K. L. Donaldson. *Centrifugal elutriation to obtain synchronous populations of cells*. Current protocols in cell biology. John Wiley, New York, 2001.

[173] X. Wang, X. Liu, C. Possoz, and D. J. Sherratt. The two *Escherichia coli* chromosome arms locate to separate cell halves. *Genes Development*, 20(13):1727–1731, Jul 1 2006.

[174] X. Wang, C. Possoz, and D. J. Sherratt. Dancing around the divisome: asymmetric chromosome segregation in *Escherichia coli*. *Genes Development*, 19(19):2367–2377, Oct 1 2005.

[175] W. Wehrl, M. Niederweis, and W. Schumann. The FtsH protein accumulates at the septum of *Bacillus subtilis* during cell division and sporulation. *Journal of Bacteriology*, 182(13):3870–3873, Jul 2000.

[176] L. S. Weinberger, J. C. Burnett, J. E. Toettcher, A. P. Arkin, and D. V. Schaffer. Stochastic gene expression in a lentiviral positive-feedback loop: HIV-1 Tat fluctuations drive phenotypic diversity. *Cell*, 122(2):169–182, Jul 29 2005.

[177] R. A. Weisberg and A. Landy. *Site-specific recombination in phage lambda*, pages 211–250. Lambda II. Cold Spring Harbor Laboratory, Cold Spring Harbor, N.Y., 1983.

[178] J. S. Weitz, Y. Mileyko, R. I. Joh, and E. O. Voit. Collective decision making in bacterial viruses. *Biophysical Journal*, 95(6):2673–2680, Sep 15 2008.

[179] H. R. Wilson, L. Kameyama, J. G. Zhou, G. Guarneros, and D. L. Court. Translational repression by a transcriptional elongation factor. *Genes Development*, 11(17):2204–2213, Sep 1 1997.

[180] H. R. Wilson, D. Yu, H. K. Peters 3rd, J. G. Zhou, and D. L. Court. The global regulator RNase III modulates translation repression by the transcription elongation factor N. *The EMBO Journal*, 21(15):4154–4161, Aug 1 2002.

[181] F. Yang, P. Forrer, Z. Dauter, J. F. Conway, N. Cheng, M. E. Cerritelli, A. C. Steven, A. Pluckthun, and A. Wlodawer. Novel fold and capsid-binding properties of the

lambda-phage display platform protein gpD. *Nature Structural Biology*, 7(3):230–237, Mar 2000.

[182] C. N. Zanghi, H. A. Lankes, B. Bradel-Tretheway, J. Wegman, and S. Dewhurst. A simple method for displaying recalcitrant proteins on the surface of bacteriophage lambda. *Nucleic Acids Research*, 33(18):e160, Oct 13 2005.

[183] X. M. Zhu, L. Yin, L. Hood, and P. Ao. Robustness, stability and efficiency of phage lambda genetic switch: dynamical structure analysis. *Journal of Bioinformatics and Computational Biology*, 2(4):785–817, Dec 2004.